NUCLEAR TOPOLOGY OF MURINE, CEREBELLAR PURKINJE NEURONS: CHANGES AS A FUNCTION OF POSTNATAL DEVELOPMENT

by

Glykeria Martou

A thesis submitted in conformity with the requirements
for the Master of Science degree

Graduate Department of Physiology
University of Toronto

Nuclear Topology of murine, cerebellar Purkinje neurons: Changes a function of postnatal development

by Glykeria Martou

A thesis submitted in conformity with the requirements
for the Master of Science degree
Graduate Department of Physiology
University of Toronto

2000

ABSTRACT

Interphase nuclei exhibit a dynamic, cell-type specific topology of chromatin in differentiated cells. We predict that this topology is established at a particular developmental stage. We assessed the number and spatial distribution of centromeric domains in murine, cerebellar Purkinje cells as a function of postnatal development, and found a redistribution of these domains from the nuclear periphery towards the centrally located nucleolus, associated temporally with differentiation events.

Centromeric sequences are not transcribed. Thus, we tested whether the above redistribution of centromeric domains is temporally associated with the *de novo* expression of Purkinje-neuron specific sequences. Fluorescence *In Situ* Hybridization to two sequences, RORα and PLCβ3, showed that the spatial position of RORα, whose levels of expression remain constant following expression at E15, does not change during development. In contrast, the *de novo* expressed PLCβ3 relocated from the nuclear periphery to the nucleolus. We conclude that this relocation may represent one level of control of gene expression.

ACKNOWLEDGEMENTS

I would like to thank my supervisor and mentor, Dr. Umberto De Boni, for making the last two years, without a doubt, the best and most rewarding years of my academic life, thus far. He is everything a student looks for in a supervisor, enthusiastic, hard-working, supporting, understanding, firm and there is so much more I am thankful for. The most important lesson I have learnt as a graduate student working with him is to be patient, no matter how "unpromising" things may appear to be. Learning to maintain a positive attitude has helped me tremendously succeed both in and outside the lab.

I would like to thank the members of my supervisory committee, Dr. W. Mackay and Dr. M. Wiley, for their guidance and support during this project.

I would like to thank Dr. Paul Park and my colleagues in the lab, Jonathan Chan, Jon Tomas, Eun Kim, Nadine Mitchel, Charly Chahwan and Paul Grossman for their friendship, their constructive criticism, their continuous support and above all for putting up with me during the last two years. Special thanks to Dr. Paul Park for his help with the molecular biology techniques during the last year.

Many thanks to Nesime Askin for her friendship, I will always remember her enthusiastic spirit, and for her drawings for this project. Also, thank you to Vassilis Kokiopoulos and Andreas Polirakis for their help with the statistical analysis.

I would like to thank Maria Kotsopoulos, for being the best friend I have ever had, for being there for me throughout the last six years, for making everything more fun, for making my life in a new country a wonderful experience. I could not have made it without her.

I would also like to thank Tassos for his love, continuous support, his wonderful surprise trip, for bringing out the best in me and for making everything easier. Μαζι για παντα.

I am grateful to my uncle George, my aunt Androulla and my cousins, Stelio, Mario and Elena for their love and support and for offering me a place in their home during my first years in Canada.

I would like to dedicate this thesis to my father, George, my mother, Irene, my brother Nikos and my uncle Dimitri. I owe everything to them and I pray that one day I will as supportive, loving and understanding to my own family.

Μπαμπα, μαμα, Νικο και θειο, αυτη η εργασια ειναι αφιερωμενη σε σας.
Δεν θα τα καταφερνα χωρις την αγαπη, την υποστηριξη και την κατανοηση σας.

TABLE OF CONTENTS

RESULTS

LIST OF FIGURES

LIST OF TABLES

LIST OF ABBREVIATIONS

BAC	Bacterial Artificial Chromosome
bp	base pair
BSA	Bovine Serum Albumin
^{0}C	degree Celcius
CABPD28K	Calcium binding protein 28kd/calbidin
CENP	Centromeric Protein
CLIP	Chromatid Linking Protein
CNS	Central Nervous System
CREST	Calcinosis, Raynauds phenomenon, Esophageal dysmotiliy, Sclerodactyly, Telangiectasia
3-D	three-dimensional
DHC	DNAse hypersensitive chromatin
DNA	Deoxyribonucleic acid
E	Embryonic
EGL	External Granular Layer
FBS	Fetal Bovine Serum
FISH	Fluorescence *In Situ* Hybridization
FITC	Fluorescein Iso-ThioCynate
g	gravity
GABA	Gamma-AminoButyric Acid

GABAA/BZ	Gamma-AminoButyric Acid A/Benzodiazepine
GER	Granular Endoplasmic Reticulum
GFP	Green Fluorescent Protein
Glu	Glutamate
GluR	Glutamate Receptor
GluRδ2	Glutamate Receptor, δ2 subunit
H1	Histone 1
h	hour
INCENP	Inner Centromeric Protein
IP_3	Inositol TriPhospate
HBSS	Hank's Balanced Salt Solution
IGL	Internal Granular Layer
kb	kilobase pair
kDa	kilodalton
LTD	Long-Term Depression
MEM	Minimum Essential Medium
µg	microgram
µL	microliter
µm	micrometer
m	meter
mg/mL	milligram per milliliter
min	minute

mm	millimeter
mL	milliliter
mRNA	messenger RNA
n.a	numerical aperture
ng	nanogram
NGF	Nerve Growth Factor
nm	nanometer
NOR	Nuclear Organizing Region
NPC	Nuclear Pore Complex
NTFI	Normalized Total Fluorescence Intensity
P	Postnatal
pcd	purkinje cell degeneration
PBS	Phosphate Buffer Saline
PC	Purkinje Cell
pcp-2	purkinje cell-specific protein - 2
PKC	Protein Kinase C
PLCβ3	Phospholipase C β3
rDNA	ribosomal DNA
RNA	ribonucleic acid
rpm	revolutions per minute
RT	Room Temperature
SC35	Splicing Component 35
sDNA	satellite DNA

sec	second
SEM	Standard Error of the Mean
SF2	Splicing Factor 2
Shh	Sonic Hedgehog
snRNP	small ribonucleoprotein
SSC	Sodium Sodium Citrate
TAE	Tris-Acetate buffer
tDNA	telomeric DNA
TFI	Total Fluorescence Intensity
UV	Ultra-Violet
V	Volt
v/v	volume per volume
wks	weeks
w/v	weight per volume
YAC	Yeast Artificial Chromosome

INTRODUCTION

The interphase nucleus is a topologically organized, three-dimensional (3-D) structure with its spatial topology being proposed to reflect compartmentalization of nuclear function (Cremer *et al.*, 1993; Marshall and Sedat, 1999; Park and De Boni, 1999). This spatial organization has also been proposed to represent one level of control of gene expression by placing actively transcribed genes to transcriptionally competent nuclear sites (De Boni and Mintz, 1986; Park and De Boni, 1998; 1999). Thus far, both these premises have been supported by a number of studies demonstrating the dynamic nature of the spatial topology of the interphase nucleus. Furthermore, evidence for the existence of components of a nuclear acto-myosin motor, via which the motion of various nuclear components is accomplished, also support the view of a dynamically compartmentalized nucleus (De Boni, 1994; Park and De Boni, 1999).

Rearrangements of chromatin domains have been shown to accompany pathological states (Borden and Manuelidis, 1988; Haaf and Schmid, 1989; Tagawa *et al.*, 1997) and conditions that alter the transcriptional demand of the cell (Holowacz and De Boni, 1991; Billia *et al.*, 1992; Janevski *et al.*, 1995). Furthermore, evidence exists to show that changes in the spatial organization of chromatin domains take place during the course of neuronal differentiation (Manuelidis, 1984a; Park and De Boni, 1991; 1992; Choh and De Boni, 1996). Differentiation is that time during which cells initiate expression of a particular part of their genome to achieve a differentiated, specialized state (Carlson, 1996; Gilbert, 1997). This, along with the fact that the spatial topology of interphase nuclei is cell-specific in fully differentiated neurons, has led to the proposal that the topological organization of the interphase nucleus is

related to the functional commitment of the cell and its state of differentiation (Manuelidis, 1984a).

One of the fundamental goals in developmental neurobiology is the identification of the mechanisms involved in orchestrating gene expression in the cell-type specific manner occurring during differentiation. Taking into consideration the above regarding a connection of a dynamically organized nuclear topology to differentiation, our hypothesis with respect to neuronal development is twofold. First, we predict that there is a particular stage during differentiation before or during which the spatial nuclear topology of adult, fully differentiated cells is established. Second, the timeframe of this establishment coincides with the *de novo* expression of cell-specific sequences.

We chose the murine, cerebellar Purkinje neuron as a model for our study for a number of reasons. According to the study by Yuasa *et al.*, (1991), the precursors of Purkinje cells undergo their final mitosis by E13. Thus, these neurons are post-mitotic at birth and any variability in nuclear topology arising from cell cycle events can be excluded. Furthermore, the majority of events leading to the fully differentiated Purkinje neuron takes place postnatally (Altman and Bayer, 1997; Dunn *et al.*, 1998b). Last but not least, the widespread use of the cerebellar cortex as the model of choice for studies in CNS development for the last three decades has led to the very well documented cytology and architecture of this region throughout postnatal development. Thus, Purkinje cells can be identified unambiguously during the course of their postnatal development.

To test part one of the hypothesis, namely, that there is a particular developmental stage before or during which the adult spatial topology is established, centromeric domains were localized via immunolabelling of associated kinetochore proteins. They were visualized by

confocal laser microscopy and analyzed with respect to their total number and spatial, intra-nuclear distribution a function of postnatal development. Kinetochore proteins represent excellent markers for centromeric domains due to their persistent association to centromeric DNA throughout the cell cycle of the cell, including interphase (Masumoto *et al.*, 1989).

To test part two of the hypothesis, according to which the timeframe of the establishment of the adult spatial nuclear topology is associated with the *de novo* expression of specific sequences, two Purkinje neuron specific sequences, RORα and PLCβ3, were labelled following Fluorescence *In Situ* hybridization to their nuclear DNA in interphase, and their spatial position was assessed as a function of postnatal development.

REVIEW OF THE LITERATURE

INTERPHASE NUCLEUS - ARCHITECTURE

Chromatin Organization/Chromosome Territories

The typical mammalian nucleus contains approximately $6x10^9$ base pairs (bps) of DNA, corresponding to a linear length of 2m, packaged into a spheroid measuring just 10μm in diameter. Thus, the necessity arises for efficient packaging that would both reduce the 2m-long DNA and maintain a structural order. To accomodate both structural and functional purposes, there is a multi-level, hierarchical organization of chromatin, ranging from strands of naked DNA to condensed structures. This organization manages to reduce the linear DNA length up to 10,000 fold, depending on the stage of the cell cycle (Becker and Deamer, 1991; Pienta *et al.*, 1991).

Specifically, six levels of organization are recognized (Fig. 1), of which the formation of the DNA double helix, about 2nm in width, represents the first. The second level consists of approximately $2^{1/2}$ turns of the double helix wrapped around a histone octamer core, the nucleosome, resulting in a 10nm chromatin or nucleosomal fiber (Becker and Deamer, 1991). The third level arises from the coiling of these chromatin fibers to form a helical coil known as the solenoid, 30nm thick (Becker and Deamer, 1991), in the form of which the majority of chromatin is found in interphase, as shown by high resolution SEM (De Boni, 1988). There is also evidence that reversible interconversions are possible between the chromatin and solenoid fibers under the control of Histone 1 (H1) (Clark and Kimura, 1990; Thomas *et al.*, 1992). In interphase, according to the most prevailing view, the solenoid fibers are arranged in discrete loops attached via a sequence-specific complex to the nuclear matrix and/or to the nuclear envelope to give rise to the fourth organizational level, the chromosome territories (see below).

Figure 1: Schematic representation of the hierarchical, conformational organization of chromatin. The DNA double helix (A) wraps $2^{1/2}$ times around the nucleosome to give rise to the chromatin fiber (B), while the coiling of the chromatin fibers results in the formation of the solenoid (C). In interphase, solenoid fibers are arranged in discrete loops, attached to the nuclear matrix and/or to the nuclear envelope via a sequence-specific complex, and forming the chromosome territories (D). In metaphase, solenoid fibers are arranged in discrete loops attached to the nuclear scaffold/matrix (D). The radial arrangement of these loops results in the formation of the minibands (E) and finally, the mitotic chromosome (F) represents the highest level of chromatin folding.

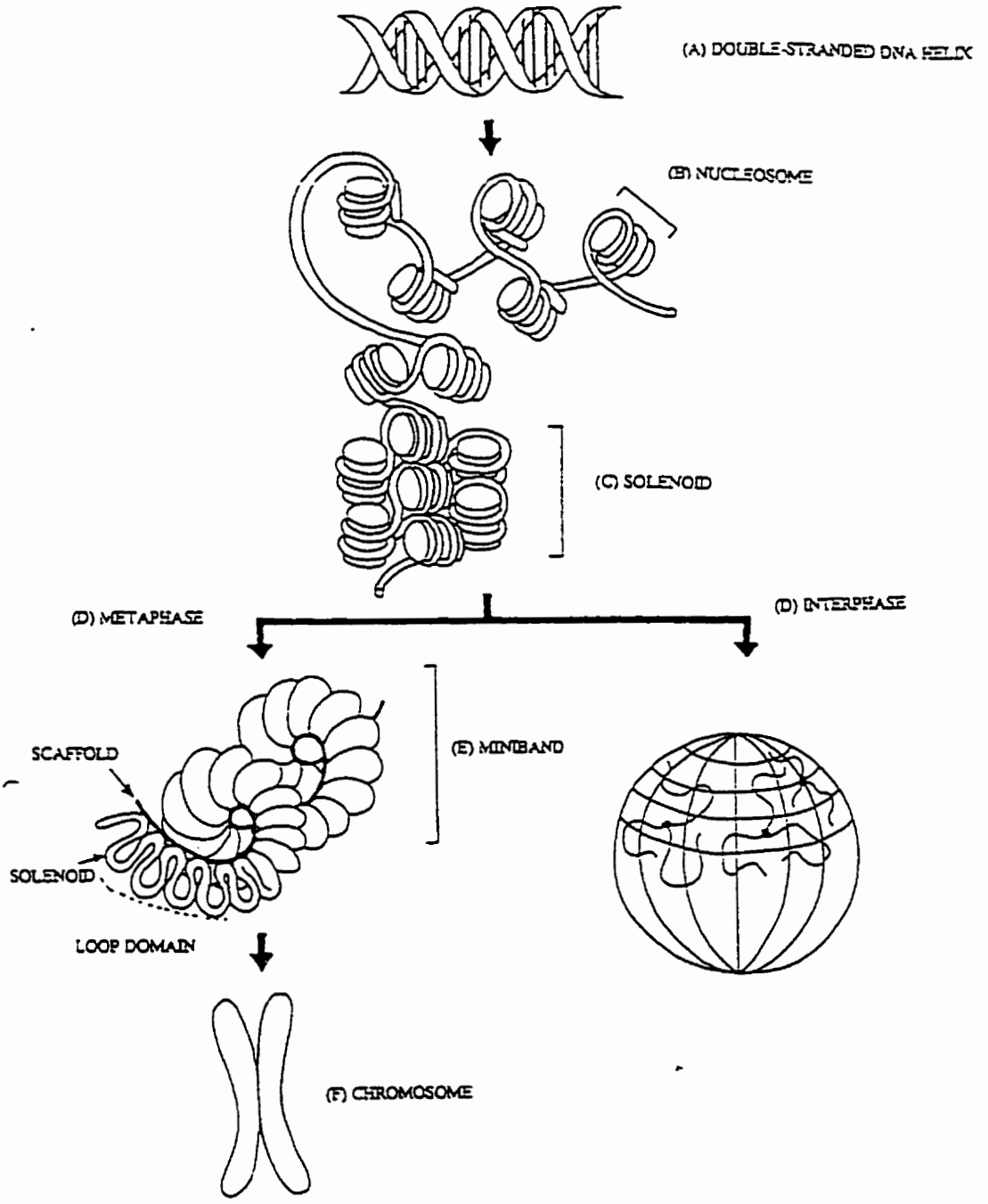
(A) DOUBLE-STRANDED DNA HELIX
(B) NUCLEOSOME
(C) SOLENOID
(D) METAPHASE
(D) INTERPHASE
SCAFFOLD
SOLENOID
LOOP DOMAIN
(E) MINIBAND
(F) CHROMOSOME

In metaphase, the fourth level is represented by the arrangement of the solenoid fibers into loop domains, 60 to 200nm in diameter, whereas the further radial arrangement of these loops at the base around a central axis to form the minibands (chromatids) leads to the fifth level (Pienta and Coffey, 1984). Finally, the formation of the mitotic chromosome represents the highest level of chromatin folding resulting in a particularly high packaging ratio (Becker and Deamer, 1991).

Eukaryotic DNA expresses itself during interphase, the timespan between two mitotic events, thus it becomes pertinent to "unravel" the organization of chromatin during this stage (Manuelidis, 1990). As stated above, the organizational pattern of nuclear chromatin during interphase is very different from the one in mitosis. Specifically, during interphase two morphological types of chromatin are evident, heterochromatin and euchromatin, that can be regarded as higher organizational levels in which there is interaction between different chromosomes (Carmo-Fonseca *et al.*, 1996; Cooper, 1997). Heterochromatin is more highly condensed and is considered to be transcriptionally inactive whereas euchromatin remains decondensed in interphase and is considered to contain active sequences (Cooper, 1997). These patterns of condensation are cell-type specific and are conserved in mammalian evolution as shown in different neuronal cells (Manuelidis, 1984a;1985a;1985b). Heterochromatin is further divided into constitutive and facultative. Constitutive chromatin consists of DNA sequences that are never transcribed, an example being satelite DNA (sDNA) in the centromeric regions (Cooper, 1997). Facultative chromatin consists of non cell-specific sequences that are expressed in some cells but not necessarily in the particular cell type examined (Cooper, 1997). However, there is some evidence showing that certain heterochromatic parts may be transcriptionally active (Manuelidis, 1990; Carmo-Fonseca *et al.*, 1996).

During anaphase, chromosomes arrange themselves toward the two poles is such a way that centromeric and telomeric regions are on opposite sides of the cell. This polarized chromatin distribution was proposed to be preserved in interphase, and is known as the Rabl model (Rabl, 1885). This was the first time the concept of territorial organization of interphase chromosomes was suggested. This view, however, was not widely accepted until direct experimental evidence was available and was shown to be the case from experiments using DNA repair following microirradiation (Cremer *et al.*, 1982a; 1982b), *in situ* hybridization studies in interspecies hybrid cells (Manuelidis, 1985b; Schhardin *et al.*, 1985) and chromosome painting (Lichter *et al.*, 1988a; 1988b; Pinkel *et al.*, 1988; Leitch *et al.*, 1990).

According to the model proposed by Cremer *et al.*, interphase chromosomes are organized as delineated, non-overlapping, compact territories presumably separated by the negative charges of chromatin at physiological pH (Cremer *et al.*, 1993; Eils *et al.*, 1996; Kurtz *et al.*, 1996; Cremer *et al.*, 1996). Moreover, this model proposes that chromosome territories are separated by interchromatin channels, devoid of DNA, continuous with nuclear pores proposed to reflect sites of post-transcriptional processing and facilitation of nucleocytoplasmic export (Spector, 1990; Cremer *et al.*, 1993). Furthermore, within territories, chromosomes have been suggested to be arranged in such a manner that active sequences are positioned towards the surface of the territory (Zirbel *et al.*, 1993). Studies that show a localization of actively transcribed sequences (Park and De Boni, 1998) and of nascent pre-mRNA (Wansink *et al.*, 1994) to the territorial surface are in support of this view. In contrast, however, the coupling of homologous chromosome pairs at the histone gene sequences in embryonic Drosophila cells (Hiraoka *et al.*, 1993) has challenged the existence of compact territories and channels (Van Driel *et al.*, 1995).

In addition, it is important to note that chromatin organization is not rigid and undergoes dynamic changes during different phases of the cell cycle and under conditions of altered transcriptional demand. Digestion of chromatin with DNase I reveals the existence of two types of structural chromatin conformations representing transcriptionally active sequences, the parts of general sensitivity and the DNase sensitive chromatin, also known as the DHC domain. The latter is characterized by an increase of two or more magnitudes in sensitivity to DNase I, and represents histone-free DNA regions 100-200bps long (Burch and Weintraub, 1983). The DNA segments of the DHC domain encode for the most part regulatory elements including promoters, enhancers, locus control regions, telomeres and silencers (Gross and Garrard, 1988). The DHC domain is suggested to be involved in changes in DNA conformation resulting in the alignment of regulatory elements with sequences to be transcribed, thus, in turn, allowing their interaction with transcriptional factors and RNA polymerase II (Rougvie and Lis, 1988; Tsukiyama *et al.*, 1994). Regions of general sensitivity, often flanking DHC domains, are associated with the coding regions of potentially active sequences (Wood and Felsenfeld, 1982).

Centromere complex

Cytologists have traditionally referred to the centromere as the primary constriction of the chromosome visible as a narrowing of the chromatin, at a certain region along metaphase chromosomes. This position represents the site of attachment of microtubules during cell division, resulting in the chromosomes aligning on the metaphase plate. This alignment, in turn, is considered to lead to the correct and timely separation of the chromosomes into each of the daughter cells (Earnshaw, 1991; Bloom, 1993; Mitchell, 1996). The importance of the

centromere is indicated by the instability and loss of chromosomes in subsequent cell divisions, both of which are associated with loss of centromeric function (Mitchell, 1996).

Even though the terms "centromere" and "kinetochore" have often been used interchangebly, studies that have dealt with the morphological and biochemical characterization of the centromeric region have shown that the kinetochore is the specific site of the centromere to which microtubules attach (Earnshaw, 1991; Bloom, 1993; Mitchell, 1996). Specifically, the centromeric region consists of three parts, different in function and protein composition. These include the pairing, the central and the kinetochore domains (Fig. 2) (Earnshaw and Rattner, 1989; Vig and Rattner, 1989). The kinetochore domain consists of a trilaminar plate attached to centromeric chromatin. The central domain confers the structural foundation for the kinetochore domain and consists mainly of chromatin, and finally the pairing domain is responsible for the pairing of sister chromatids and comprises of both DNA and protein (Earnshaw and Rattner, 1989).

Mammalian centromeric regions contain large amounts of redundant or sDNA (Pardue and Gall, 1970). For instance, the murine centromeric regions have been shown to consist of two types of sDNA, the major type accounting for 5-10% of the total genome and the minor type accounting for less than 1%. Both are found at the centromeres of murine chromosomes (Jones, 1970; Wong and Rattner, 1988). In humans, Mitchell *et al.*, (1985) showed that alphoid DNA, a family of sDNA characterized by tandem arrays of 170bp repeats arranged in groups of dimeric and pentameric units, is found at the centromeres of all chromosomes. Furthermore, sequences homologous to the human alphoid DNA have also been found in higher primates suggesting a degree of evolutionary conservation (Baldini *et al.*, 1991).

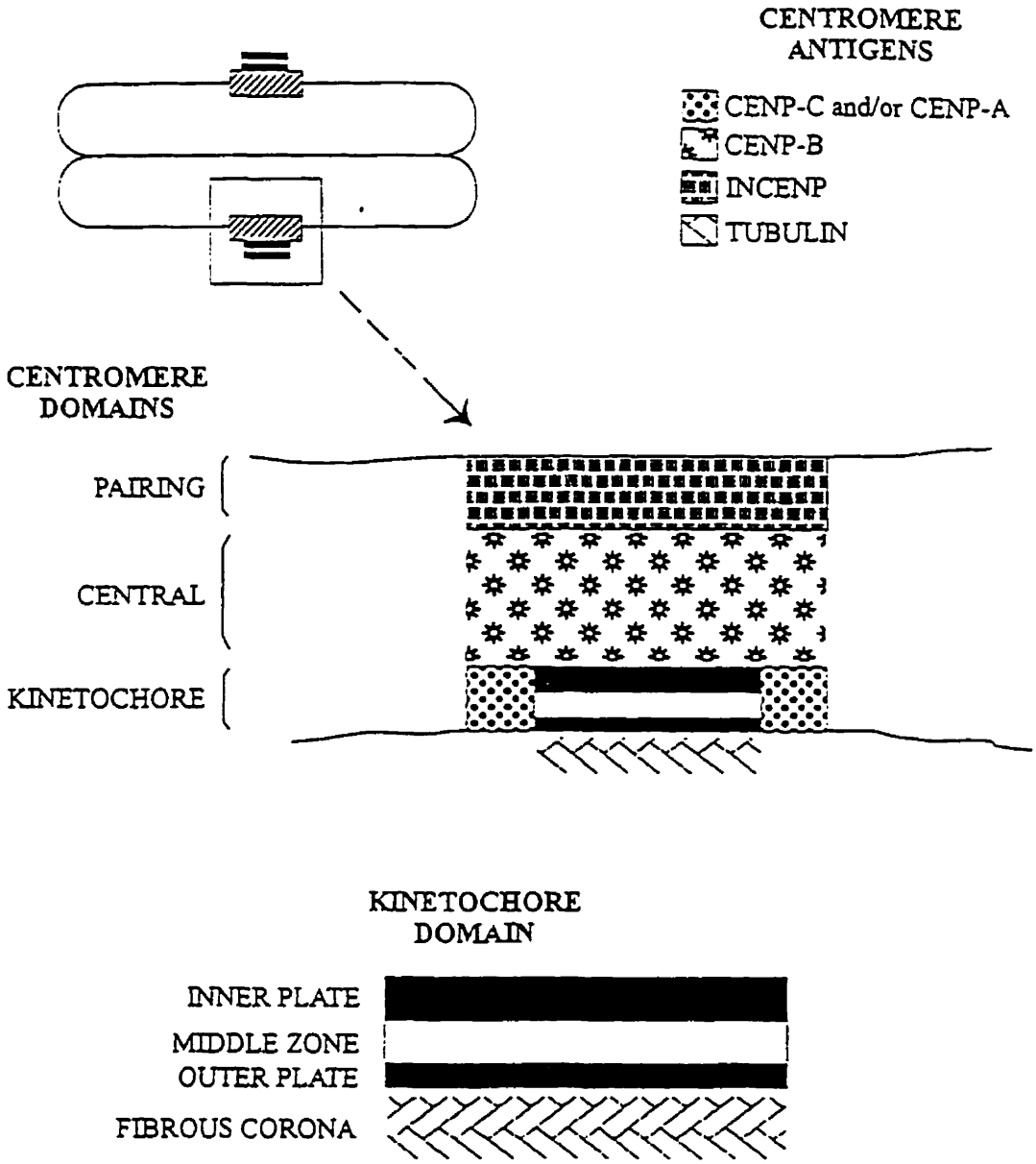

Figure 2: Structural map of the vertebrate centromere complex. Shown are the three constituents, the pairing domain, the central domain and the kinetochore domain, along with the distribution of the corresponding diagnostic antigens (Adapted from Pluta *et al.*, 1990). The kinetochore domain is the site of microtubule attachment while the pairing domain is responsible for the pairing of the sister chromatids. The centromeric protein via which centromeric domains are immunolabelled is CENP-B, a constituent of the central domain.

In murine centromeres, fractions of major sDNA are found throughout the centromeric region and are a major component of the central domain while minor sDNA sequences are restricted to the lateral kinetochore domain (Wong and Rattner, 1988; Rattner, 1991).

As mentioned above, all centromeric domains consist of both DNA and protein. Although the task of identifying the protein components was perceived to be daunting originally, the discovery that the sera of patients with CREST (Calcinosis, Raynauds phenomenon, Esophageal dysmotility, Sclerodactyly, Telangiectasia) contain autoantibodies that recognize some of the centromeric polypeptides changed this perception (Brenner *et al.*, 1981; Moroi *et al.*, 1981). Centromeric proteins are divided into two groups, constitutive proteins found in association with the centromere throughout the cell cycle, including interphase, and facultative proteins associated with the centromere as function of cell cycle (Brinkley *et al.*, 1992; Rattner *et al.*, 1993). Constitutive proteins include centromeric protein (CENP) -A (Guldner *et al.*, 1984; Valdivia and Brinkley, 1985), CENP-B (Earnshaw and Rothfield, 1985; McNeilage *et al.*, 1986), CENP-C (Earnshaw *et al.*, 1984; Earnshaw and Migeon, 1985), and CENP-D (Cox *et al.*, 1983; Earnshaw and Migeon, 1985). Facultative proteins include CENP-E (Yen *et al.*, 1991) and CENP-F (Rattner *et al.*, 1993), both members of a group known as inner centromeric proteins (INCENPs) (Mackay *et al.*, 1993). Additional facultative proteins include calmodulin, tubulin, dynein (Pfarr *et al.*, 1993), chromatid linking proteins (CLIPs) (Rattner *et al.*, 1988), cytoskeletal proteins knowns as chromosomal passenger proteins (Mackay *et al.*, 1993) and a collection of high molecular weight proteins associated with the chromosomal scaffold (Yen *et al.*, 1991).

Studies which focused on how the DNA and protein contents of the centromeric region interact and how this interaction reflects on the precise role of the centromere in chromosomal segregation have provided valuable insight in the role of each of these proteins. For example,

CENP-A, a histone-like molecule found in centromeric nucleosomes, is proposed to provide a structure that can withstand the stronger stress forces required in chromosome segregation during cell division (Mitchell, 1996). CENP-C, shown to be part of the inner kinetochore plate (Saitoh *et al.*, 1992; Tomkiel *et al.*, 1994), has been suggested to function in stabilizing microtubule attachment and in maintaining the kinetochore size (Tomkiel *et al.*, 1994). For the purposes of this review, however, we will focus on CENP-B since this is the centromeric protein via which centromeric domains are commonly immunolabelled (see Methods).

CENP-B has been shown to be distributed in the heterochromatin of the central domain as opposed to the kinetochore domain in which it was previously thought to be localized (Earnshaw *et al.*, 1987). In fact, studies using monospecific antibodies and colloidal gold techniques have shown that only 1% of the CENP antigens is associated with the kinetochore domain (Pluta *et al.*, 1990). CENP-B has provided the most insight in terms of CENPs-DNA interactions. Masumoto *et al.*, (1989) showed that human alphoid DNA can be immunoprecipitated using serum from patients with CREST and that CENP-B binds alphoid DNA directly via a 17bp motif known as the CENP-B box (Masumoto *et al.*, 1989; Pluta *et al.*, 1992). This interaction gives rise to a stable dimer structure maintained by protein-protein hydrophobic bonds (Kitagawa *et al.*, 1995) that is, in turn, proposed to be involved in the condensation of the long arrays of sDNA (Mitchell, 1996). Most importantly, however, binding sites for CENP-B have been found in murine sDNA of the central domain and it is this association of the constitutive CENP-B with centromeric sDNA that renders this centromeric protein an excellent marker for the localization of centromeric domains during interphase (Vig and Rattner, 1989; Haaf and Schmid, 1991; Holowacz and De Boni, 1991; Janevski *et al.*, 1995; Martou and De Boni, 2000).

Nucleolus

The nucleolus is the most prominent, morphologically recognizable nuclear compartment, responsible for rRNA transcription and processing, and for ribosome assembly (Cooper, 1997). It is composed of ribosomal DNA (rDNA) sequences, rRNA and ribosomal proteins (Cooper, 1997). rRNA sequences are arranged in clusters on different chromosomes, each cluster representing a nucleolus-organizing region (NOR). To meet the need for transcription of a large number of rRNA molecules, each NOR contains multiple rRNA transcription units arranged as tandem repeats, segregated by nontranscribed spacer sequences (reviewed in Scheer and Weisenberger, 1994). The distribution of rDNA is species specific (Howell, 1982). For example, in Xenopus laevis NORs are associated with only one chromosome, chromosome 12 (Schmid and Steinein, 1991), whereas in human cells NORs are found on chomosomes 13, 14, 15, 21 and 22 (Henderson *et al.*, 1972). In murine cells NORs are associated with three chromosomes, 12, 15 and 19 (Oud and Reutlinger, 1981).

Morphologically, ultrastructural studies have revealed three nucleolar components, namely, one or more fibrillar centers, the dense fibrillar component and the granular component (Hozak, 1996). Each fibrillar center is surrounded by dense fibrillar components and both are surrounded by the granular component (Hozak, 1996). The granular component, accounting for the majority of the nucleolar mass, consists of ribosomal precursor particles and is suggested to represent the site of post-transcriptional processing of rRNA (Hilliker and Apples, 1989).

Fibrillar centers consist of rDNA, representing aggregation of NORs, and members of the transcriptional apparatus such as RNA polymerase I, topoisomerase I along with other proteins (Scheer and Rose, 1984). Nucleoli form during telophase at the regions of chromosomal NORs. It is suggested that association of the NOR-bearing chromosomes with the nuclear matrix (see

below) provides a focal point for the formation of the fibrillar centers (Hilliker and Appels, 1989). The presence of enzymes involved in rDNA transcription in these centers strengthens the view that active rDNA is present in the fibrillar centers. More recent studies, however, propose that active rRNA along with the nascent transcipts give rise to dense fibrils that, in turn, are arranged in such a manner that they extend outside the fibrillar centers forming the surrounding dense fibrillar components (Wachtler *et al.*, 1989; 1990; Hozak, 1996). Thus, transcribed rRNA undergoes processing as it proceeds from the centrally located fibrillar center through the dense fibrillar component and finally to the granular component where maturation of the pre-ribosomal RNA takes place (Wachtler *et al.*, 1990).

- Nucleolar organization and morphology depend on the cell type and physiological state of the cell. For example, since ribosomes are required for cytoplasmic protein synthesis, changes in the protein demand reflect changes in the nucleolar activity. In rat sympathetic neurons, increased rRNA synthesis in the nocturnal rat was found to be associated with a concomitant increase in the size of the fibrillar center, whereas during the day, nucleoli appeared reticulated (Pebusque *et al.*, 1981). In adult, murine Purkinje cells nucleoli appear prominent and occupy primarily a central, intranuclear position, whereas some younger Purkinje cells were characterized by multiple, smaller, peripherally located nucleoli (Martou and De Boni, 2000).

Nuclear Matrix

The concept of a nuclear matrix as the structural skeleton of the nucleus was first introduced in 1974, when, following DNase digestion and extraction with high salt buffers to remove histones and other nuclear proteins, a network of insoluble material "survived" and

maintained the size and shape of rat liver nuclei (Berezney and Coffey, 1974). This residual network had three components, namely, a peripheral nuclear lamina, a residual nucleolar structure and an internal network of granular fibers. The lamina eventually was shown to consist of the interfilament-like proteins lamin A, B and C and to associate with the inner lining of the nuclear envelope. Thus, it was considered to provide an attachment site for the matrixed nuclear membrane and nuclear pore complexes (Gerace and Burke, 1988; Nigg, 1989).

The proposed role for the nuclear matrix is analogous to that of the cytoskeleton as the structural framework of the cell (Pienta *et al.*, 1991; Hozak, 1996). In addition, the nuclear matrix is proposed to anchor the chromatin loop domains during the formation of metaphase chromosomes (Vogelstein *et al.*, 1980; Manuelidis, 1990) (see below).

Following the seminal study by Berezney and Coffey in 1974, 25 years later, there still exists controversy surrounding the existence of a nuclear matrix. According to advocates who argue against this concept, the nuclear matrix is a residual structure, representing an artefact from aggregation of proteins and nucleic acids arising during preparation, a notion supported by the variability of results depending on the extraction procedure (Stuurman, 1991; de Jong, 1996).

Nonetheless, even though the structural proteins that polymerize to give rise to the filamentous nuclear network collectively termed the nuclear matrix, are not clearly identified, there remains evidence supporting the existence of a nuclear scaffold. Comparisons of the number and distribution of various nuclear components, labelled with specific probes, before and after the extraction procedure show that both variables remain unchanged despite the harsh conditions employed during the isolation method (Nickerson *et al.*, 1995). In addition, nuclear structures, such as nuclear bodies linked to cellular changes in promyelocytic leukemia (PML bodies), that appear prominent *in situ*, are part of this nuclear scaffold (Stuurman *et al.*, 1991;

Dent *et al.*, 1996). Studies showing that the fibrillar centers of nucleoli are anchored to the nuclear matrix also strengthen the concept of the presence of a nuclear, structural skeleton (Dundr and Raska, 1993; Hozak, 1996).

Finally, additional evidence comes from the field of biochemistry according to which actin is a component of the nuclear matrix. Actin has been identified as a proteinaceous component in the matrix from nuclei of amphibian oocytes (Clark and Rosenbau, 1979), of marine green algae (Tischendorf *et al.*, 1987) and of insect cells (Henderson and Locke, 1992). Even though actin was argued to appear as part of the nuclear matrix only as a result of cytoplasmic contamination during the isolation procedure, this view was challenged by studies that showed nuclear actin to be unique because of a markedly more acidic isoelectric point than its cytoplasmic counterpart (Bremer *et al.*, 1981; Kumar *et al.*, 1984). The uniqueness of nuclear actin was further demonstrated by immunocytochemical findings according to which neuronal, nuclear actin is antigenically distinct from the cytoplasmic isoforms and is more closely related to the alpha sarcomeric isoform (Milankov *et al.*, 1991). The functional significance of nuclear actin as a nuclear matrix component is discussed in the following section.

ASSOCIATION OF SPATIAL ORGANIZATION OF THE INTERPHASE NUCLEUS WITH NUCLEAR FUNCTION

Functional significance of non-chromatin components

Traditionally, the interphase nucleus was viewed as a membrane-bound reaction chamber in which interactions between molecules were regulated solely by the laws of mass action and diffusion (Park and De Boni, 1999). In contrast, the interphase nucleus is emerging as a

topologically organized, 3-D structure with its spatial topology proposed to reflect compartmentalization of nuclear function.

The structural entities within the interphase nucleus including the nucleolus, the nuclear matrix and the chromosome territories (all discussed above), are proposed to interact with DNA or RNA in order to serve specific functional roles in processes such as transcription, splicing, mRNA transport and repair (Spector, 1993; Park and De Boni, 1999). Studies employing a variety of labelling protocols suggest that the nuclear machinery required for the various nuclear functions is localized in specific domains, further supporting the notion of a functionally compartmentalized interphase nucleus. This section provides a summary of evidence which outlines the functional significance of the nucleolus, nuclear matrix, nuclear pore complexes and interchromatin channels, how they interact with both chromosomal and non-chromosomal components and how these interactions translate to nuclear functions.

The nucleolus

Nucleolar organization is proposed to affect the spatial organization of chromatin domains in the interphase nucleus (Comings, 1968; Manuelidis, 1984a; 1984b; Hochstrasser and Sedat, 1987). Centromeric domains have been shown to occupy reproducible, cell-type specific positions at the nucleolar periphery and have been suggested to represent the acrocentric NOR-bearing chromosomes (Haaf and Schmid, 1989; Billia and De Boni, 1991). In human cells, heterochromatic parts of chromosomes, including the Y chromosome that contains no rRNA genes, are also reproducibly localized at the nucleolar region (Borden and Manuelidis, 1988).

Moreover, as stated above for both murine and human neuronal cells, NORs are found on more than one chromosome. This, along with the fact that there is a single nucleolus in these

cells, has led to the suggestion that these chromosomes arrange themselves by extending their NORs towards the nucleolus (Goessens, 1984). Taking into consideration that neuronal cells have been shown to exhibit more than one nucleolus at young, immature stages, the localization of all NORs on the single nucleolus at the fully differentiated state could result from the fusion of multiple nucleoli. Such a phenomenon has been reported to occur during the *in vitro* differentiation of dorsal root ganglion neurons (Park and De Boni, 1992). The grouping of all rRNA genes in the fibrillar center of the nucleolus has been proposed to provide a functional advantage arising from the accumulation of transcriptional factors and others involved in RNA processing (see below) (Park and De Boni, 1999).

Finally, in higher order eukaryotes, nucleoli have been shown to be associated with the nuclear envelope either via their peripheral positioning or via large invaginations of the nuclear envelope (Dupuy-Coin *et al.*, 1986; Fricker *et al.*, 1997). This association has been suggested to facilitate nucleocytoplasmic transport of nucleolar products (Bourgeois *et al.*, 1979).

Nuclear matrix

As stated above, the proposed role for the nuclear matrix is analogous to that of the cytoskeleton. However, the nuclear matrix is also proposed to have a multi-functional role in providing a scaffold for chromosome territories (van der Valden and Wanka, 1987; Bekkers *et al.*, 1986), DNA replication and transcription, presumably at the level of the inter-chromatin channels (Cremer *et al.*, 1993; Zirbel *et al.*, 1993; Cremer *et al.*, 1996) and RNA processing (van der Valden and Wanka, 1987; Verheijen *et al.*, 1988).

Specific DNA sequences, known as matrix attachment regions (MARs) have been shown to associate with the matrix (Gasser and Laemmli, 1986) and are proposed to anchor

chromosomal loops to the nuclear matrix (Mirkovitch *et al.*, 1984; Cockerill and Garrard, 1986). Notably, the dynamic nature of the nuclear matrix is demonstrated in *Physarum* by the fact that transition to metaphase is characterized by a transformation of the nuclear skeleton to form the metaphase chromosomal scaffold (Bekers, 1981).

In addition, evidence exists providing a functional link between the nuclear matrix and transcription. Specifically, the matrix is suggested to activate transcription via an association of DNA with the matrix, an association that is further proposed to be species specific. Specifically, when transcription is stimulated by estrogen in chick oviducts, there is a selective, hormone-activated association of the ovalbumin gene with the matrix (Robinson *et al.*, 1983). Also, following the *de novo* activation of the vitellogenin gene via estrogen administration in *Xenopus laevis*, the promoter region of the B2 vitellogenin gene, the estrogen receptor protein involved and the unspliced vitellogenin mRNA have all been shown to be associated with the nuclear matrix, indicating that this association precedes the transcription of this gene (Thorburn and Knowland, 1993).

Given such findings, the nuclear matrix is suggested to be a transcriptionally competent site (Jackson *et al.*, 1981; Berezney, 1984; Smith and Rothblum, 1987; Zhao *et al.*, 1993; Thompson *et al.*, 1994), a view further supported by studies that show an association with the matrix of RNA polymerase II, and of nascent mRNA in cells pulse labelled with tritiated uridine (Jackson *et al.*, 1981; 1986; 1991). In addition, specific genes and gene clusters are flanked by boundaries of matrix attachment regions (Mirkovitch *et al.*, 1984; Jarman and Higgs, 1988; Phi-Van *et al.*, 1990), regions that are proposed to facilitate the allignment of genes to matrix components that contain transcriptional machinery (Boulikas, 1995).

The nuclear matrix is also implicated in splicing of newly formed mRNA due to its demonstrated association with spliceosome complexes (Smith *et al.*, 1989), heterogenous nuclear RNA, small nuclear RNA and splicing intermediates (Van Eekelen and Van Venrooij, 1981; Nakayasu *et al.*, 1982; Long and Och, 1983). Furthermore, Lawrence *et al.*, (1989) have proposed that the matrix is involved in the nucleocytoplasmic transport of nascent mRNA by providing "pathways", visualized by *in situ* hybridization.

The actin found associated with the nuclear matrix has been proposed to be involved in modifying chromatin architecture (Scheer *et al.*, 1984), in nuclear transport mechanisms (Ueyama *et al.*, 1987) and also to act as an initiation factor in transcription (Ankenbauer *et al.*, 1989). Moreover, nuclear actin has been suggested to be a component of a motor responsible for chromatin motion (Milankov and De Boni, 1993; De Boni, 1994). Specifically, chromatin motion, defined as the rearrangement of chromatin components, is proposed to be taking place via an acto-myosin contractile mode (De Boni, 1994). This view is supported by studies that show a fraction of the nuclear actin to exist in a filamentous form (Amankwah and De Boni, 1994) and by the presence of an isoform of myosin in the nucleus, antigenically related to myosin I (Rimm and Pollard, 1989; Milankov and De Boni, 1993). In fact, nuclear myosin has been shown to be myosin I beta, unique to the nucleus (Dr. P. Hozak, *personal commun.*)

Evidence exists to show that in neurons, nuclear components such as nucleoli and chromosomes undergo motion during interphase (De Boni and Mintz, 1986; Holowacz and De Boni, 1991). This evidence, along with the presence of a contractile mechanism acting as a driving force for the mobilization of nuclear components and the association of these components to the nuclear matrix, points towards a dynamic nuclear structural organization (De Boni, 1994). Such an organization is proposed to accommodate the alignment of transcribed

genes with transcriptionally competent sites, nascent mRNA with the appropriate processing compartments and eventually spliced mRNA with the nuclear pores for export to the cytoplasm (Cremer *et al.*, 1996).

Splicing of pre-mRNA

Splicing reactions are mediated by heterogeneous macromolecular complexes, termed spliceosomes, via interactions with pre-mRNA whereas the specificity of these reactions is directed by RNA flanking the exon and intron borders (Rymond and Rosbach, 1992). Spliceosomes consist of small nuclear ribonucleoproteins (snRNPs) and have been demonstrated to participate in RNA metabolism (Baserga and Steitz, 1993). Besides snRNPS, additional spliceosomes' components include a large number of proteins, certain enzymes (Ruskin and Green, 1985; Query *et al.*, 1994) and a collection of auxiliary factors that associate with the spliceosome in a stage-specific manner mediating recognition of splice sites (reviewed in Park and De Boni, 1999). Splicing factor protein (SF2) (Krainer *et al.*, 1990a; 1990b) and the spliceosome component protein (SC35) are examples of auxilliary factors, rich in serine and arginine, suggested to play a role in the commitment of the RNA to the splicing pathway by binding to pre-mRNA and recruiting additional splicing factors (Wu and Maniatis, 1993; Kohtz *et al.*, 1994).

Splicing factors are concentrated in discrete foci within the nucleus referred to as speckles (Lerner *et al.*, 1981). In support of the hypothesis that speckles are functional sites of splicing, it has to be shown that they contain all the necessary molecular factors involved in the production of mature mRNA. However, there is controversy regarding the actual role of speckles in splicing reactions (reviewed in Park and De Boni, 1999). In support of the prevailing

view, speckles are shown to contain certain required splicing factors and to be in close spatial association with active sequences. These findings propose that speckles may potentially represent functional nuclear compartments (Xing *et al.*, 1993; 1995).

The compartmentalization of splicing machinery at specific sites, represented in mammalian nuclei by approximately 20-40 distinct foci, presents evidence pointing towards the localization of this process to these sites (Lawerence *et al.*, 1989; Xing *et al.*, 1993). In addition, the dispersion of these speckles during mitosis, when levels of transcription are low, along with their reassembly once mitosis is over, further strengthen the compartmentalization of splicing in speckles (Leser *et al.*, 1989; Spector *et al.*, 1990; Ferreira *et al.*, 1994). Results from a number of studies employing immunocytochemistry and FISH to components of splicing machinery have also strengthened the notion that speckles are indeed functional splicing sites. Specifically, the speckled distribution pattern of major snRNPs paralleled the distribution of the Sm proteins with which they associate during splicing (Carmo-Fonseca *et al.*, 1992; Huang and Spector, 1992; Matera and Ward, 1993; Visa *et al.*, 1993). The localization of intron-containing RNA microinjected into nuclei at these speckles further strengthens the notion of their functional significance (Wang *et al.*, 1991).

The spatial coupling of splicing and transcription also points towards a splicing function in speckles. A hyperphosphorylated form of RNA polymerase II has been shown to immunoprecipitate with splicing factors (Mortillaro *et al.*, 1996; Yuryev *et al.*, 1996; Du and Warren, 1997), while in mammalian nuclei labelling of intron sequences and intron-exon junctions has demonstrated that nascent mRNA is found spatially associated with transcription sites (Zhang *et al.*, 1994; Huang and Spector, 1996). Furthermore, poly-A RNA, the majority of which represents pre-mRNA (Harpold *et al.*, 1981), has been shown to be distributed in 20-40

specific nuclear sites (Carter *et al.*, 1991; 1993) termed "transcription domains". Notably, this distribution is paralleled by the speckled distribution of Sm proteins and SC35 domains (Carter *et al.*, 1991; 1993). These findings, along with a demonstrated association of actively transcribed sequences with the periphery of SC35 (Xing *et al.*, 1995) point toward a spatial co-localization of active genes and splicing speckles. The latter is also supported by the demonstrated colocalization of DNase sensitive domains with snRNPs in PC12 cells (Park and De Boni, 1996).

Collectively all the findings described, thus far, propose that transcription of DNA sequences occurs peripherally to the speckles, thus, facilitating splicing (Clemson and Lawrence, 1996). However, until more active genes are shown to localize at the sites of speckles, the above model cannot be verified. Furthermore, the concept that these sites may merely represent storage and assembly pools for the splicing machinery renders the issue of functional significance of speckles controversial.

Specifically, even though several studies have identified a number of splicing factors associated with speckles, there are other members of the splicing machinery for which such an association has not been established. These include auxiliary factors required for spliceosome assembly (Zamore and Green, 1991) and SC35, which does not always colocalize with snRNPs (Sahlas *et al.*, 1993). In addition coiled bodies, once proposed to represent transcription/splicing sites due to the presence of snRNPS, genes and Sm antigens (Lamond and Carmo-Fonseca, 1993; Frey and Matera, 1995), have also been shown to lack additional splicing factors (Carmo-Fonseca et al., 1992; Huang and Spector, 1992; 1996).

According to the alternative view, speckles represent sites of storage/assembly of splicing machinery and splicing takes place diffusely, independantly from speckles (Spector, 1993; Carmo-Fonseca *et al.*, 1996). Thus, instead of sites of transcription, speckles have been proposed

to be storage pools and assembly sites of splicing factors represented by a diffuse pool of splicing machinery (Jimenez-Garcia and Spector, 1993). If this is the case, it is suggested that speckles are located in near proximity of transcription sites so that upon demand soluble splicing factors can be recruited by active genes (Misteli and Spector, 1997). In support of this, gene activation in polytene chromosomes of *Chironomus tentans* leads to the recruitment of splicing factors to the site of transcription. These factors appear as puffs that disappear upon completion of transcription (Bauren *et al.*, 1996). Notably, the strongest evidence in support of the model that speckles are involved in storage and assembly of splicing machinery comes from experiments in live viral-infected cells, in which localization of the alternative splicing factor, fused to green fluorescent protein (GFP), was monitored (Misteli *et al.*, 1997). In these cells, observed live, transcriptional activation of the viral genome was accompanied by an actual morphological projection of splicing factors from nearby speckles to the transcription site.

Thus, it is evident that the exact functional role of speckles remains unclear along with the question of whether the observed topological organization of certain nuclear factors indeed reflects compartmentalization of nuclear function.

Chromatin domains and their rearrangements

As previously stated, the Rabl model provided the first piece of evidence indicating that chromatin in interphase exhibits a higher-order, specific topological arrangement (Rabl, 1885). Results from more recent studies in a variety of cells have shown that a diversity exists in chromatin arrangement. Nuclei that exhibit the Rabl model include the polytene nuclei of salivary gland cells in Drosophila (Hochstrasser and Sedat, 1987a; 1987b) and the interphase

nuclei of plant cells such as rye, barley and oat (Dong and Jiang, 1998). In contrast, in the same study, nuclei of sorghum, rice and maize exhibited a non-Rabl arrangement, in which both centromeres and telomeres were dispersed throughout the nucleus.

Labeling of individual chromosomes, via chromosome painting, (Pinkel *et al.*, 1986; Borden and Manuelidis, 1988; Cremer *et al.*, 1988; Hilliker and Appels, 1989) has shown that chromosomes occupy compact, non-overlapping domains whose position is reproducible and cell-type specific (Manuelidis, 1985b; Borden and Manuelidis, 1988). Labeling of the non-transcribed, centromeric, sDNA sequences, via *in situ* hybridization, has shown that these sequences also exhibit a cell-type specific arrangement in interphase nuclei (Rae and Franke, 1972; Moroi *et al.*, 1981; Manuelidis, 1982; 1984a; 1985a; Chaly and Brown, 1988; Joseph *et al.*, 1989; Haaf and Schmid, 1989; Masumoto *et al.*, 1989a; 1989b; Manuelidis and Borden, 1988; Billia and De Boni, 1991; Holowacz and De Boni, 1991; Haaf and Schmid, 1991). Finally, telomeric DNA has also been shown to exhibit reproducible, distinct intranuclear sites (Mathog *et al.*, 1984; Hochstrasser *et al.*, 1986; Katsumata and Lo, 1988; Rawlins and Shaw, 1990a; 1990b; Billia and De Boni, 1991).

Given the cell-type specific nature of the spatial topology in interphase nuclei, especially in fully differentiated neurons, it can be postulated that the establishment of the adult topology takes place during differentiation and is associated with the functional commitment of the cell (Manuelidis, 1984a; Park and De Boni 1999). Furthermore, evidence exists to show motion, during interphase, of various nuclear components including nucleoli (De Boni and Mintz, 1986), nuclear matrix components, coiled bodies (Janevski *et al.*, 1997) and other DNA containing domains. This motion has been proposed to be accomplished via a nuclear acto-myosin motor, for which evidence exists, leading to the postulate that such motion serves gene expression by

placing specific chromatin domains into transcriptionally competent nuclear sites (De Boni, 1994).

This premise proposes that the spatial topology of the interphase nucleus has a dynamic nature, dependent on the differentiation state and/or cell function (Park and De Boni, 1999). Such a dynamic nature has been demonstrated by the alterations in the cell-specific patterns of nuclear topology which accompany pathological states, development and changes in gene expression. Pioneering work by Borden and Manuelidis (1988) showed that the spatial position of the X chromosome in nuclei of human cerebral cortical neurons from epileptic seizure foci is different in comparison to the nuclei from adjacent regions. Specifically, the X chromosome was shown to relocate from the nuclear periphery in normal neurons to a more central position in those from the seizure foci. Differences in spatial nuclear topology have also been shown to exist between normal and cancer cells (Haaf and Schmid, 1989; Tagawa *et al.*, 1997).

In studies which employed physiological stimuli, a redistribution of chromatin domains has been demonstrated in murine, dorsal root ganglion neurons upon exposure to gamma-aminobutyric acid (GABA) (Holowacz and De Boni, 1991), in hepatocytes of Xenopus laevis following *de novo* activation of vitellogenin genes upon estrogen stimulation (Janevski *et al.*, 1995) and in hippocampal neurons undergoing long term potentiation (Billia *et al.*, 1992). Long-term potentiation has been shown to be associated with altered gene expression (Cole *et al.*, 1989), *de novo* protein production (Abraham and Otani, 1989) and RNA synthesis (Goelet *et al.*, 1986). Moreover, altered patterns of clustering of sDNA sequences have been reported as one type of rearrangement of chromatin domains in certain cells (Billia *et al.*, 1991; Janevski *et al.*, 1995; Carmo-Fonseca *et al.*, 1996).

Furthermore, there is evidence pointing towards changes in the spatial topology of chromatin domains during the course of cell differentiation (Manuelidis, 1984a). Specifically, in dorsal root ganglion neurons, nucleolar domains have been shown to relocate to spatially restricted territories during *in vitro* differentiation (Park and De Boni, 1991). Also, a redistribution and clustering of centromeric domains along with fusion of nucleoli have been linked to *in vitro* differentiation of sensory neurons (Park and De Boni, 1992; Choh and De Boni, 1996).

Studies have shown that changes in gene expression are accompanied by changes in the spatial organization of both DNase sensitive domains and speckles, compartments that have been proposed to be transcriptionally competent. Specifically, DNase sensitive domains have been shown to undergo a change in their spatial distribution following growth-factor induced changes in cell function and under "reverse transformation" of cancer cells mediated by secondary messenger analogues (Hutchison and Weintraub, 1985; De Graaf *et al.*, 1990; Krystosek and Puck, 1990). In addition, both snRNPs and DNase sensitive domains are relocated into the form of a 3-D shell at the nuclear periphery following nerve growth factor (NGF)-induced differentiation of PC12 cells, whereas in the non-transformed cells they are both localized throughout the nucleus (Sahlas *et al.*, 1993; Park and De Boni, 1996). This change in spatial distribution into the shell is temporally associated with the upregulation of genes such as the neurofilament light chain (Park and De Boni, 1996).

In addition, an association between an active sequence and DNase sensitive domains has recently been demonstrated in breast cancer cells. Specifically, it was shown in these cells that chromosome 17 exhibits a specific conformation that results in the placement of an active sequence of this chromosome, ERBB-2, towards the nuclear periphery, and, as colabelling of

DNase sensitive domains showed, into a DNase sensitive domain (Park and De Boni, 1998). Furthermore, the existence of a specific, spatial organization at the level of a single chromosome territory associated with gene expression is demonstrated by a recent study by Vershure *et al.*, (1999). In this study, nascent RNA was immunolabelled and chromosome territories were visualized by FISH in human female fibroblasts. Results show that transcriptionally active chromatin is compartmentalized within the chromosome territories with active genes found predominantly at or near the surface of the territories while nascent RNA extends into the interchromatin space.

PURKINJE NEURONS

Overview

When observing the structure of the cerebellum, one is immediately struck by the apparently para-crystalline nature of its anatomical organization that is, in turn, characterized by a highly specific and uniform laminar arrangement and microcircuity (Middleton and Strick, 1998). These features have rendered the cerebellum an ideal system for the study of CNS development, and results from developmental studies have provided valuable insight in the developmental mechanisms involved in the orderly assembly of the nervous system such as cell lineage, migration, formation of topographic maps, target-dependent cell death, axon projection, etc.

This part of the review of the literature provides a summary of the main events in cerebellar development with an emphasis placed on the central player of the cerebellar microcircuitry, the Purkinje cell (PC). The first section deals with cerebellar anatomy and function whereas the second section provides an overview of cerebellar development focusing on all of the cerebellar cells except the PC. Understanding the environment within which the PC operates from an anatomical, functional and developmental perspective is of key importance in understanding the anatomy, function and development of the PC itself. Sections three and four deal with a detailed analysis of the migration and development of the PC, respectively, whereas the fifth section provides a summary of changes in gene expression in PCs as a function of postnatal development. The sixth section refers to the controversial issue of PC polyploidy and contrasts the results from studies representing both views, i.e., diploidy vs. polyploidy.

The last section, abnormal cerebellar development, provides a detailed description of the *staggerer* mutant, regarding a proposal for future work, which may be undertaken to enhance the

further understanding of a potential association between spatial nuclear organization and control of gene expression.

Cerebellum: anatomy and function

The distinguishing feature of brain cells is the ability of groups of neurons to produce behaviour in the functional brain, a feature dependant on development and neuronal integrative properties (Middleton and Strick, 1998). The cerebellum (little brain) represents the system of choice for studying neuronal development (1700-1900 publications per year) during the last 4 decades. Results from these studies also strongly propose a role for the cerebellum in both motor and cognitive processes.

In general terms, the cerebellum, operating entirely at a subconscious level, compares intent and performance with regard to muscular activity and makes certain that any movement is accurate, smooth and coordinated with appropriate force and direction (McClintic, 1985). This is accomplished via error control, damping the tendency for pendular motion and calculating when a motion should be slowed down and stopped. Thus, the cerebellum acts as the overseer for coordination and ultimate adjustor of movement (McClintic, 1985).

Regarding its anatomy, the cerebellum is located on the posterior aspect of the brainstem and consists of two hemispheres with the vermis located between (Voogd and Glickstein, 1998). Each hemisphere is further divided into three lobes, anterior, middle and posterior or flocculo-nodular, each exhibiting a specific set of connections and functions with some overlap (McClintic, 1985). The cerebellar surface is characterized by convolutions with folds, termed folia, that provide an increased surface area for neuron placement (McClintic, 1985). The outer surface portion of each folium is a layer of gray matter, the cerebellar cortex, deeper to which

lies an internal core of white matter that is, in turn, overlying the three cerebellar, deep nuclei, the fastigial, the interposed and the dentate nucleus (McClintic, 1985).

The cerebellar cortex contains the circuitry responsible for the cerebellar functions and is organized in three layers, an organization common to all cerebellar parts (Fig. 3). These layers, from outer to inner, include the molecular layer (stellate and basket cells), the PC layer and the granule cell layer (Voogd and Glickstein, 1998). The stellate and basket cells are GABAergic interneurons that provide feed-forward inhibition to PCs whereas Golgi cells, another type of inhibitory interneuron found between the molecular and PC layers, provide feed-backward inhibition to granule cells (Voogd and Glickstein, 1998). Granule cells are small, glutamatergic neurons whose unmyelinated axons, the parallel fibers, project upwards towards the molecular layer where they bifurcate and synapse with the distal spines of the Purkinje dendrites (Voogd and Glickstein, 1998). PCs are large, GABAergic neurons arranged in a single layer between the molecular and granule layers (Voogd and Glickstein, 1998). These cells are characterized by their dendritic arborization that extends towards the molecular layer in a fan-like fashion and in a single plane across the folia perpendicular to the parallel fibers (McClintic, 1985; Voogd and Glickstein, 1998). The single axon of PCs synapses with the deep seated cerebellar nuclei (Voogd and Glickstein, 1998). The final cell type found in the cortex is the Bergmann glia whose cell bodies are located among PCs and their pallisades extend into the molecular layer (Voogd and Glickstein, 1998).

Regarding its functional anatomy, the cerebellum operates in sets of 3's (Teyler, 1999). There are 3 main inputs, 3 main outputs from 3 deep nuclei and 3 highways via which information enters and exits the cerebellum (Teyler, 1999).

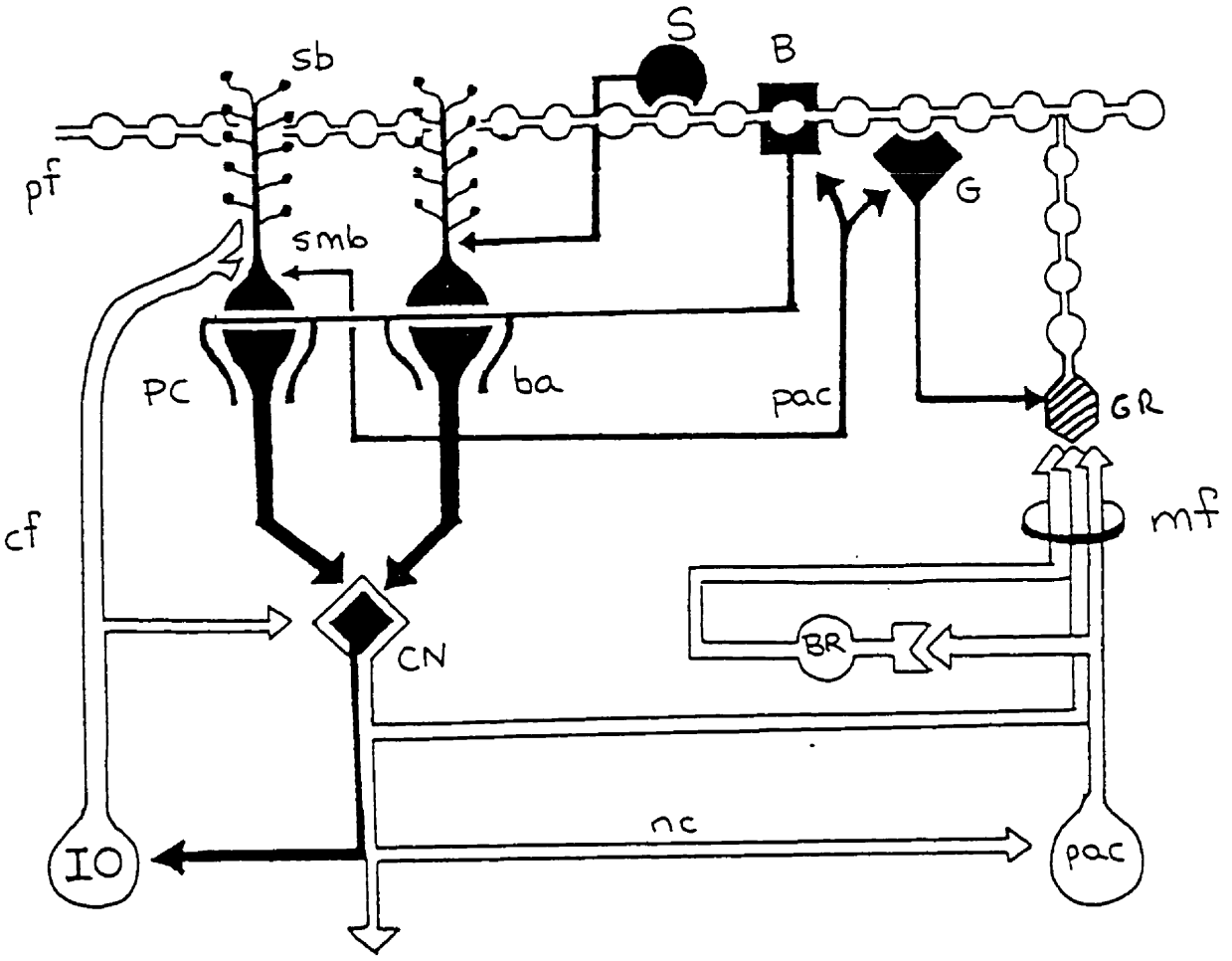

Figure 3: Schematic representation of the cerebellar circuitry, showing inputs to and outputs from cerebellar cells . Inhibitory interneurones are shown in black.

B, basket cell; ba, basket terminal; bb, efferent basal bundle; cf, climbing fiber; CN, cerebellar nuclei; G, Golgi cell; IO, inferior olive; nc, collateral of nuclear relay cell; pac, Purkinje-cell axon collateral; PC, Purkinje cell; S, stellate cell; smb, proximal smooth branches; mf, mossy fiber; sb, spiny branchlets; BR. brush cells; GR, granule cell; pf, parallel fiber. (Adapted from Voogd and Glickstein, 1998)

The three inputs include the mossy fibers from the spinocerebellar pathways and the pons that synapse with the granule cells, and the climbing fibers originating exclusively from the inferior olive that synapse directly with the smooth, proximal branches of the Purkinje dendritic arbor (Teyler, 1999). Thus, the PC receives input directly from the climbing fibers but indirectly from the mossy fibers via the granule cells (Teyler, 1999). There is a significant difference in the convergence ratios of parallel (100,000:1) and climbing (1:1) fibers onto PCs (Houk *et al.*, 1999). Climbing fibers also reach the other cerebellar cells including the deep nuclei. All input to the cerebellum is excitatory but the sole cortical output from the PCs to the deep nuclei is invariably inhibitory and ultimately all output from the deep nuclei to the cortex is excitatory (Teyler, 1999). Thus, PCs help refine and control movement by providing a waxing and waning inhibitory effect on the deep nuclei that are already excited by cerebral cortical and peripheral information (Teyler, 1999). The three main outputs originate from the fastigial, interposed and dentate nuclei and the three highways are the inferior, middle and superior penducles (Teyler, 1999).

In addition to coordination of goal-directed/spontaneous movement, the cerebellum has been proposed to be involved, at least partly, in motor learning and adaptive plasticity (Ito, 1984). The mechanism suggested to facilitate such an involvement is Long-Term Depression (LTD) of synaptic transmission at the point of parallel fiber-PC synapse, a form of synaptic, physiological plasticity (Daniel *et al.*, 1998). LTD along with other forms of PC synaptic plasticity are part of a negative feedback loop acting at a local level to prevent PCs from being overstimulated by parallel fiber input (De Schutter, 1995). LTD occurs when coincident signals along parallel and climbing fibers arrive at the PC and the role attributed to the climbing fiber input is the timely generation of an intracellular Ca^{2+} transient in Purkinje dendrites, an event

necessary for the activation of a molecular cascade that eventually results in depression of coincidentally active parallel fiber synapses (Strata and Rossi, 1998). Despite the fact that climbing fibers have been shown to undergo dynamic anatomic rearrangements that might enable them to participate in physiological plasticity there is still no clear evidence that this is indeed the case (Strata and Rossi, 1998).

Cerebellar development

The cerebellum has many traits that render it an excellent model for the study of neuronal development. It is overall a relatively simple system with its developmental program characterized well enough to allow the study of events such as cellular interactions, pattern formation and synaptic formation and stabilization.

The cerebellum arises from the alar plate of the neural tube and has a dual, mesencephalic-metencephalic origin as demonstrated from the results of chick-quail chimera systems (Goldowitz and Hamre, 1998; Baader *et al.*, 1998). All cerebellar cells originate from a germinal matrix region, bounded by the isthmus anteriorly and the choroid plexus posteriorly, that consists of two germinal zones, the neuroepithelial ventricular zone and the more caudally located rhombic lip (Goldowitz and Hamre, 1998). The deep cerebellar nuclei, eventually settling deep in the cortex, are the first neurons to exit the ventricular zone (E10-E12) followed by the PCs that undergo their last mitosis and exit the neuroepithelial zone by E13 (Yuasa *et al.*, 1991; Goldowitz and Hamre, 1998). By E13 the rhombic lip gives rise to the external granular layer (EGL) whose cells migrate towards the cerebellar surface while Golgi neurons are born from the diminishing ventricular zone (Goldowitz and Hamre, 1998). Postnatally, the EGL gives rise to the granule neurons that will migrate in an inward fashion to finally settle in the internal

granular layer (IGL) below the PC layer (Goldowitz and Hamre, 1998). Concomitantly with the seeding of the IGL, the stellate and basket cells of the molecular layer are born (Goldowitz and Hamre, 1998). Regarding the generation of these interneurons, results from chimeric systems show that it is a two-way process with an initial birth taking place in the ventricular zone followed by migration to the white matter of the cortex where they undergo further mitotic events before finally settling to the molecular layer (Zhang and Goldman, 1996).

It is during the inward migration of the granule neurons that the cerebellum starts assuming its adult shape with deep fissures and folia (Goldowitz and Hamre, 1998). The EGL is completely diminished by the end of the third postnatal week at which point synaptogenesis between the climbing fibers of the inferior olive and the PCs, and between the spinoreticular mossy fibers and granule cells, is also close to the apex of differentiation (Goldowitz and Hamre, 1998).

Regarding the regulation of neuron number in the cerebellum, it appears that PCs determine the size of the granule cell population, thus, maintaining a tight ratio of PCs to granule cells (Crossley and Martin, 1995). A number of possible mechanisms have been proposed to function in the formation of this tight ratio, including the removal of trophic factors resulting in cell death and the inhibition of mitosis (Goldowitz and Hamre, 1998). The timeframe of this regulation appears to coincide with the seeding of the IGL, with PCs controlling the mitotic activity of granule cell neuroblasts within the EGL as the latter appears to inform the PCs of the size of the mitotically active population (Smeyne *et al.*, 1995). Specifically, in this study, the ablation of PCs in transgenic mice resulted in the thinning of the overlying EGL and a selective loss of proliferative cells (Smeyne *et al.*, 1995). The PC-derived Sonic Hedgehog (Shh) is the signaling molecule proposed to control the proliferation of neuroblasts in the EGL via action on

genes such as Patched (Ptc) and Gli 1, expressed by EGL cells (Wallace, 1999). PCs have also been implicated in the developmental regulation of granule cell specific proteins such as "parallin" located on the parallel fibers, whose expression levels appear to depend on the presence of PCs. In fact, in the *staggerer* and *purkinje cell degeneration (pcd)* mutants which are characterized by loss of PCs, parallin cannot be detected (Smith and Mullen, 1997).

In addition, the establishment of migration patterns is essential for the proper assembly of the nervous system and the migration of the cerebellar cells has provided valuable insight for the mechanisms behind neuronal migration. The first migratory events include the exit of the deep cerebellar nuclei and PCs and it appears that this initial migration is essential since it defines the future boundaries of the cerebellum (Goldowitz and Hamre, 1998). Mutants of genes encoding for Netrin, a molecule implicated in neuronal migration, and its receptor Unc5H3 exhibit an ectopic migration and settling of granule and Purkinje neurons all the way to the inferior colliculus and hindbrain (Goldowitz and Hamre, 1998). The inward migration of granule neurons is presumed to be mediated partly by radial glial fibers, since upon distortion and atrophy of the radial glia both the survival and the migration of the granule cells are severely affected (Rakic and Sidman, 1973; Ross *et al.*, 1990).

Additional molecules that appear to play a role in neuronal migration in cerebellar development include *reelin*, an extra-cellular matrix molecule and *disabled,* a tyrosine kinase signaling adaptor molecule (Goldowitz and Hamre, 1998). R*eeler* and *scrambler* mutants, in which the expression of these molecules is altered, are also characterized by altered migration patterns of PCs and severely compromised numbers of granule cells (Goffinet *et al.*, 1984; Goldowitz *et al.*, 1997).

Furthermore, a number of studies suggest that lineage plays an important role in cerebellar development along with environmental factors (Herrup *et al.*, 1984). Mathis *et al.*, (1997), using a novel cell-marking construct, showed that all cerebellar neurons, except granule neurons that arise from the rhombic lip, are clonally related and ongoing research is aimed at the cellular interactions and molecules that determine commitment to each lineage.

Finally, regarding the early molecular events involved in cerebellar development, most of the information about the key genes is coming from the study of naturally occurring mutated genes and null mutations of other genes. The formation of the anatomical and molecular compartmentalization of the adult cerebellum along both the rostrocaudal and mediolateral axes has a strong genetic component and the two segmentation genes that appear to be of key importance are *en*-1 and *en*-2, expressed by the isthmus, the midhindbrain junction that gives rise to the cerebellum (Millen *et al.*, 1994; Kuemerle *et al.*, 1997; Baader *et al.*, 1998;). A null mutation of *en*-1 results in the deletion of the cerebellar primordium at E9 (Wurst *et al.*, 1994) while the one of *en*-2 has more subtle effects on cerebellar development (Millen *et al.*, 1994). Specifically, elimination of *en*-2 results in a general developmental delay including a delay in the fusion of the cerebellar rudiments at the midline. Additional effects include abnormal formation of specific fissures with the posterior region greatly affected, altered transgene expression and a uniform 30-40% decrease in the cells of the olivocerebellar circuit (Millen *et al.*, 1994; Kuemerle *et al.*, 1997). Ectopic expression of *en*-2 by PCs resulted in a 40% reduction in PC number uniformly across the mediolateral axis and a subtle effect on sagittal banding, with the cells residing in the fissures being the most sensitive. This sensitivity extended to alterations in cellular interactions required for the formation of EGL (Baader *et al.*, 1998).

Results from these studies have lead to the double-patterning hypothesis according to which there are two levels of action of the *en* genes in cerebellar patterning (Kuemerle *et al.*, 1997). The first patterning event occurs prior to the bulk of neurogenesis (E8-E10) and establishes the cerebellar field and the precursors of the cerebellar cells. This initial patterning is then lost as demonstrated by the extensive cell mixing occurring during cortical development, and once neurogenesis is complete, a second patterning event takes place that establishes the size and shape of the folia and the sagittal bands (Kuemerle *et al.*, 1997).

Purkinje cell migration

During the course of CNS development, neuroblasts generated from the ventricular neuroepithelia start migrating towards their destined locations once they undergo their last division (Yuasa *et al.*, 1991). In the murine cerebellum, PC precursors complete their final mitosis between E11 and E13 (Miale and Sidman, 1961; Inouye and Murakami, 1980). Specifically, there is a latero-medial gradient in the time of origin: PCs born on E11 and E12 end up in the paravermian and hemispheric regions, whereas cells born at E12 and E13 end up in the vermis (Inouye and Murakami, 1980). Thus, postnatally, early developing regions may have received many of later born PCs (Inouye and Murakami, 1980).

The clonal nature of PCs and the determination of the size of their precursors' pool have been the focus of many studies considering the fact that lineage has long been recognized as one of the mechanisms in CNS development. Initial studies using *lurcher*-wild type aggregation chimeras indicated that the entire PC population arises from a rather limited number of progenitor cells, namely, 8 (Wetts and Herrup, 1982; Herrup *et al.*, 1984; Herrup, 1993). Recent studies, however, using X-inactivation mosaics, laacZ-lacZ recombinant mosaics and embryonic

stem cells chimeras have shown independently that the initial pool consists of approximately 80 cells per half cerebellum (Baader, *et al.*, 1996; Mathis, 1997; Hawkes, *et al.*, 1998). Overall, these studies have demonstrated that this number of precursor cells generates clonally related PC groups, each of which contributes to the rostrocaudal spectrum of the cerebellum. However, this contribution is rather constrained in the mediolateral axis suggesting that there is no agreement between PC lineage and the compartmentalization seen in adult mice (Baader *et al.*, 1996; Hawkes *et al.*, 1998). Both the initial and the more recent studies, however, agree on the timeframe of commitment which, for PCs, occurs before their last division during the neural plate to neural fold stage (Wetts and Herrup, 1982; Mathis, 1997).

Regarding their mode of migration, PCs have been shown to migrate radially from the neuroepithelium of the fourth ventricle to the cortical surface between E13 and E18, towards the end of murine gestation (Yuasa *et al.*, 1991). At E13 most of the PCs are found in the subventricular zone with a few having already migrated to the intermediate zone and even fewer to the caudal half of the primordial cortical region (Yuasa *et al.*, 1991). At E14, PCs are found in both zones with an increasing number in the intermediate zone and the caudal half of the primordial cortical layer (Yuasa *et al.*, 1991). As migration continues, at E15 the number of migratory cells originating from the lateral half of the neuroepithelium is still higher in the intermediate and cortical zones of the caudal half (Yuasa *et al.*, 1991). At E16, PCs from the lateral half have reached the cortex while the ones from the medial half are still found in the intermediate zone (Yuasa *et al.*, 1991). By E18, all PCs have reached the cortex where they are arranged in several layers (Yuasa *et al.*, 1991). At P2 they form an uneven layer 4 cells thick while the characteristic monolayer is established by P5 (Swisher and Wilson, 1977). It is hypothesized that this final settling into the monolayer is a mechanical process due to the parallel

inward migration of granule cells and growth of parallel fibers over the PCs (Altman and Bayer, 1997).

Thus, the overall migration pattern reveals a temporal gradient from caudal to rostral cerebellar cortex along with a latero-medial gradient in the origin of the PC population (Yuasa *et al.*, 1991). The retardation of PCs from the medial part in migrating to the cortex is attributed to the concomitant appearance of the cerebellar nuclei that causes certain groups of PCs to deviate from their migratory course (Yuasa *et al.*, 1991). Furthermore, the projection of the vestibulo-cerebellar fibers, the earliest cerebellar afferents, to the intermediate zone and finally to the caudal half of the primordial cortex, could also be partly responsible for the retardation of PC migration to the rostral part of the cortex (Yuasa *et al.*, 1991). Regarding the medio-lateral regional differences, they are attributed to an inherent PC heterogeneity considering that final mitotic division occurs first for the lateral PCs (Inouye and Murakami, 1980), extrinsic factors, differences in the chemical microenvironment and developing cerebellar afferents (Yuasa *et al.*, 1991).

Regarding the mechanism behind the migration of PCs, contact guidance appears to be one possibility (Yuasa *et al.*, 1991). According to contact guidance, first described as an underlying mechanism in neuroblast migration by Sidman and Rakic (1973), migratory cells adhere to the radial fibers formed by glial or matrix cells. Specifically, in the study by Yuasa *et al.*, (1991) radial and tenanscin fibers were colabelled with the migratory PCs in an attempt to correlate these fibers to PC migration. Tenanscin is a substrate molecule shown to be involved in neuron-glia interactions (Crossin *et al.*, 1990). Both radial and tenanscin fibers were shown to extend from the subventricular zone to the pial surface with a higher density in the medial cerebellar part and with the density diminishing around E17-E18, when the migration process is

complete (Yuasa *et al.*, 1991). These results indicated that both fibers are involved in PC migration (Yuasa *et al.*, 1991).

Purkinje cell development

PCs, named after the anatomist Evangelista Purkinje who first described them in 1837, represent the central player in the cerebellar circuitry (McClintic, 1985; Teyler, 1999). The PC undergoes a rather long timeframe of development before it reaches its fully differentiated state (Altman and Bayer, 1997). The mature PC is characterized by a prominent polarization arising from both compartmentalization and synaptic interactions and by unique subcellular features such as an extensive hypolemmal cisternal system and the Granular Endoplasmic Reticulum (GER)-mitochondria complexes (Dunn *et al.*, 1998b; Altman and Bayer, 1997). The extensive, monoplanar dendritic tree, usually originating from a single root segment and terminating with an abundance of branchlets covered in spines, permits the PC to be at the receiving end of a synaptic density higher than any other neuronal cell (Dunn *et al.*, 1998b).

The overall developmental course of this neuron has been divided traditionally into four stages with the end of the third postnatal week marking the end of differentiation (Altman and Bayer, 1997; Dunn *et al.*, 1998a; Dunn *et al.*, 1998b). According to the study by Dunn *et al.*, (1998b), in which PC development was followed in dissociated cerebellar cultures from E16 cerebellar anlagen, these four stages are roughly defined as follows: E16-P3, P4-P11, P12-P19, P20-P27. Despite the disruption of intercellular contacts and tissue geometry caused by the dissociation, the similarities of the timeframe of the developmental course and of the morphological features of PCs in each of the stages between this study and others done *in situ*, suggest that there was faithful recapitulation of the PC developmental program (Dunn *et al.*,

1998b). Furthermore, this study provides the most detailed account, to date, of the developmental events surrounding dendritic differentiation, synaptic maturation and formation of cell-specific features in PCs.

During the first stage, also referred to as the "stellate" stage (Armengol and Sotelo, 1991), the cell body (approximately 10μm in diameter) contains an eccentric nucleus, immature cytoplasmic organelles (Golgi apparatus, rich complement of coated/uncoated vesicles, mitochondria) and is already polarized (Dunn *et al.*, 1998b). Specifically, at around P2 the cytoplasm forms a rounded apical cap which bulges towards the cortical surface by P4-P5 and eventually moves basally by P7 (Swisher and Wilson, 1977). In addition, dendritic differentiation is rather rudimentary at this stage (Armengol and Sotelo, 1991; Dunn *et al.*, 1998a; 1998b). The rough contour of the cell body is attributed to protruding appendages such as spines (short and thick), filopodia (long and thin) and protodendrites (short, tapering with growth cones at their tip, either branching further to spines and filopodia or remaining unbranched).

There are also rudimentary afferent and efferent synapses such as axosomatic and axodendritic synapses from parallel fibers (Dunn *et al.*, 1998b). The fate of spines and filopodia will depend on appropriate axon contact, that is, they may develop to dendritic branchlets and mature spines or be retracted in the case that functional contact is not achieved (Dunn *et al.*, 1998b). Regarding axonal development, the axon is already prominent at this early stage with many of its mature features such as the tapering base giving rise to beaded collaterals terminating in growth cones (Dunn *et al.*, 1998a; 1998b). *In situ,* the axon arises from the cell body, whereas in dissociated cultures it often originates from a protodendrite, an event attributed to cutting of axons during dissociation (Dunn *et al.*, 1998a). Overall, it is evident from this early stage that

even though axonal differentiation is a cell-autonomous process, dendritic differentiation is dependent on external signals (Schilling *et al.*, 1991) such as granule cell signals (Dunn and Mugnaimi, 1993; Baptista *et al.*, 1994). Furthermore, dendritic differentiation depends on axonal differentiation as demonstrated by studies in which inhibition of axon-specific tau protein prevents axonal elongation and dendritic differentiation (Caceres *et al.*, 1991). Thus, by the end of this stellate stage, PC polarity is established and intercellular contacts are in the process of being established (Armengol and Sotelo, 1991; Altman and Bayer, 1997; Dunn *et al.*, 1998a; 1998b).

During the second stage, i.e., P3-P11, there is a cytoplasmic enlargement resulting in a 16 μm-somatic diameter concomitantly with somatic elongation and smoother contours (Dunn *et al.*, 1998b). By P10-P11 the apical cytoplasm tapers into the root of the primary dendrite, whereas the basal cytoplasm forms a rounded bulge, both movements resulting in the achievement of the adult, flask-type shape (Swisher and Wilson, 1977). Despite the increase in the soma size, ultrastructural features remain immature. The nucleus is still eccentric, the Golgi apparatus and mitochondria remain the predominant organelles, cisterns of GER are found in pairs or individually and occasionally cisterns of smooth endoplasmic reticulum (SER) are found beneath the plasmalemma (Dunn *et al.*, 1998b).

This second stage is further characterized by significant dendritic differentiation. Dendritic processes thicken, become longer, start to bifurcate and all dendritic projections emit spines and filopodia (Dunn *et al.*, 1998). There is dendritic outgrowth to the point of a second but no more than third order (Smith and Mullen, 1997; Swisher and Wilson, 1977; Dunn *et al.*, 1998b). Primary dendrites exhibit an irregular contour and a rich array of organelles such as microtubules, fewer neurofilaments and tightly packed mitochondria (Dunn *et al.*, 1998b).

Synaptic contacts, afferent and efferent on both the dendritic shafts and the appendages, remain immature and are characterized by boutons with round synaptic vesicles and both asymmetric and symmetric densities (Dunn *et al.*, 1998b). Axonal differentiation also progresses. The proximal part of the axon thickens as it becomes packed with mitochondria and coated vesicles, the initial axon segment (tapering point) becomes prominent and there is an appearance of a modest number of synaptic vesicles in the axonal boutons (Dunn *et al.*, 1998b).

The third stage (P12-P19), overall, is characterized by major somatic development, synaptic maturation and further dendritic outgrowth (Dunn *et al.*, 1998b). Specifically, the somatic diameter reaches 20μm (22μm in the long axis), the nucleus is found centrally located and assumes a regular contour and the nucleolus increases in size suggesting increased ribosomal protein production (Dunn *et al.*, 1998b). Most importantly, however, this is the time of formation of cell class specific features, namely the hypolemmal cisternal system and the GER-mitochondrion complex (Dunn *et al.*, 1998b). These complexes, first described by Rosenbluth (1962) are possible sites of IP_3-sensitive channels potentially involved in calcium fluxes (Takei *et al.*, 1992), thus, suggesting special cell signaling mechanisms (Dunn *et al.*, 1998b). Axon morphology does not change significantly but the axon does grow longer, often extending as much as 3mm from the soma (Dunn *et al.*, 1998b). The increase in dendritic branching is indicated by an increase in the number of dendritic bifurcations up to the 7^{th} order and of spines. There is no more filopodia emission, all portions of the dendritic arbor are rich in organelles, spines acquire mature features and both asymmetric and symmetric synapses are found on the cell body and dendrites (Dunn *et al.*, 1998b). The fourth and final stage is not characterized by new events but merely by elaboration of growth and maturation of the soma, dendrites and

synaptic contacts, suggesting that PCs have reached the apex of their differentiation (Dunn *et al.*, 1998b).

Regarding the two major excitatory inputs to PCs, namely the climbing and parallel fibers, synaptic maturation is achieved by the end of stage 3. Parallel fibers begin to contact the Purkinje dendritic shafts and spines and slowly form immature synapses during the first postnatal week (Smith and Mullen, 1997; Yamada *et al.*, 1997; Dunn *et al.*, 1998a). Features of these immature contacts include the presence of few synaptic vesicles, small contacts and absence of astroglial enclosure (Yamada *et al.*, 1997). By P16 synaptic contacts mature and exist only on distal spines as seen in the mature state (Smith and Mullen, 1991; Yamada *et al.*, 1997). Climbing fibers from the inferior olive, once in the cerebellum, project to their target neurons without undergoing a stage of random dispersion (Sotelo and Wassef, 1991). Climbing fibers begin to contact PCs early at birth, before the formation of the PC monolayer, when they are rather immature morphologically themselves with relatively unbranched terminal arbors and small tapered growing tips (Mason *et al.*, 1990). By P3-P4, climbing fibers branch over more than one adjacent PC somata and by P7 these contacts become more focused on individual PC somata, even though dendritic differentiation has already begun (Mason *et al.*, 1990). It is not until P8-10 that climbing fibers project to the PC dendritic tree to form contact with the proximal spines of large, low order dendritic branches (Mason *et al.*, 1990).

Finally, the mode of regulation of the number of PCs has been the focus of several studies. Naturally occurring cell death, a mechanism involved in the regulation of the size of nerve cell populations such as the EGL, is one possibility that until recently was not thought to occur in the case of PCs (Goldowitz and Hamre, 1998). However, in a recent study transgenic mice that overexpressed Bcl-2, a gene which represses cell death, exhibited a PC population

significantly larger than the wild type, suggesting that cell death is partly involved in regulating the number of PCs (Zanjani *et al.*, 1996).

Changes in gene expression during Purkinje neuron development

PC heterogeneity

The mammalian cerebellum is a compartmentalized structure as revealed by patterns of gene expression and of input and output fiber projections along both the mediolateral and rostrocaudal axes (Voogd and Bigare, 1980; Hawkes *et al.*, 1985; Oberdick *et al.*, 1993; Kuemerle *et al.*, 1997; Baader *et al.*, 1998). The results of the action of specific genes in the form of highly patterned markers strongly suggest the functional significance of this compartmentalization in aspects such as the guidance of major input and output fiber systems (Oberdick *et al.*, 1998).

Studies involving transplants (Sotelo and Alvarado-Mallart, 1987) and chimeras (Smeyne and Goldowitz, 1982) show that PC development is not synchronous and furthermore, that these neurons follow a developmental program which, for the most part, is autonomous of environmental influences, i.e., it is intrinsic. There are a number of PC markers, expressed early in embryonic stages, each following a different developmental pathway, that establishes a transient biochemical heterogeneity among PCs (Smeyne *et al.*, 1991; Sotelo and Wassef, 1991). Furthermore, their expression patterns reveal two types. A characteristic example of the first type is L7 encoded by pcp-2 (Berrebi and Mugnaini, 1992) that is first expressed embryonically by certain groups of PCs found in four parasagittal bands, two on each side of the midline,

(Smeyne *et al.*, 1991). As development progresses there is a caudal-rostral and mediolateral gradient of L7 expression until P9 at which point all PCs are positive for L7 (Smeyne *et al.*, 1991). A comparison of the L7 expression pattern between wild type and *reeler* mice, characterized by clusters of PCs positioned ectopically, indicates that the induction of the L7 is cell-autonomous whereas results from work *in vitro* shows that it is also independent of mossy and climbing fibers input (Smeyne *et al.*, 1991). Additional PC markers of this type, first expressed by some PCs and then by all of them, include calbindin 28kD (CABPD28K) and PEP19 (Christakos *et al.*, 1989).

The other type of markers, the best understood example being the zebrins, follows a different developmental expression pattern (Leclerc *et al.*, 1988; 1992; Ozol *et al.*, 1999). Specifically, zebrin expression begins around P5-P6. By P12-P15 all PCs are positive, followed by a selective suppression in zebrin expression between the third and fourth postnatal weeks. This suppression results in the parasagittal zebrin positive bands seen in the adult cerebellum (Leclerc *et al.*, 1998; Lannoo *et al.*, 1991).

The compartmentalization conferred by the differential expression patterns of these markers is proposed to direct the formation of the cerebellar topographic/projectional maps. Specifically, it is proposed that PCs are essential in organizing the proper projection of the climbing and mossy fibers by matching of positional cues between the growth cones of incoming afferent axons and themselves (Wassef *et al.*, 1990; Sotelo and Wassef, 1991). This is based on the fact that the boundaries of the intrinsic biochemical compartments are in agreement with those of the projectional maps (Sotelo and Wassef, 1991). Comparisons with mutant mice in which synaptology of the cerebellar circuitry is disrupted indicates that synaptogenesis with the target neuron is not involved in the formation of the maps but that the latter is an early event

preceding synaptogenesis (Sotelo and Wassef, 1991). However, neuronal activity is proposed to be involved in fine-tuning and refining of the projections to the single cell level (Sotelo and Wassef, 1991).

An additional level of compartmentalization, less understood and appreciated, exists at the cellular level of the PC as revealed by the separation of afferent input to this neuron (Oberdick *et al.*, 1998). Specifically, following a proximo-distal direction, the initial axon segment is contacted by the terminals of the inhibitory basket and stellate interneurones. In addition, the proximal dendrites are surrounded by climbing fibers whereas parallel fibers connect to the distal dendritic spines (Oberdick *et al.*, 1998). This morphological subdivision is respected by an intracellular compartmentalization of mRNA distribution and it appears that the latter serves as a level of local translational control either by being a source of protein gradients or by facilitating the deployment of protein to specific subcellular compartments (Oberdick *et al.*, 1998). Some of the proteins whose mRNAs have been shown to be differentially distributed are CABPD28K, L7 and PEP19. Specifically, the mRNA of CABPD28K is found at the axonal pole of the perikaryon, around the initial axon segment, whereas the mRNA of L7 is localized throughout the cell from the axon to the distal dendrites (Wanner *et al.*, 1997). Furthermore, the faithful replication of these differential distributions in PCs *in vitro* suggest that the mechanism underlying this mRNA localization pattern is cell-intrinsic (Wanner *et al.*, 1997). Notably, this compartmentalization of the cerebellum at the cellular level is proposed to serve a role in synaptic plasticity and learning (Oberdick *et al.*, 1998).

Expression patterns of PC-specific sequences

GABA, is the major, inhibitory neurotransmitter in the mammalian cerebellum. Purkinje neurons receive GABAergic afferents via their GABAA/benzodiazepine receptors (GABAA/BZ) (Zdilar *et al.*, 1992). Among the subunits that make up the Cl^- channel of this receptor are β1, β2 and β3 (Olsen and Tobin, 1990) whose distribution and temporal expression are different during cerebellar development (Zdilar *et al.*, 1992). PCs in particular appear to express very low levels of β1 and somewhat higher levels of β3. The β2 subunit, however, detectable at birth mostly in the molecular/Purkinje layer, is maintained during the first postnatal week and is significantly upregulated as development and foliation progress achieving the adult distribution by P20 (Zdilar *et al.*, 1992). The α1 subunit of GABAA/BZ, responsible for the binding of flunitrazepam, follows a different expression pattern; the low levels detected in PCs at P1 are followed by an upregulation during the first postnatal week (Zdilar *et al.*, 1991) before the formation of afferent inhibitor synapses. This timeframe of upregulation, thus, excludes a role of GABAergic synaptic input for the expression of the α1 subunit (Zdilar *et al.*, 1991). Finally, the γ2 subunit, that appears to facilitate the interaction between the α and β subunits, is expressed by PCs embryonically, followed by an upregulation during the first and second postnatal weeks (Luntz-Leybman *et al.*, 1993). Again, the timeframe of expression indicates that GABAergic input is not required for expression.

Glutamate (Glu), the major neurotransmitter involved in fast excitatory synaptic transmission in the mammalian CNS, appears to be a signal for cell migration, neuronal differentiation, activation of second-messenger cascades and is also thought to be involved in synaptic plasticity, learning and memory (Sutherland *et al.*, 1996; Yamada *et al.*, 1997). There are four subtypes of the Glu transporter each with a distinct structure, function and expression

pattern, EAAT 1,2, 3, and 4. PCs receive Glu from granule cells and the inferior olive and specifically express EAAT4, localized exclusively on their dendritic spines (Yamada *et al.*, 1997). The EAAT4 mRNA is already detectable at birth in the somata of PCs in the caudal cerebellum. By P7, there is significant upregulation resulting in a homogeneous expression of EAAT4 by all PCs (Yamada *et al.*, 1997). The intracellular distribution of the protein product indicates a PC-specific transcriptional control along with translational regulation resulting in synaptic localization during P0-P14. The latter correlates temporally with the formation and structural maturation of the parallel fiber-PC synapses suggesting a role for EAAT4 in the regulation of synaptic transmission (Yamada *et al.*, 1997).

Subunits 2 and 3 of the α–amino-3-hydroxy-5-methyl-4-isoxazole-propionic acid (AMPA)-type Glu receptor (GluR) are quasi-exclusively expressed by PCs (Martin *et al.*, 1993). The mRNA of these two subunits is first expressed embryonically and the protein product is already present at P1 in both the PC somata and primary dendrites (Bergmann *et al.*, 1996). There is a significant upregulation during the first postnatal week and by P8 GluR 2/3 appear at some post-synaptic sites (Bergmann *et al.*, 1996). During the second postnatal week, concomitantly with an increase in dendritic differentiation, there is an increase in the levels of expression of subunits 2 and 3 in the higher order dendritic branches so that in adult PCs both subunits are found predominantly at the distal branches and postsynaptic densities (Bergmann *et al.*, 1996). The GluRδ2 is an additional subunit of the GluR that is exclusively expressed in PCs (Takayama *et al.*, 1996). Expression begins embryonically (E15) and the moderate mRNA signal detected at P0 in posteriorly located PC somata is followed by a significant upregulation that results in a uniform expression by all PCs by P7 (Takayama *et al.*, 1996). It appears that during the first postnatal week there is a caudal to rostral gradient in GluRδ2 expression,

followed by an additional upregulation at P14 (Takayama *et al.*, 1996). It is noteworthy that, while synaptogenesis does not appear to affect the expression of this subunit, the intracellular distribution of the protein product undergoes a shift from non-synaptic to synaptic sites during the time of parallel fiber-PC synapse formation, thus indicating a role for GluRδ2 in this event (Takayama *et al.*, 1996).

Additional sequences that undergo upregulation during PC development include the cerebellum-specific glycoprotein P400 (Maeda *et al.*, 1989). This molecule undergoes a PC-specific, significant upregulation during the first postnatal week and the protein product is localized in the plasma membrane, endoplasmic reticulum and postsynaptic densities (Maeda *et al.*, 1989). The postnatal increase in the expression levels proceeds concomitantly with growth and differentiation of the dendritic tree, thus, suggesting a role for this glycoprotein in this process (Maeda *et al.*, 1989). The PC-specific calcium binding protein CaBPD28k is also upregulated during the first postnatal week reaching a peak at week 2 and decreasing to steady levels at week 4 (Iacopino *et al.*, 1990). This developmental expression pattern, along with the fact that levels of this protein decline dramatically in aging PCs, implicate CaBPD28k in PC maturation and maintenance (Iacopino *et al.*, 1990). Other postnatal proteins significantly upregulated during the first two postnatal weeks include calmodulin (Messer *et al.*, 1990), zebrin I (Sotelo and Wassef, 1991), mGluR1α (Ryo *et al.*, 1993), inositol 1,4,5-triphospate receptor type 1 ($InsP_3R1$) (Nakawaga *et al.*, 1991) and L7 (Hamilton *et al.*, 1996).

The following two subsections provide a detailed description of the developmental expression patterns of two PC-specific sequences, RORα and PLCβ3. The spatial, intra-nuclear position of these sequences was analyzed as a function of development for the purposes of the present study.

RORα

RORα is a member of the nuclear hormone receptor gene superfamily, whose deletion is responsible for the *staggerer* mutation (Hamilton *et al.*, 1996). The nuclear hormone receptor gene superfamily codes for a variety of transcriptional regulators (Evans, 1988; Mangelsdorf *et al.*, 1995) and its members are classified into two groups, one activated by known lipophilic hormones such as steroids, thyroid hormone and retinoic acids while the ligands for the other group, the orphan nuclear receptors, are still unidentified (Nakagawa *et al.*, 1997). For both groups, binding of the ligands triggers activation and most of these receptors bind as monomers, homodimers and heterodimers to specific DNA sequences termed the response elements and, thus, have a diverse function in the cell (Nakagawa *et al.*, 1997). RORα is expressed at the highest level in the PC, with low levels of expression detected in certain thalamic nuclei (Matsui *et al.*, 1995; Hamilton *et al.*, 1996). Regarding its developmental expression pattern, RORα mRNA first appears at E15 in the migrating PCs. Following this early appearance, levels of expression remain constant until P21 at which time PCs have completed their differentiation (Nakagawa *et al.*, 1997). There is are mediolateral or rostrocaudal differences in the expression of RORα and at all stages it is found in the PC perikaryon (Nakagawa *et al.*, 1997). The severe compromise PCs undergo in the *staggerer* mutation (discussed below) indicates that RORα is a

gene required for proper phenotypic differentiation of PCs (Hamilton *et al.*, 1996; Nakagawa *et al.*, 1997).

PLCβ3

The activation of neurotransmitter and hormone receptors, coupled to the Gq subclass of GTP-binding protein, results in the further activation of phosphoinositide-specific phospholipase C (PLC). PLC is, in turn, responsible for the hydrolysis of phosphatidylinositol 4,5-biphosphate to two second messengers; diacylglycerol and inositol 1,4,5-triphosphate (IP_3) (Exton, 1993). Diacylglycerol then stimulates protein kinase C (PKC) while IP_3 moves Ca^{2+} from intracellular stores via the IP_3 receptors (Watanabe *et al.*, 1998). There are three subtypes of PLC, β, γ, δ, different in structure and activation mechanism (Watanabe *et al.*, 1998). PLCβ has four isoforms, 1-4, that have two conserved X and Y domains followed by the long C- terminal sequence that interacts with the alpha subunit of the Gq subclass of GTP-binding protein (Wilkie *et al.*, 1989).

In a study of the developmental expression patterns of all four isoforms, PLCβ3 was found to be PC-specific while the highest levels of the β4 isoform were also detected in the PCs (Watanabe *et al.*, 1998). Very faint signals of PLCβ3 were detected over the ventricular zone of the fetal brain but disappeared perinatally; there was no signal at P0 and P1 (Watanabe *et al.*, 1998). According to this study, the first mRNA signal appears at P7 and levels of expression remain constant from thereon, indicating that this PC-specific sequence is *de novo* expressed between P2 and P7. In addition, no mediolateral or rostrocaudal gradient was observed in the expression of PLCβ3 as development progressed (Watanabe *et al.*, 1998). These isoforms

appear to form a functional phosphoinositide signaling cascade, involved in synaptic plasticity, synapse development and normal brain function (Watanabe *et al.*, 1998).

Notably, PLCβ4 mutants were recently studied to investigate the role of this isoform in the elimination of excess climbing fiber-PC synapses. These mutants are viable but display locomotor ataxia and developmental elimination of excess climbing fiber-PC synapses is impeded in the anterior portion of the vermis where this isoform is normally expressed in particularly high levels (Kano *et al.*, 1998). Such impairment is absent in the caudal cerebellum where low levels of PLCβ4 are found. Thus, it is proposed that this isoform is required to transduce signals necessary for climbing fiber synapse elimination in the rostral cerebellum (Kano *et al.*, 1998).

On the DNA content of Purkinje cells

Neuronal cells have traditionally been assumed to be of the standard diploid range regarding their DNA content, a trait typical of non-dividing, somatic cells. However, certain neuronal cell types and particularly cerebellar PCs have been proposed to be polyploid. Specifically, early cytophotometric studies deduced that cerebellar PCs of the rat achieve a permanent tetraploid state during early postnatal development (Lentz and Lapham, 1970; Mares *et al.*, 1973). Since then, numerous studies have been undertaken to resolve this issue of polyploidy using cytophotometric, radiographic and biochemical techniques. However, the results of these studies remain contradictory and potential deficiencies in methodology and/or interpretation continue to render the issue of PC polyploidy unresolved.

The cytophotometric studies using Feulgen stained PC nuclei have been challenged the most and a number of parameters have been identified as potential sources of error such as non-

specific light loss due to false-positively stained and unstained background areas and improper selection of control haploid and diploid cells (Swartz and Bhatnagar, 1981). Nonetheless, even after an attempt to correct these factors, it remains inconclusive whether PCs are polyploid (Swartz and Bhatnagar, 1981). In addition, the different fixatives and hydrolysis kinetics in cytophotometry have been shown to influence the chromatin availability to the Feulgen reaction, thus, resulting in an overestimation of DNA staining in PCs (Scherini, 1982). An additional suggested source of error includes nonspecific cytoplasmic and nuclear absorption of the Feulgen stain (Manuelidis and Manuelidis, 1974).

Results from biochemical studies also appear insufficient to permit conclusions since they have been performed on cell "enriched" rather than pure fractions and the polyploid level of the non-PCs in these fractions has been assumed to be diploid (Swartz and Bahtnagar, 1981). Finally, according to the results of radioautographical studies, the absence of incorporation of radiographic precursors by cerebellar PCs in the first 10 postnatal days both *in vivo* and *in vitro* indicates that PCs are of the standard diploid range (Manuelidis and Manuelidis, 1974), a finding also supported by some biochemical studies (Cohen *et al.*, 1973). The findings from autoradiographical studies represent the most serious challenge of the polyploidy suggested by results obtained from Feulgen staining. Possible sources of error for this type of study deal primarily with time and level of exposure to the various radiographic isotopes as well as with subjectivity in determining level of staining (Swartz and Bahtnagar, 1981).

In conclusion, it appears that the two views, polyploidy versus diploidy, are supported primarily by the results of Feulgen cytophotometry and radioautographical studies, respectively, Notably, it is proposed that the radioautographic approach appears to have greater potential for resolving this controversial issue (Swartz and Bahtnagar, 1981).

ABNORMAL CEREBELLAR DEVELOPMENT

There is a number of cerebellar mutants whose abnormal morphological/ behavioural traits and genetic events have been identified, namely, the *staggerer*, *lurcher*, *weaver*, *reeler*, *purkinje-cell degeneration* (*pcd*), *nervous*, *waggler* and *weaver*. The *staggerer* mutant and cerebellin, a PC-specific neuropeptide whose expression pattern is altered in this mutant, are described in detail below as part of a future study proposed at the end of the Discussion.

Staggerer

- The primary target of this mutation is the PC (Herrup and Mullen, 1979a) and as shown from chimera experiments, PC development is affected in a direct, cell-autonomous manner in these mutants (Herrup and Mullen, 1979b; 1981; Soha and Herrup, 1995). Overall, homozygous *staggerer* mice, (sg/sg), exhibit a characteristic cerebellar ataxia with PCs being reduced in number and exhibiting an immature morphology, synaptic arrangements, biochemical properties and altered gene expression (Hamilton, *et al.*, 1996). Furthermore, in heterozygous *staggerer* (sg/+) mice PCs undergo accelerated dendritic atrophy and there is cell loss (Hamilton, *et al.*, 1996). In sg/sg mice PCs are small and ectopically positioned (Soha *et al.*, 1997) and their number is substantially lower than normal (Herrup and Mullen, 1979a). The dendrites, besides being atrophic and sparsely branched, do not express dendritic spines that are normally postsynaptic to the parallel fibers (Landis and Sidman, 1978). Furthermore, PCs abnormally retain their immature polyinnervation by climbing fibers (Crepel *et al.*, 1980) and either fail to express or have very low levels of early postnatal proteins such as calmodulin (Messer *et al.*, 1990), zebrin I (Sotelo and Wassef, 1991), mGluR1α (Ryo *et al.*, 1993), inositol 1,4,5-

triphospate receptor type 1 ($InsP_3R1$) (Nakawaga *et al.*, 1996), calbindin (Nakawaga *et al.*, 1996) and L7 (Hamilton *et al.*, 1996). The early timeframe of the normal expression patterns of these sequences, along with the fact that *staggerer-lurcher* double mutants do not express the *lurcher* phenotype, that normally appears by P7 (Messer *et al.*, 1991), indicate that PC development is impaired at an early stage in *staggerer* mice (Soha *et al.*, 1997).

The *staggerer* mutation also affects the granule cells in an indirect manner. Specifically, granule cells are generated at a slower rate than normal and soon after their successful migration to the internal granular layer they begin to die in such large numbers that by maturity the staggerer cerebellum is agranular (Sidman *et al.*, 1962; Soha *et al.*, 1997). Herrup (1983), studying wild type-*staggerer* chimeras showed that this dramatic loss of granule cells is not a cell autonomous effect of the *sg* gene but an indirect consequence of the target population of PCs instead. This target-dependent death of granule cells (Herrup and Sunter, 1987) is secondary to the primary PC defects and together the two result in complete cerebellar failure in the first postnatal weeks (Zanjani *et al.*, 1994; Herrup and Basser, 1995).

Although the effects of this mutation have been studied for almost three decades, the molecular basis underlying the *staggerer* phenotype has only recently been defined. Hamilton *et al.*, (1996) mapped *staggerer* to a 160kb-interval on mouse chromosome 9, which contained the gene for RORα, a member of the nuclear hormone-receptor superfamily (described above). Specifically, it was found that sg/sg mice carry a deletion within the RORα thus eliminating a ligand-binding domain required for transcriptional activity *in vitro* (Hamilton *et al.*, 1996). These results were further confirmed by an additional, independent study of the genetic cause of the *staggerer* mutation. (Matysiak-Scholze and Nehls, 1997).

Considering the severe effects of this deletion as described above, it is evident that RORα is a gene required for proper PC postnatal maturation. In an attempt to define the mechanism via which RORα exerts its effects, research was directed towards the thymus, an organ that also expresses RORα albeit at much weaker levels (Hamilton *et al.*, 1996). It is noteworthy that sg/sg mice exhibit delayed thymic development along with a defect in the termination of T-cell response (Trenkner and Hoffmann, 1986). It is also of interest that among the effects of hypothyroidism are reduced dendritic arborization of PCs and granule cell proliferation similar to sg/sg mutants, defects that can be assuaged in a dose-dependent manner by thyroid hormone replacement (Legrand, 1979). In addition, the *staggerer* mutation prevents PC response to the thyroid hormone (Messer, 1988). Taken together, these findings strongly suggest the possibility of an interaction of RORα with the thyroid hormone signaling pathway involved in PC maturation (Hamilton *et al.*, 1996). A potential target of the thyroid hormone is L7 (encoded by pcp-2) which responds to thyroid hormone levels *in vivo* (Zou *et al.*, 1994) and is undetectable in sg/sg mutants (Hamilton *et al.*, 1996).

Cerebellin

The levels of expression of cerebellin are developmentally regulated and cerebellin has been used previously as a marker for PC development (Slemmon *et al.*, 1985). Although its exact function is not known, results from immunological (Mugnaini *et al.*, 1985) and biochemical (Slemmon *et al.*, 1984) studies indicate that both cerebellin peptides (cerebellin and des-Ser1-cerebellin) are found in the postsynaptic parts of PCs. In addition, the homology between the cerebellin sequence and the polyimmunoglobulin receptor (Mugnaini *et al.*, 1988)

suggests that the cerebellin precursor may participate in the recognition and transport of a ligand (Slemmon *et al.*, 1988).

In the wild type mouse, the cerebellin peptides are first detected at P3-P4 followed by a significant upregulation that leads to maximum levels at P25 whereafter there is a decline to adult, stable values (Slemmon *et al.*, 1988). The upregulation parallels events such as granule cell migration, parallel fiber synaptogenesis, PC dendritic differentiation and overall formation of adult cytoarchitecture (Slemmon *et al.*, 1988). The expression of the two cerebellins is uniform, i.e., they are expressed by all PCs and are localized in the PC perikaryon and dendrites but not the axon (Slemmon *et al.*, 1988).

Sg/Sg mice are characterized by cerebellin-negative PCs in every cerebellar region and this observation together with the indirect effect of this mutation on granule cells reveals a role for this molecule in the relationship between the PC and the granule cell. In *sg/sg* mice, granule cells die and do not synapse with the PC dendritic spines that normally express cerebellin, whereas in wild type mice, the increase and decrease in the number of parallel fiber-PC synapses parallel the increase and decrease in the cerebellin levels. Thus, cerebellin expression is proposed to be regulated by the formation of these synapses (Slemmon *et al.*, 1988). It has been proposed that the granule cell induces cerebellin expression possibly by producing a signal that, in turn, controls cerebellin transcription. Alternatively, it has been suggested that the formation of the parallel fiber-PC synapses somehow affects the proteolytic processing of the cerebellin precursor molecule (Slemmon *et al.*, 1988).

In conclusion, it is evident from the above that the cerebellin is developmentally regulated by a relationship of key importance for the control of cerebellar development in terms

of regulation of cell number, migration of precursor cells and cell differentiation, the one between the Purkinje and the granule cell (Goldowitz and Hamre, 1998).

OBJECTIVE

Taking into consideration studies that point towards a function-dependent nuclear topological organization and an involvement of this topology in the functional commitment of the cell, the following figure (Fig. 4) is a schematic representation of the premises onto which the present study is based as well as the proposed two-fold hypothesis and the protocols applied.

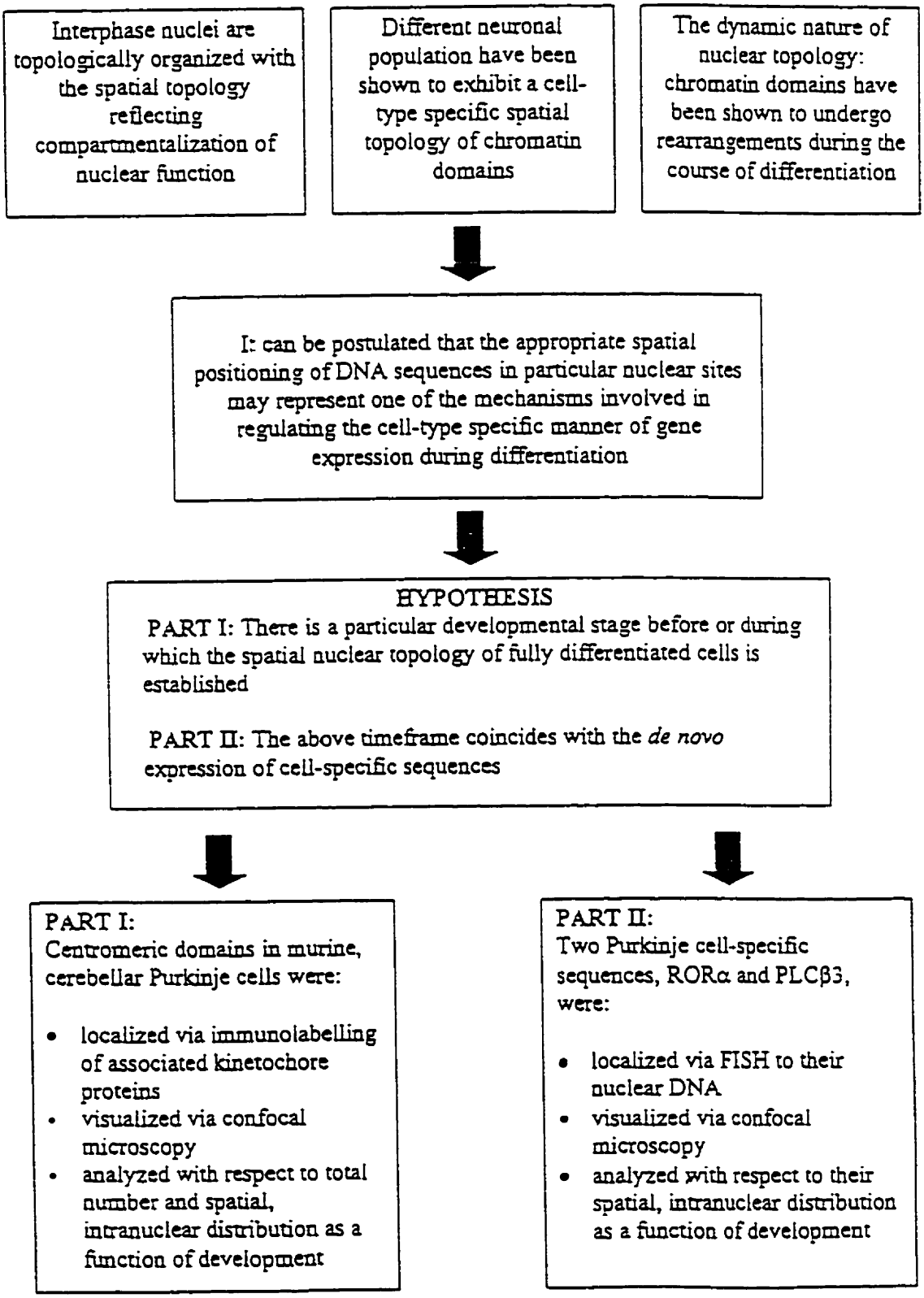
Interphase nuclei are topologically organized with the spatial topology reflecting compartmentalization of nuclear function
Different neuronal population have been shown to exhibit a cell-type specific spatial topology of chromatin domains
The dynamic nature of nuclear topology: chromatin domains have been shown to undergo rearrangements during the course of differentiation
It can be postulated that the appropriate spatial positioning of DNA sequences in particular nuclear sites may represent one of the mechanisms involved in regulating the cell-type specific manner of gene expression during differentiation
HYPOTHESIS
PART I: There is a particular developmental stage before or during which the spatial nuclear topology of fully differentiated cells is established
PART II: The above timeframe coincides with the de novo expression of cell-specific sequences
PART I:
Centromeric domains in murine, cerebellar Purkinje cells were:
• localized via immunolabelling of associated kinetochore proteins
• visualized via confocal microscopy
• analyzed with respect to total number and spatial, intranuclear distribution as a function of development
PART II:
Two Purkinje cell-specific sequences, RORα and PLCβ3, were:
• localized via FISH to their nuclear DNA
• visualized via confocal microscopy
• analyzed with respect to their spatial, intranuclear distribution as a function of development

MATERIALS AND METHODS

STOCK SOLUTIONS

Blocking buffer: 4% BSA in 1x PBS. Stored at -20^{0}C.

Culture medium (100mL): 89% MEM (v/v) with Hank's salts containing L-glutamine (MEM, GIBCO-BRL 11575-032), 10% FBS (v/v), 0.5% (v/v) of penicillin - streptomycin and supplemented with 1mL of D-glucose to a final concentration of 5mg/mL. Final concentrations for penicillin and streptomycin are 50units/mL and 50μg/mL, respectively. Stored at 4^{0}C for up to a month.

Detection Buffer: 0.1M Tris-HCl, p.H 8, 0.1M NaCl, 0.05M $MgCl_2$. Adjust p.H to 9.5.

Denaturation buffer: 70% (v/v) deionized formamide, 2X SSC. Stored at 4^{0}C.

Ethidium Bromide (stock): 10 mg/mL ethidium bromide (Sigma # E-7637) in distilled H_2O. Stored at RT in a light-tight container. Gloves should be worn when handling solutions or gels containing ethidium bromide.

Hybridization buffer: 50% deionized formamide, 2XSSC, 10% (w/v) dextran sulfate (Sigma D-8906). Rigorous vortexing recquired. Stored in 1mL aliquots at -20^{0}C.

Luria-Bertani, (LB) Broth: 1% (w/v) bacto-tryptone (Difco #0123-01). 0.5% (w/v) bacto-yeast extract (Difco #0127-01), 1% (w/v) NaCl and pH was adjusted to 7.5 using NaOH. Final solution was steam-sterilized and stored at 4^{0}C with the culture media.

Loading dye (buffer) (6x): 0.25% (w/v) bromphenol blue (SIGMA #B-6896), 0.25% (w/v) xylene cyanole ff (SIGMA #X-4126), 30% (v/v) glycerol (SIGMA # G-5516) in H_2O. Stored at RT.

Re-equilibration buffer: 50% (v/v) deionized formamide, 2X SSC. Stored at 4^{0}C.

PBS (10X): Phosphate buffer saline. Dissolve 80g NaCl, 2g KCl, 14.4g Na_2HPO_4, and 2.4g KH_2PO_4 in 800mL of distilled $H_2O$and adjust p.H to 7.4. Add H_2O to 1L in a volumetric flask and steam sterilize. Stock solution was stored at 4^0C.

Protease buffer (10x): 0.01M Tris (p.H 7.8), 0.005M EDTA, 0.5% SDS. Stored at -20^0C. Dilution to 1X was done with distilled H_2O and the 1X solution was stored at 4^0C.

SSC (20X): Sodium sodium citrate. 3M NaCl, 0.3M sodium citrate, p.H 7.0. Solution was steam sterilized and stored at RT.

TAE buffer (10X): Tris-acetate buffer. 400mM Tris-HCl, 2.28% (v/v) glacial acetic acid, 20mM EDTA (p.H 8.0). Stored at RT.

CELL CULTURE

Preparation of coverslips

Glass coverslips (22 x 22mm) that were to be used for cell culture were cleaned to remove organic contaminants, the presence of which could interfere with the subsequent coating of the coverslips using adhesion substrate. Specifically, coverslips were placed vertically on acid resistant porcelain racks (Fisher Scientific) and immersed in 50% (v/v) acqueous nitric acid in a hot water bath for at least 2h. The coverslips were then removed from the acid, thoroughly washed with distilled water to ensure that all nitric acid was removed, dehydrated in absolute alcohol one at a time and stored in absolute ethanol.

Prior to cell seeding, coverslips were air-dried, both sides sterilized by a 5min exposure to ultraviolet light, and transferred to sterile polystyrene dishes with tight-fitting lids (Falcon #1006) to prevent evaporation of medium. They were then coated with aqueous poly-L-lysine hydrobromide solution (Sigma #P9011, 0.1mL per coverslip, 0.1mg/mL, 15min). Following the removal of the poly-L-lysine, coverslips were washed once in 0.5mL (per coverslip) of sterile Type I distilled water prior to cell seeding.

Derivation and culture of murine kidney fibroblasts

Fibroblasts in culture were used to quantify signal intensities of single kinetochores, i.e., to determine the "unitary value" corresponding to the kinetochore of a single chromosome (described below). Cultured fibroblasts were also used to perform preliminary Fluorescent *In Situ* Hybridization (FISH) experiments.

For the primary cultures, kidneys of a female CD1 mouse were aseptically removed and minced into fragments of approximately $1mm^3$. The resected tissue was then placed in 0.25% trypsin (2mL, Gibco BRL #15050-065) for 30min, before inactivation of trypsin with the addition of fetal bovine serum (FBS, 1mL, Sigma #F-2442). Following trituration, the tissue was centrifuged for 3min, 500g. The resulting pellet was resuspended in 2mL of culture medium and seeded onto glass coverslips (22 x 22mm) coated with poly-L-lysine hydrobromide. The coverslips, with approximately 0.3mL of culture medium, were placed into plastic culture dishes with "tight fitting lids" (Falcon #1006) to reduce evaporation. The cultures were then incubated at 37^0C in a humidified incubator supplemented with CO_2.

The cultures were fixed in freshly prepared (from paraformaldehyde) 4% (w/v) formaldehyde in phosphate buffered saline (PBS, pH = 7.3). The fixation time varied depending on the experiments performed. Specifically, having determined empirically that kinetochores could not be detected if fixation time exceeded 30min, cells were fixed for 30min for kinetochore analysis. For FISH cells were fixed for 90min. Kinetochores were labelled and detected following the immunocytochemistry and confocal laser microscopy protocols described below for the Purkinje neurons. The labelling and detection parameters for these two types of cells were kept the same since the unitary value determined from the fibroblasts was used to determine the existence and extent of clustering of kinetochores in Purkinje neurons.

Subculture of kidney fibroblasts

Cell cultures, maintained in $25cm^2$ culture flasks (Falcon #3013), were subcultured upon reaching confluency. The medium was aspirated and the cultures were briefly washed with 2mL of pre-warmed, calcium and magnesium-free Hank's Balanced Salt Solution (HBSS, GIBCO

BRL 14170-112) to remove any residual calcium and magnesium ions from the medium that could, in turn, interfere with the action of trypsin. Following the aspiration of HBSS, the cultures were incubated in 0.25% trypsin (2mL, 37^{0}C, 15min), followed by inactivation of the trypsin with FBS. The cells were gently triturated, transferred to a 10mL polystyrene test tube (Falcon #2057) and sedimented by centrifugation (3min, 500g). The supernatant was aspirated and the cell pellet resuspended with 2mL of pre-warmed culture medium. Depending on the cell density in this suspension, an appropriate volume (2 to 6 drops) was transferred to new culture flasks already containing 5mL of culture medium. For subculturing onto coverslips, the above cell suspension was diluted (usually 5-fold) with culture medium. Sterile, freshly coated coverslips, preconditioned with HBSS (0.5mL per coverslip) were seeded with approximately 8 drops of the cell suspension following the removal of the HBSS solution. These cultures were fixed after three days *in vitro* according to the immunocytochemistry and FISH protocols.

PURKINJE NEURONS

Kinetochore analysis

Tissue and Fixation

Mice (CD1) of either sex, ranging in age from postnatal day 0 (P0) to adult (6wks), following euthanasia, were decapitated, the skull removed and cerebella resected. The vermis was separated from the hemispheres using a scalpel and fixed for 30min in freshly prepared (from paraformaldehyde) 4% (w/v) formaldehyde in phosphate buffered saline (PBS, pH = 7.3). An optimal fixation time of 30min was empirically determined based on preliminary experiments, which showed that fixation times in excess of 30min rendered the centromeric

protein (CENP) resistant to immunolabelling by the primary antibody. In contrast, fixation times of less than 30min resulted in poor preservation of morphology. Following fixation, the tissue was washed (PBS, 3x10min) and stored in PBS with 0.02% sodium azide at 4^0C.

Immunocytochemistry

The cerebellar vermis was sectioned parasagitally at 50μm nominal thickness, using a Vibratome equipped with a chilled bath (4^0C, PBS, 0.02% sodium azide). Tissue sections were then transferred into wells of polystyrene plates containing PBS with sodium azide. The PBS was aspirated and the sections were incubated in RNAse A (Roche #84969521-74, 100μg/mL, PBS, 2h, 37^0C) to restrict subsequent counter-staining to nuclear DNA. Subsequently, the sections were incubated in 4% (w/v) bovine serum albumin (BSA, Sigma A-2153, PBS, 0.02% sodium azide, 2h, RT) to reduce non-specific binding of antisera. Tissue sections were then incubated in human CREST-type scleroderma anti-centromeric autoimmune serum (a gift from Dr. L. Rubin, cross-referenced with Centre for Disease Control Reference Serum #8, 1:1000 in PBS, 2% Triton-X 100 (BDH #R06433), 3.2% BSA, 37^0C, 21h). The primary antibody was diluted in a BSA solution so that blocking (reduction of non-specific binding of antisera) could be continued during the overnight incubation and, thus, further decrease background immunolabelling. Following washes (PBS, 3x20min) and additional blocking (4%BSA, 2h, RT), bound antibody was detected with Alexa-conjugated goat anti-human IgG (Molecular Probes, A-11013, 7μg/mL, 21h, 37^0C). Sections were then washed (PBS, 3x20min), counterstained with ethidium bromide (1μg/mL, PBS, 10 min) and mounted onto slides in 20μL of anti-fading reagent (p-phenylenediamine, 1mg/mL, 50% (v/v) glycerol, PBS).

Confocal Microscopy

Immunofluorescence was detected using a ZEISS LSM410, laser scanning confocal microscope equipped with an argon/krypton laser. Alexa and ethidium bromide signals were detected by excitation with the 488-nm and 568-nm, lines respectively. Electronic amplification parameters were kept constant within each experiment to acquire comparable images and to permit normalization of the calculated kinetochore signal sizes (see below). For evaluation of changes in nuclear topology, nuclei were optically sectioned at 0.33mm with a pinhole size of 20, using a 100x, 1.3 n.a oil-immersion objective. Dual-channel confocal images (128 X 128 pixels) of each optical section were recorded. Using the computer program furnished with the confocal microscope, these optical sections were then assembled into galleries and three-dimensional volumes. Both the constructed galleries were, in turn, used to assess kinetochore signal sizes and changes in their number and spatial, intra-nuclear position as a function of developmental age.

Analysis of the spatial, 3-D distribution of kinetochores

The spatial position of each kinetochore signal was assigned to one of three, arbitrarily defined, nuclear compartments, as follows (Fig. 5). Signals in direct contact with the nuclear membrane as well as those associated with aggregates of heterochromatin that were, in turn, associated with the nuclear membrane, were assigned to the compartment termed the nuclear periphery. Kinetochore signals associated with the nucleolus, or the nucleolar surface, were assigned to a compartment termed nucleolar. Signals that were associated with neither the peripheral nor the nucleolar compartments were arbitrarily assigned to a compartment termed

nucleoplasmic. The relative association of kinetochore signals in nuclei of Purkinje neurons with respect to these three compartments was compared among the different postnatal age groups.

The same criteria were applied for the assignment of sequence signals to different, intra-nuclear compartments (see below).

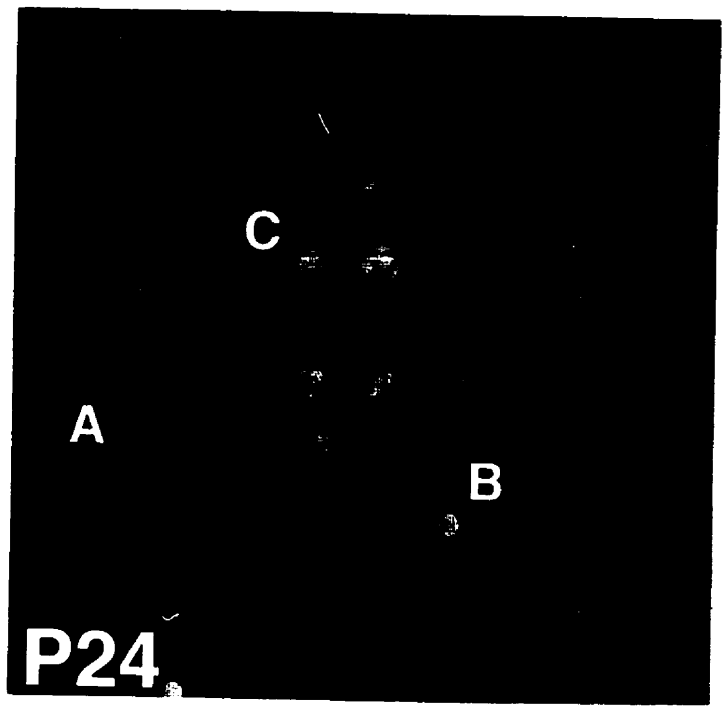

Figure 5: Nucleus of a Purkinje neuron shown as a projection of serial cofocal sections, exhibiting kinetochore signals representative of the three intranuclear compartments as defined in this study. Kinetochore signals associated directly with the nuclear periphery such as indicated by A, were termed "peripheral". Kinetochore signals, such as the one indicated by C, were termed "nucleolar" due to their association with the centrally located nucleolus. Signals associated with neither of the latter two compartments, such as B, were assigned to a compartment termed "intermediate/nucleoplasmic".

Kinetochore signal size

The size of each kinetochore signal and the extent of their clustering were determined as described previously (Janevski *et al.*, 1995). Briefly, kinetochore signal sizes were quantified by image analysis of optically-sectioned interphase nuclei, immunofluorescently labelled for kinetochores. In the study by Janevski *et al.*, (1995) "Fluoresbrite" fluorescent latex beads (Polysciences Inc.), used as models, were optically sectioned using confocal laser microscopy, and since fluorescence from each bead could be detected in several optical sections, the section at which maximum bead fluorescence was observed was chosen for image analysis and quantification of the bead size. Analysis of the fluorescence intensity for single, adjacent and aggregated beads showed that increases in the levels of fluorescent material corresponded to analogous increases in both the fluorescent area and mean pixel intensity.

In the present work, using the paradigm from the study described above and the public domain image analysis program NIH Image 1.61, the size of each kinetochore signal was expressed as the product of the area and mean pixel intensity of that optical section at which the signal exhibited maximum fluorescence. This product was termed Total Fluorescence Intensity (TFI). These TFI values were normalized, to account for cell to cell differences, by each being expressed as a fraction of the sum of all the TFIs of kinetochore signals within a nucleus, and were termed Normalized TFI (NTFI). In cells from the kidney cultures, most likely fibroblasts, the number of kinetochore signals per nucleus was found to be 40.00 ± 0.00 (mean $\pm$ SEM), equal to the 2n chromosome complement of the mouse. The NTFI of each kinetochore signal in these nuclei was, thus, considered to represent the unitary value of a single kinetochore. This unitary value was subsequently used in the analysis of kinetochore signals in interphase nuclei of

Purkinje neurons to determine the extent of kinetochore clustering, i.e., to determine the number of chromosomes which contribute their centromeric domains to a given cluster.

Analysis of Purkinje-neuron specific sequences

Isolation of sequences

Preparation of agar plates

1.0% (w/v) of bacto-agar (Difco # 0140-01) was added to Luria-Bertani (LB) broth. Following steam-sterilization, the solution was allowed to cool to below 65^{0}C, and 30mL aliquots were poured into sterile 100 x 15mm plastic petri dishes (Fisher # 8-757-13) in a laminar flowhood, avoiding bubble formation. The agar was allowed to solidify (10-15min) and the plates were then closed, sealed with parafilm and stored at 4^{0}C. When adding antibiotics, the steam-sterilized solution was again allowed to cool below 65^{0}C, the appropriate amount of antibiotic was added, followed by gentle mixing before pouring to the plates. Working concentration for ampicillin (Sigma # A-9518) and chloramphenicol (Sigma # C-0378) were 50μg/mL and 20μg/mL, respectively. Plates with agar containing antibiotic could be stored for up to a month at 4^{0}C.

Long-term storage of bacteria

For long–term storage of bacteria, 0.5mL of the bacterial culture was transferred to a sterile screw-cap Sarstedt (1.5 mL) tube, already containing 0.5mL of 60% sterile glycerol in distilled water. The contents were mixed thoroughly by vortexing, the tube was labelled accordingly and stored in liquid nitrogen. Viable bacteria could be recovered by scratching the surface of the frozen stock with a sterile needle.

1. Phospholipase C β3 (PLCβ3)

This sequence was not commercially available in a BAC or YAC clone. Thus, a 153bp-cDNA (see below), kindly donated by Dr. Watanabe (Hokkaido University, School of Medicine, Japan), after being amplified, vector- and gel-purified, was used to screen a mouse library at the MRC Genome Resource Facility (Hospital for Sick Kids, Toronto, ON). A BAC clone, 100kb, was provided by them containing the genomic DNA sequence for PLCβ3 and was used in FISH experiments. The following protocols were applied to obtain the vector-free and gel-purified PLCβ3 cDNA.

Transformation of bacteria

Competent bacteria (*E.coli*, TOP10S) were kindly donated by Dr. P.C. Park (Ontario Cancer Institute). The 153bp-cDNA for PLCβ3 was subcloned between BamH I and EcoR I restriction sites in the ampicillin-resistant, 4.9kb p-GEX4T-2 plasmid (Fig. 6).

Tubes containing the plasmid as supplied were briefly centrifuged and placed on ice along with β-mercaptoethanol (β-ME, 0.5M, Invitrogen, # 46-0123) and two tubes of frozen E.*coli* competent cells. 2μL of β-ME were pipetted into each tube of competent cells and the contents were mixed by stirring gently with the pipette tip. Mercaptoethanol was added to complete the process of rendering the bacteria competent for transformation. 2μL of the ligation reaction mixture were pipetted directly into one of the tubes containing the competent bacteria and were mixed gently by stirring gently with the pipette tip. The other tube containing no plasmid represented the negative control. Both tubes were incubated on ice for 30min. The remaining plasmid was stored at -20^{0}C. Following the 30min incubation period, the tubes containing the bacteria were heat shocked for *exactly* 30sec in a 42^{0}C water bath and then placed

on ice for 2min. Care was taken so that the tubes were not mixed or shaken during the heat shock to avoid leaking of plasmid DNA. Subsequently, 250μL of LB broth at RT were added to each tube followed by incubation (37^0C, 1h, 225rpm, rotary shaking incubator). The tubes were then placed on ice and, both tubes i.e., transformed and non-transformed bacteria, were spread on separate LB agar plates containing 50μg/mL of ampicillin to verify transformation. Specifically, 20μL of transformed bacteria (full concentration and 1:10 dilution in LB broth) and of non-transformed bacteria were spread on 3 ampicillin-containing agar plates. The same was done for 3 agar plates containing no ampicillin. The bacteria were spread using a heat-sealed Pasteur pipette. Once the liquid was absorbed (2-3min), the plates were inverted and placed in a 37^0C incubator for 24h.

All three plates without the antibiotic exhibited growth as expected. The plates with the ampicillin, on the other hand, exhibited patches of growth representing colonies of transformed bacteria. The latter together with the fact that non-transformed bacteria did not grow on the ampicillin plate indicated that the transformation was successful.

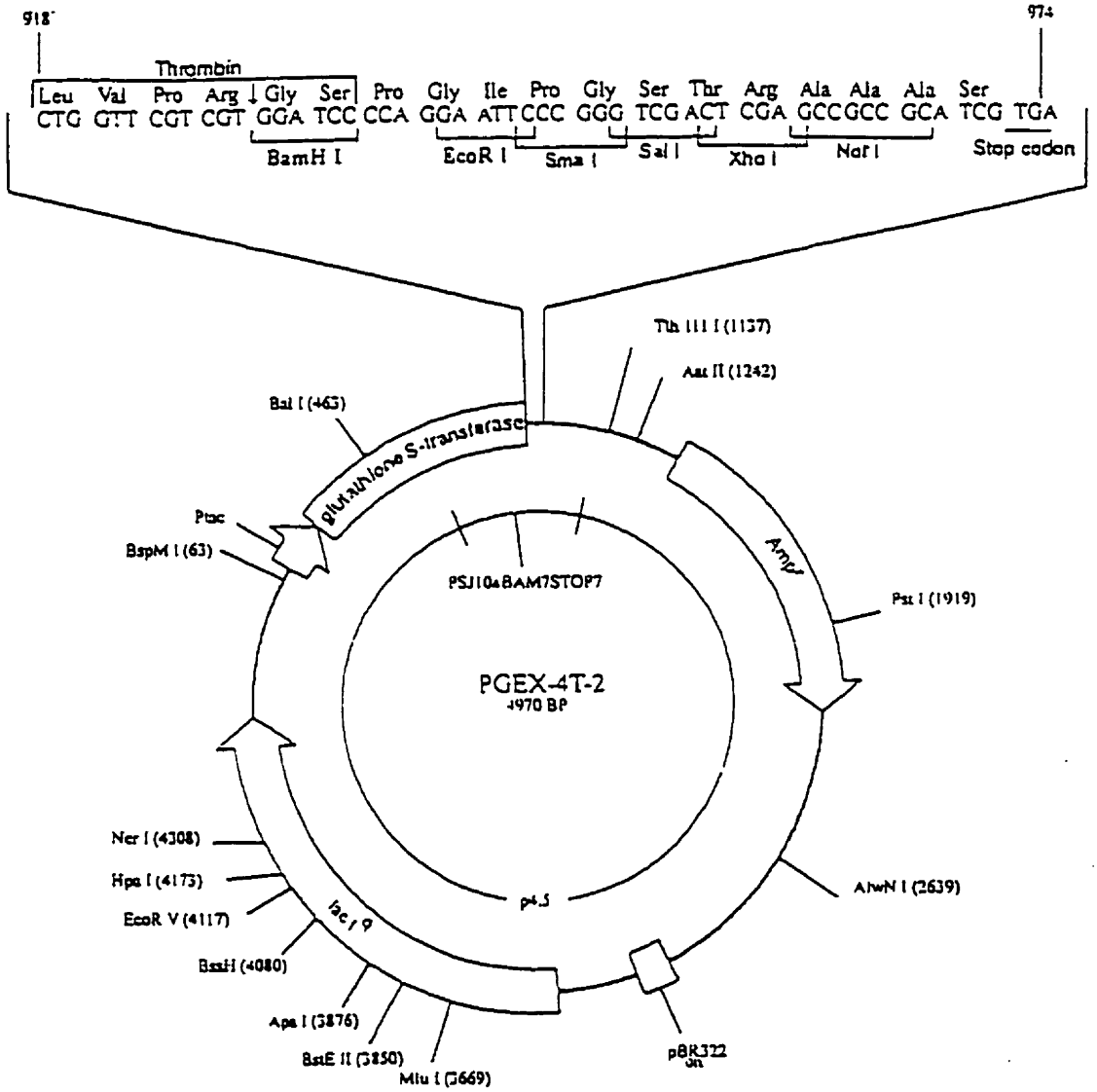

Figure 6: Restriction map of pGEX4T-2. The enzymes used to digest the plasmid and isolate the PLCβ3 cDNA are Bam HI and Eco RI.

Plasmid (p-GEX4T-2) isolation

Single colonies from freshly streaked selective plates (ampicillin) were picked and used to inoculate 5mL cultures (LB broth, 50μg/mL ampicillin), one colony per culture, which were then were grown overnight (37^{0}C, 250rpm, rotary shaking incubator). Plasmid isolation was performed for 4 such cultures following the instructions of the Miniprep kit manufacturer, Qiagen (27104).

The plasmid was then digested with NotI (Biolabs, #189S), a restriction enzyme that, according to the vector map, linearizes this plasmid. Upon running a 1% agarose (GIBCO BRL 5510UA) analytical gel (described in the next section) a band corresponding to the size of the whole plasmid (4.9kb) was observed (Fig. 7). Double digestion with *Bam*H I (Biolabs, #136S) and EcoR I (Biolabs, #101S) releases, according to the vector map, the 153bp DNA sequence of interest from the remainder of the plasmid. The results of the 2% agarose gel for all four samples can be seen in Fig. 8. The higher agarose concentration offers better resolution of the smaller size DNA bands. This gel verifies that the appropriate sequence is present and indicates the absence of contamination.

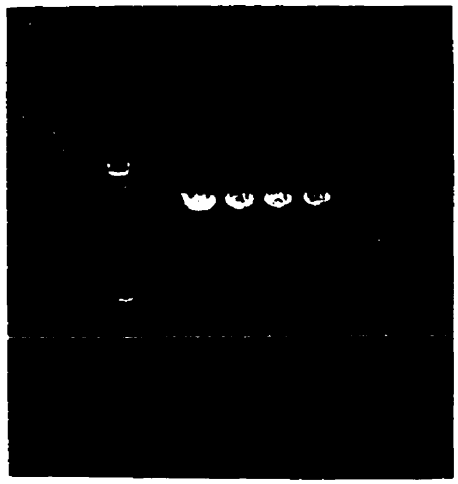

Figure 7. Gel electrophoresis (1% agarose) of p-GEX4T-2 for verification of plasmid size, following linearization with Not I. Left lane represents the molecular weight ladder (1Kb). Right lanes represent 4 samples (4 different colonies) of the linearized plasmid. Position of the bands indicate the correct size (4.9kb)

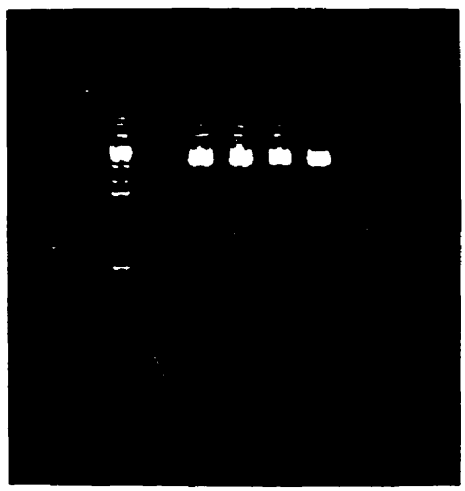

Figure 8. Gel electrophoresis (2% agarose) of p-GEX4T-2 for verification of insert size (153bp), following double digestion with BAM HI and ECO RI. Left lane, molecular weight ladder (1Kb). Right lanes, 4 samples (from 4 different colonies) of the isolated insert. Position of band verifies correct size.

The plasmid isolated using the Qiagen miniprep kit was then used to transform more bacteria as described above. A larger culture was then prepared (500mL) and a maxi prep (Qiagen #12162) was performed following the instructions of the manufacturer to isolate a larger quantity of desired plasmid. The resulting DNA concentration was determined via UV spectrophotometry:

DNA concentration = A260 x 0.05 x Dilution factor.

This larger amount of plasmid DNA containing the sequence of interest was subjected to double digestion and was assayed by a 2% LMPA (Low Melting Point Agarose, GIBCO BRL 5517UB) preparatory gel. Two lanes were employed representing the DNA ladder (1kb, GIBCO BRL 15615-016) and the double-digested plasmid DNA. Once the band representing the 153bp DNA piece was sufficiently separated from the rest of the plasmid, it was removed using a sterile blade and the desired sequence was extracted from the gel following the instructions of the Gel Extraction Kit by Qiagen (28704).

Agarose gel electrophoresis of plasmid DNA (p-GEX4T-2)

Agarose gel electrophoresis was employed to determine the efficiency of the isolation procedure and the integrity of the isolated plasmid DNA, using a 76 x 100mm gel tray. Powdered agarose (GIBCO BRL, # 5510UA) was added to 39mL of 1X TAE buffer to achieve a final 1% (w/v) concentration. This agarose solution was placed in an 125mL Erlenmeyer flask and was heated in a boiling water bath until completely dissolved. The gel solution was allowed to cool until it was comfortable to hold and 20µL of ethidium bromide from a 1mg/mL stock were added to achieve a final concentration of 50µg/mL. The gel mixture was mixed gently, poured into the gel tray with the gel comb already placed in position and was allowed to sit at RT

for 45-60min. The combs and the masking tape were then removed, the gel tray was placed in position in a GNA-100 gel box (Pharmacia # 18-1517-01) and 1X TAE buffer was added in the gel box to cover the gel to a depth of at least 1mm.

The sample volume that can be applied in a well depends upon the thickness of the gel used and the dimensions of the comb. In the present case, the total volume of the sample was 10-12 μL, 80% of which was the digested plasmid DNA while the loading buffer made for the remaining 20%. The samples were carefully loaded into the wells using a fresh, sterile micropipette, one for each sample.

Once the wells were loaded, the electrodes were connected to the EPS 500/400 power supply (Pharmacia # 19-1907-01). At pH = 8.0, DNA is negatively charged and migrates towards the anode during electrophoresis. Thus, the gel box was connected in such a way that the cathode was closest to the sample wells. The voltage was initially set to 100V for 1min, to ensure that the DNA had entered the gel, and was then reduced to 45V. The electrophoresis was allowed to continue until the bands were well separated and was monitored by UV excitation of ethidium bromide.

2. **RORα**

This sequences was kindly provided in a BAC clone from Dr. Bruce Hamilton (University of California San Diego). The BAC clones for both sequences (PLCβ3, RORα), required for the FISH experiments, were isolated following the QIAGEN Large-Construct Kit protocol (Qiagen, # 12462), a protocol designed specifically for the isolation of BAC, PAC, and cosmid DNA.

Fluorescent *In Situ* Hybridization (FISH)

Coverslip coating for FISH experiments

To ensure maximum adhesion of the tissue sections during the hybridization experiments, the coverslips were coated with aminopropyltriethoxysilane (Sigma #A-3648). Specifically, the coverslips were placed vertically in a porcelain rack (Fischer Scientific) and immersed in a detergent solution (2% Decon 75, BDH #B56019, 30min, RT). Using a specifically designed clamp to hold the rack, the coverslips were then thoroughly washed in distilled water to remove any traces of the detergent. Excess water was drained off and the rack was immersed in acetone for 1-2min. Excess acetone was drained off and the coverslips were then placed in acetone containing 2% (v/v) 3-aminopropyltriethoxysilane for 5 min (this step was performed in the fume hood). Excess coating solution was again allowed to drain off and the coverslips were washed briefly in distilled water. Upon draining excess water, they were left to air-dry at RT overnight and were stored at RT.

Biotinylation of insert DNA

Biotinylation of the BAC DNA for all three sequences was performed following the BioNick Labelling System Protocol (Gibco BRL, #18247-015) with the following modifications. Upon addition of the stop buffer, 1μL of the final volume was placed on a nylon transfer membrane (Hybond Nucleic acid transfer membranes). This was termed the "before clean-up" sample. Removal of unincorporated nucleotides was carried out according to the protocol of the QIAquick Nucleotide Removal Kit (using a microcentrifuge, Qiagen, #28304). To maximize binding and retrieval of biotinylated DNA, the centrifugation step using PN buffer (supplied with the kit) was extended to 2min and during the second centrifugation with PE buffer (also supplied

with the kit) the lid of columns was left open. The latter was done to ensure complete evaporation of the alcohol whose presence could prevent the elution of the DNA during the final step.

Upon elution of the biotinylated DNA (termed "after-clean up" sample), 1μL was also placed on the nylon transfer membrane. The rest of the biotinylated DNA was then precipitated by adding 10μL of salmon sperm DNA (Roche #1467 140, 10mg/mL) to assist DNA precipitation, 40μL of distilled water, 10μL (1/10 of the final volume) of sodium acetate (pH = 5.2) and 220μL (2 volumes) of absolute ethanol. The final mixture was vortexed briefly and stored at -20^{0}C. It was centrifuged (4^{0}C, 20min, 13000g) the following day and the supernatant was carefully removed. The DNA pellet was suspended in 50μL of hybridization buffer and stored at -20^{0}C.

Immunoblotting of biotinylated insert DNA

Immunoblotting of the insert was carried out routinely to ensure that the probe used in each hybridization experiment was indeed biotinylated. On the nylon transfer membrane, 1 μL of the following was applied: negative control (unbiotinylated DNA in distilled H_2O), positive control DNA (previously biotinylated, after clean-up), before- and after- clean up biotinylated DNA (see above). The membrane was submerged in blocking buffer (4% BSA, PBS, 30min, RT) in a 50 x 9 mm petri dish (Falcon # 10006). The blocking buffer was then aspirated and the membrane was further incubated in strepavidin-alkaline phosphatase (1:2000 in 4% BSA, 2h, RT) followed by washing (3x5min, PBS). The membrane was then washed with detection buffer followed by incubation (approximately 20-30min, RT) in substrate solution (22μL of NBT and 16.5μL of BCIP in 5μL of detection buffer). For instructions on the making of the substrate

solution, the BCIP/NBT combo (Gibco BRL, # 18280-016) protocol was followed. Both the detection buffer and the substrate solution were freshly prepared and the latter was kept in the dark prior to use.

FISH on cultured kidney fibroblasts

Cells, grown on coverslips, were previously fixed for 90min, washed (PBS, 3x5 min) and stored at 4^0C, PBS (0.02% sodium azide). At the beginning of every FISH experiment, cells were washed with distilled H_2O, 3x5min, to remove any traces of PBS that could interfere with the following, extraction step. The cells were then extracted (0.25% Triton X-100, 0.25% NP-40, Sigma #127087-87-0, in 0.2N HCl, 30min, RT), washed with PBS (3x5min) to ensure removal of the detergent, and incubated in RNAse A (100µg/mL, 37^0C, 1h). After washing with PBS (3x5min), the cells were rinsed once with protease buffer before digestion with proteinase K (10µg/mL, protease buffer, 20min, RT). The duration of the digestion treatment was empirically determined based on preservation of morphology and hybridization efficiency. Cells were monitored during this step and signs of adequate digestion included pale nuclei and nucleoli.

Cells were then equilibrated overnight in 70% deionized formamide (EM/BDH # 4650) 2XSSC, to avoid any morphological distortion associated with dehydration. Following equilibration, cells were denatured (70^0C waterbath, 70% formamide, 2XSSC, 2min) and then re-equilibrated in 50% formamide, 2XSSC, 0^0C, 10min). Prior to the denaturation step, the biotinylated probe, already in hybridization buffer, was placed in a boiling waterbath for 2min and then immediately returned on ice, so that it would be at the same temperature as the re-equilibrated tissue. Each coverslip was inverted and mounted onto a microscope slide in 25 µL

(500ng) of the biotinylated probe and carefully sealed with rubber cement to prevent evaporation of the hybridization mixture. This "sandwich" was incubated at 37^{0}C, 48h.

At the end of the hybridization, the rubber cement was pealed off and the coverslips were carefully lifted off the slides by placing the latter in a slide rack filled with 2XSSC. Cells were first washed in 50% formamide, 0.1XSSC, 45^{0}C, 3x15min and then in 0.1XSSC also at 45^{0}C, 3x15 min. Following the second post-hybridization wash, an immunocytochemistry protocol was carried out to detect the hybridization signals. Specifically, following blocking (4% BSA, 2h, RT), the probes were marked by an anti-biotin monoclonal Ab (Boehringer Mannheim, # 1 297 597, 1:1000 4% BSA, PBS, 2h, 37^{0}C) and unbound antibody was removed by washing (PBS, 3x5min). Following an additional blocking period, probes were detected by a FITC-conjugated anti-mouse IgG (Boehringer Manheim, # 821462, 1:100 4% BSA, PBS, RT, 2h). Finally, the cells were washed again (PBS, 3x5min), counterstained with ethidium bromide (0.5µg/mL, RT, 10min) and mounted using p-phenylenediamine as an anti-fading agent (see immunocytochemisty section above). The resulting hybridization signals were visualized using confocal microscopy as described above.

FISH on cerebellar tissue sections

Cerebellar tissue was sectioned using a vibratome as described above and sections were immediately adhered to silane-coated coverslips (22 x 22mm). They were then stored in PBS (0.02% sodium azide, 4^{0}C) for at least 2-3 days before used in a hybridization experiment. Such storage ensured the adherence of the sections on the coverslips throughout the steps of the hybridization. Upon removal from the fridge, excess PBS was carefully shaken off and the sections are placed in a 45^{0}C, dry incubator for 15min. This step was also determined to enhance

the adherence of the sections on the coverslips, while upon confocal analysis, this drying step was not found to affect the retention of morphology of the tissue. The sections were subsequently washed in distilled H_2O (3x5min) to remove any excess PBS, followed by an extraction step (0.2N HCl, 45min, RT). Sections were then washed once in PBS and permeabilized overnight (1% Tx-100, 1% NP-40, PBS, RT). Sections were subsequently washed, PBS (3x10min), RNAse A treated (100μg/mL, 2h, 37^{0}C) and washed again, PBS (3x10min). They were then rinsed once with protease buffer followed by digestion with proteinase K (40μg/mL, protease buffer RT). The digestion step was interrupted by washing, PBS (3x10min). The duration of the digestion was again empirically determined based on preservation of morphology and hybridization efficiency. Specifically, the optimal digestion times for PLCβ3 and RORα were determined to be 15 and 30min, respectively.

Following digestion, the sections were equilibrated, 70% Formamide-2X SSC, RT, overnight. The sections were then denatured (70% formamide-2X SSC, 70^{0}C waterbath, 12.5min) and re-equilibrated (50% formamide-2X SSC, 0^{0}C, 10min). The coverslips were then mounted using biotinylated probe (35μL per coverslip, 0.02μg/μL), sealed with rubber cement and incubated at 37^{0}C for at least 48h. Prior to mounting, biotinylated probe was prepared as described above under *FISH on cultured cells*. Following hybridization and post-hybridization washes (50% formamide-2X SSC and 0.1X SSC, both 3x15min, 45^{0}C), the hybridized probes were marked and detected by applying the immunocytochemistry protocol followed for kinetochore labelling in cerebellar tissue sections (see above). The primary and secondary antibodies were as those used for FISH on cultured cells. The signals were visualized using dual-channel confocal laser microscopy as described above.

Morphometric analysis of radial position of RORα and PLCβ3 signals

An alternative method of analysis of the spatial, intra-nuclear position of both the RORα and PLCβ3 signals was applied that permitted statistical analysis. For this, two representative sets of Purkinje neurons were analyzed, each set labelled for one of the two sequences at different postnatal days. For each nucleus, a 3-D volume along with a series of projected views of the 3-D nuclear volume rotated at 10^0 increments were constructed using ZEISS LSM software. For each signal, the view at which it was maximally displaced from the axis of rotation was considered to represent the optimal orthogonal view and was chosen for analysis. In this 3-D view, the radial vector connecting the centroid of the nucleus to the signal was expressed as a fraction of the same vector extended to the nuclear envelope. These fractions of radial vectors (or distances) were plotted (Fig. 19) and the differences in the means among different postnatal days were compared using the Tukey test.

STATISTICAL ANALYSIS

To test for significant differences between means (three and above) a normality test was employed at the $p \leq 0.05$ level of confidence followed by a test that allowed multiple comparisons, namely the Tukey test, at the $p \leq 0.001$ level of confidence. In cases where the normality of the population could not be assummed, the Kolmogorov-Smirnov non-parametric test was employed and comparisons between observed and expected distributions of kinetochore signal sizes were carried out at the $p \leq 0.05$ level of confidence.

RESULTS

PART I:Centromeric domains

Comparison of Kinetochore Signal Size and Number between Fibroblasts and adult Purkinje Neurons

In the fibroblasts from the kidney cultures the total number of kinetochore signals observed per nucleus (n = 680 kinetochore signals, 17 nuclei) was found to be 40 ± 0.00 (mean ± SEM). This number was consistently greater than the number of signals observed in adult Purkinje neurons (Table 1). In addition, the sizes of kinetochore signals in fibroblasts exhibited a very low variability compared to those in adult Purkinje neurons (Table 1). Considering the fact that these fibroblasts are rapidly cycling cells, the kinetochore signals observed in interphase were deemed to represent kinetochores associated with single chromosomes (Fig. 9). The differences in the number of kinetochores between the fibroblasts and the adult Purkinje neurons (Figs. 9 and 10, Table 1) suggest that the smaller number of signals together with the larger variability in size in nuclei of Purkinje neurons are not a result of inadequate detection of all kinetochores present. Rather, the differences were found to be attributable to clustering of kinetochore regions of different chromosomes (see below), a common observation in neurons (Manuelidis, 1985; Billia and De Boni, 1992; Park and De Boni, 1992).

Table 1: Number and size of kinetochore signals in fibroblasts and Purkinje neurons

	Signals/nucleus (mean ± SEM)	Mean Relative Signal size (mean ± SEM)
Fibroblasts	40.00 ± 0.00	0.0249 ± 0.0004
Purkinje neurons (adult)	10.8 ± 0.46	0.084 ± 0.068

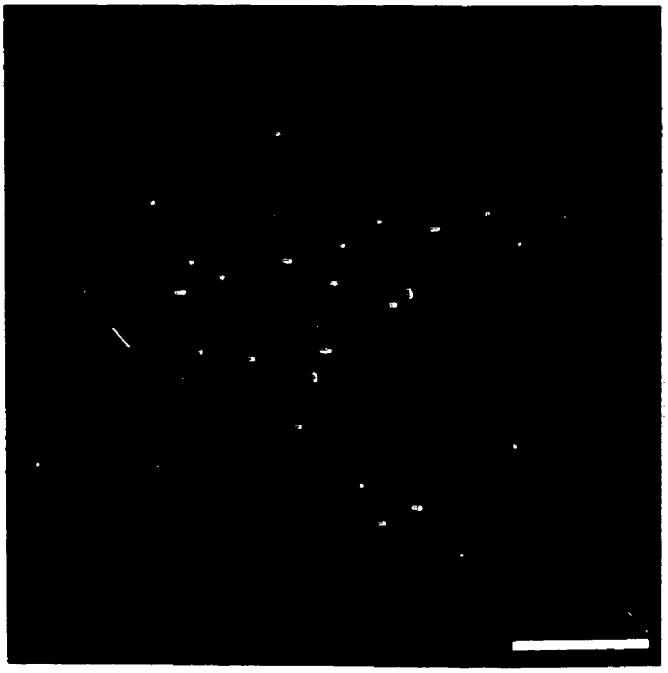

Figure 9: Single confocal section of a fibroblast nucleus (counterstained with ethidium bromide) in interphase. Note that the number of kinetochore signals (white) is larger and their variability in size, is lower, compared to those in Purkinje neurons (Fig. 15). Bar = 5 μm.

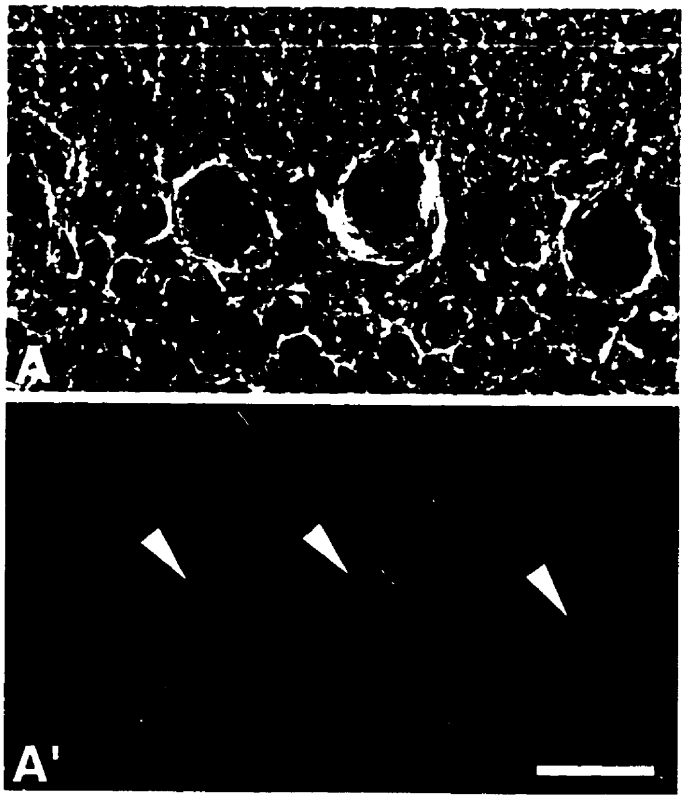

Figure 10: Confocal images of adult cerebellum showing architecture of cortex and characteristic monolayer of Purkinje neurons (arrowheads). A. Phase contrast image. A'. Corresponding fluorescence image, showing kinetochore clusters (yellow) in nuclei of Purkinje neurons. Bar = 20 μm.

Determination of the number of kinetochore signals

a. Fibroblasts

Kinetochore signal sizes, when normalized, exhibited a mean NTFI of 0.0249 ± 0.0004 (n = 680 kinetochores, 17 nuclei). This mean value compares favourably with 0.025, the equivalent of the theoretical signal size of one of the 40 kinetochores present in a murine, interphase nucleus. Each NTFI value and the above mean were then divided by 0.025 to obtain the relative signal size of each kinetochore. Relative signal size is defined as the number of kinetochores that contributes to each individual signal. The resulting values exhibited a new mean of 0.997 ± 0.017, which was rounded to 1.000 ± 0.017 and defined as the "unitary" value. A frequency histogram of these relative signal sizes (Fig. 11) shows that the majority of signals clusters around a relative size of 1, i.e. is representative of single kinetochores. The unitary value of 1.000 with its associated variance of 0.199, was then used to construct expected theoretical distributions of kinetochore signal sizes resulting from the potential clustering of kinetochores of more than one chromosome in Purkinje neurons (see below). The kinetochore signal to which the unitary value corresponded could still be detected in more than one optical section. Any signal that could not be detected in at least two optical sections was considered to represent noise and, thus, neither was it included in the count of signals nor was its size determined.

b. Purkinje neurons

To determine the presence and extent of clustering of kinetochores in nuclei of Purkinje neurons, the calculated NTFIs of kinetochore signals from a representative subset of nuclei (n =

793 kinetochore signals, 81 nuclei) were divided by 0.025 to obtain relative signal sizes. These were then plotted as a frequency histogram as well as a line plot (solid line, Fig.12) to show the distribution of kinetochore cluster sizes.

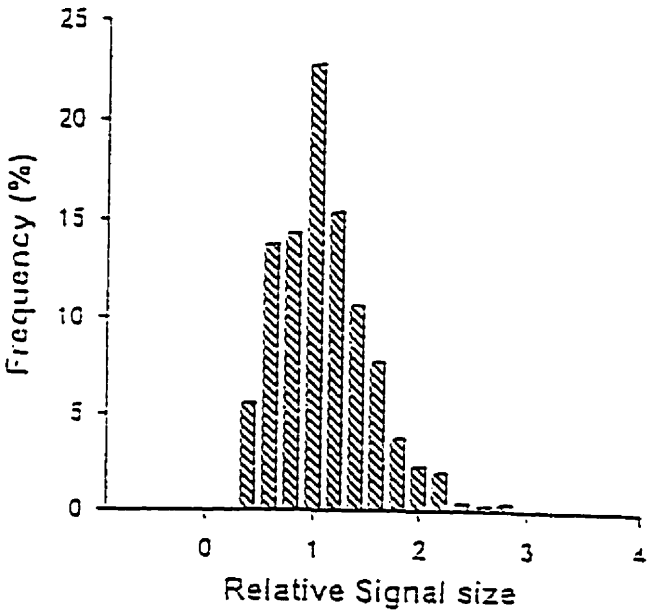

Figure 11: Frequency histogram of relative kinetochore signal sizes (n = 680 signals, 17 nuclei) in cycling fibroblasts. Note clustering around the mean relative signal size of 1, representative of the size of a single kinetochore.

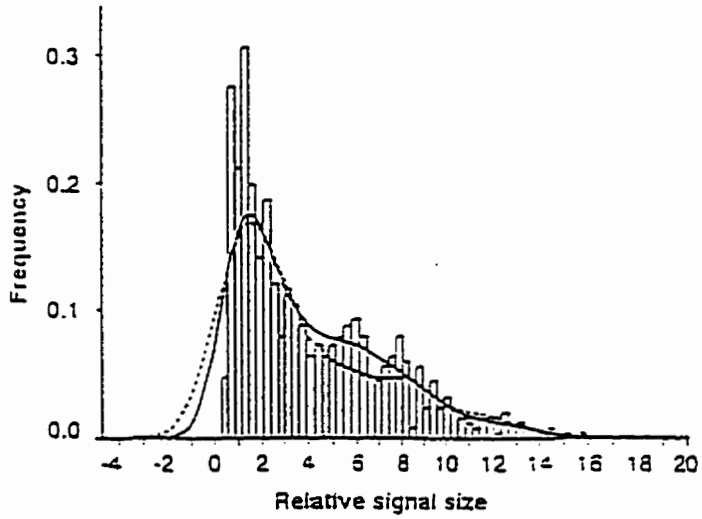

Figure 12: Frequency histogram of relative kinetochore signal sizes (n = 793 signals, 81 nuclei) in Purkinje neurons (open bars) and corresponding distribution curve (solid line, arbitrary units). This observed distribution curve could not be shown to be different (p=0.22; Kolmogorov-Smirnov) from the expected distribution resulting from seven Gaussian populations of signal sizes at different means (dotted line).

To confirm that this distribution results from contributions from several populations which exhibit clustering of kinetochores, i.e. with means at multiples of the signal size corresponding to a single kinetochore, a theoretical distribution was constructed (dotted line, Fig. 12), from seven Gaussian populations. The first of these was assigned the mean and variance (1.000 ± 0.199) of the relative signals sizes derived from fibroblasts. The remaining 6 populations were assigned multiples of the above mean and variance. Populations with higher means were assigned variances at multiples of that of the first, to maintain constant the contribution of each population to the final, theoretical curve. The population with a mean of 2, for example, was assigned a variance double that exhibited by the population with a mean of 1, etc. In order to determine whether this propagation of variance was justifiable, the individual TFIs of all signals within each of 17 nuclei were summed and their mean determined. The resulting, tight distribution (1083.87 ± 75.70) was taken to indicate that the variance is due to variability in individual signal sizes and not measurement error, and could thus be propagated.

Group limits for the composite, theoretical curve, that is, the points at which populations 1 and 2, 2 and 3 etc. meet, were defined by calculating the probability with which a particular signal was expected to be found in one of the contributing Gaussian distributions. The observed distribution (solid line, Fig. 12) could not be shown to be different ($p = 0.22$, Kolmogorov-Smirnov) from the theoretical, composite distribution (dotted line, Fig. 12).

The above result shows that the larger kinetochore signals in the nuclei of Purkinje neurons indeed arise from clustering of single chromosomes at their kinetochore region. This conclusion permitted the assignment of kinetochore signals, in terms of their size, to groups representative of either one or multiple kinetochores. Upon classification of the sizes of 793 kinetochore clusters (81 nuclei), a value equivalent to 3308 individual kinetochore signals was

obtained. This corresponds to 40.8 kinetochore signals per nucleus, a value close to the theoretical chromosome complement of 40. When calculated individually for each nucleus (n = 81), the mean number of kinetochores was similarly found to be 40.8 ± 0.114, with a range from 38 to 43. These results thus support our position that the quantification technique employed is indeed sufficiently sensitive to detect all of the centromeric domains present in a nucleus and permits the determination of the number of individual structures contributing to each kinetochore signal.

Changes in the Nuclear Topology of Purkinje Neurons with postnatal development

a. Number and Size of Kinetochore Signals

The number of kinetochore signals in nuclei of Purkinje neurons decreased significantly ($p \leq 0.001$) from a mean of 11.44 ± 0.44 (n = 52 nuclei) at postnatal day 0 (P0) to 8.78 ± 0.24 (n = 36 nuclei) at P3. The mean number of signals then remained constant until P12, and increased again to 11.16 ± 0.27 (n = 62 nuclei) at P15. The latter persisted into adulthood (Fig. 13). The decrease and increase in the number of signals are taken to indicate the clustering and de-clustering of kinetochores, respectively. The existence of such events is further illustrated by age-dependent changes in the frequency distribution of signal sizes (Figs. 14, 15). While kinetochore signals of small size are prominent at P0, the distribution shifts to larger signal sizes between P3 and P12. From P15 onward, however, the distribution returns to a pattern similar to that at P0 (Fig. 14). Thus, the changes in the number of kinetochore signals are paralleled by changes in the distribution of their sizes.

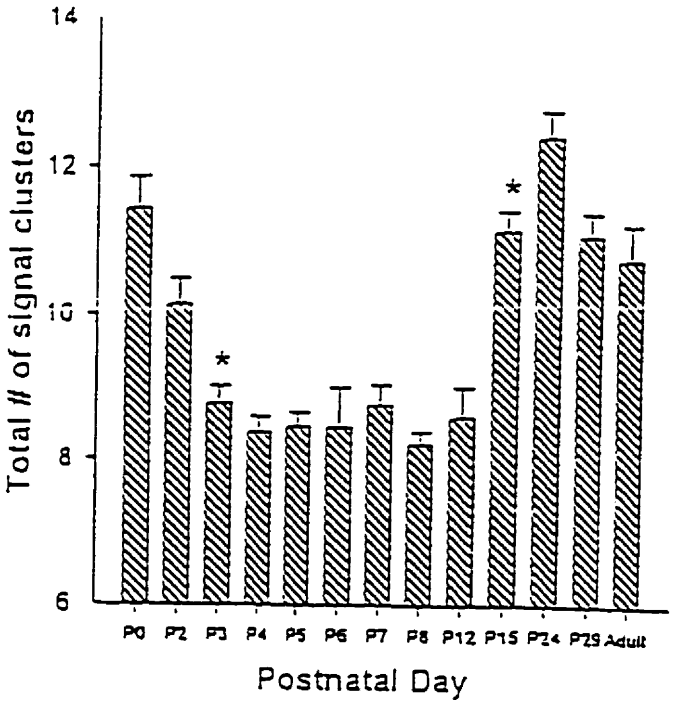

Figure 13: Change in the total number of kinetochore signal clusters in Purkinje neurons as a function of postnatal age. Note the decrease at P3 (asterisk) and the increase at P15 (asterisk) associated with clustering and de-clustering of kinetochore signals, respectively ($p \leq 0.001$, Tukey Test). Error bars represent SEM.

b. Spatial distribution of kinetochore signals and chromosomes

The spatial distribution of signals in the three nuclear compartments, namely the periphery, the nucleoplasm and the nucleolus, also changes with development (Fig. 16). The fraction of the number of signals in the peripheral compartment decreases with ongoing differentiation, while the number in the nucleolar compartment increases. The number of signals in the nucleoplasmic compartment increases transiently at a stage preceding that at which the

increase in the nucleolar compartment occurs. Therefore, there exists a re-distribution, with development, of kinetochore signals towards the nucleolus.

Each kinetochore signal represents one or more kinetochores. By determining the number of kinetochores, i.e. chromosomes, contributing to each signal, changes, with postnatal development, in the fraction of the chromosome number in each nuclear compartment, could be determined. These changes (Fig. 17) were found to exhibit a pattern similar to that displayed by the changes in the compartmentalization of kinetochore clusters (Fig. 16). Thus, in Purkinje neurons of newborn mice (P0), the majority of chromosomes are found at the nuclear periphery. As development progresses, centromeric domains of chromosomes shift from the nuclear periphery towards the nucleoplasmic compartment and finally towards the nucleolus.

Figure 14: (next page). Frequency histograms of relative kinetochore signal sizes in Purkinje neurons at four postnatal ages. Note the shift of the distribution to the larger signal sizes with ongoing differentiation (P3 onwards) and the re-establishment of the distribution characteristic of P0, at P24 (adult). Changes in the distribution of signal sizes correspond to changes in the number of signal clusters that occur with postnatal development (Fig. 13).

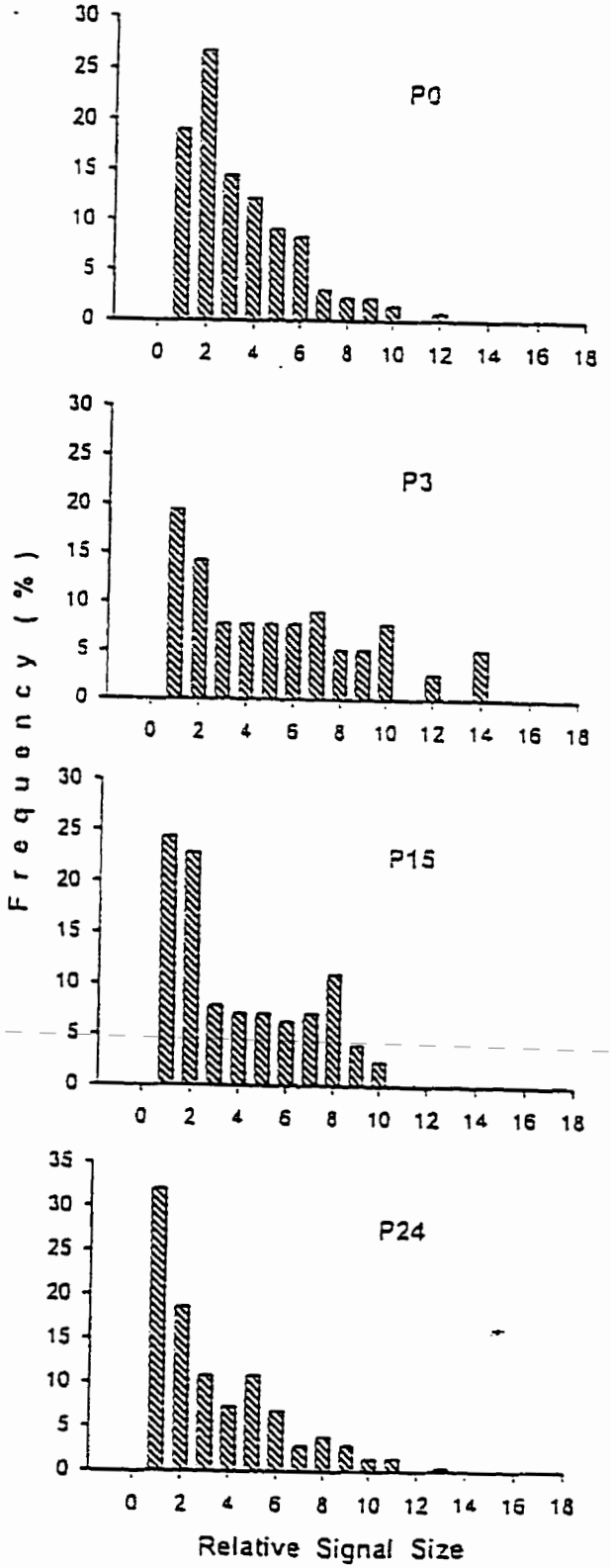
P0
P3
P15
P24
Frequency (%)
Relative Signal Size

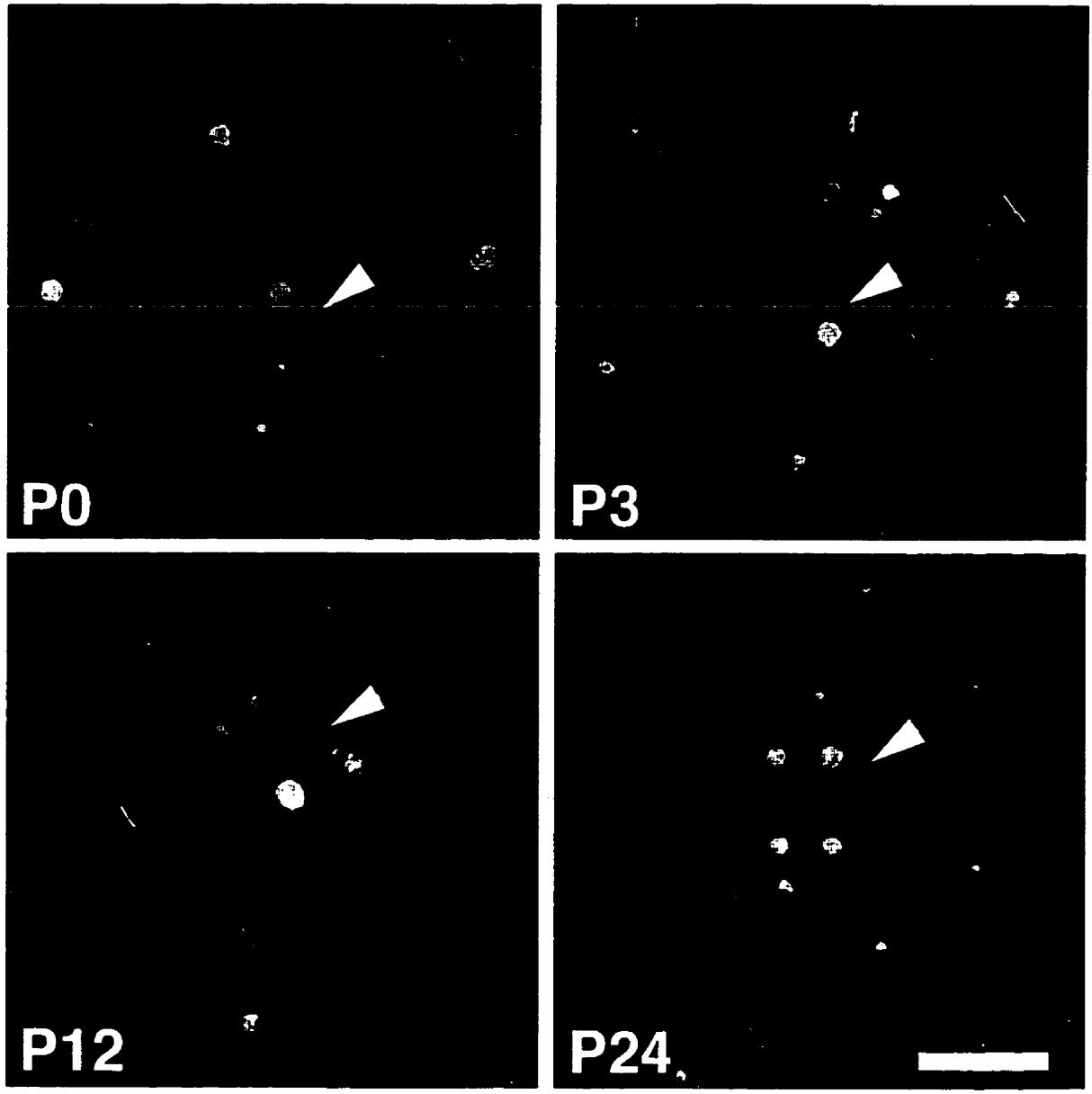

Figure 15: Nuclei of Purkinje neurons at different developmental ages, shown as composite projections of serial confocal sections. Note increased association of kinetochore signals with the nucleolus (arrowheads) at P12 and P24. Note also the decrease in signal number by P3 and increase by P24. The superposition of optical sections in these face-on views obscures some kinetochore signals. Bar = 3 μm.

Figure 16: (next page). Changes in the spatial distribution of the fraction of kinetochore signals in the three nuclear compartments with postnatal development. Note decrease in the periphery at P2 and P4 and a corresponding, transient increase in the nucleoplasmic compartment. The latter precedes an increase in the fraction of kinetochore signals at the nucleolus, taken to indicate a redistribution of signals from the periphery to the nucleoplasmic compartment and ultimately to the nucleolus. Note different scale of y-axis for the nucleoplasmic compartment. Asterisks indicate those postnatal days showing the first significant difference (Tukey test, $p \leq 0.001$). Error bars represent SEM.

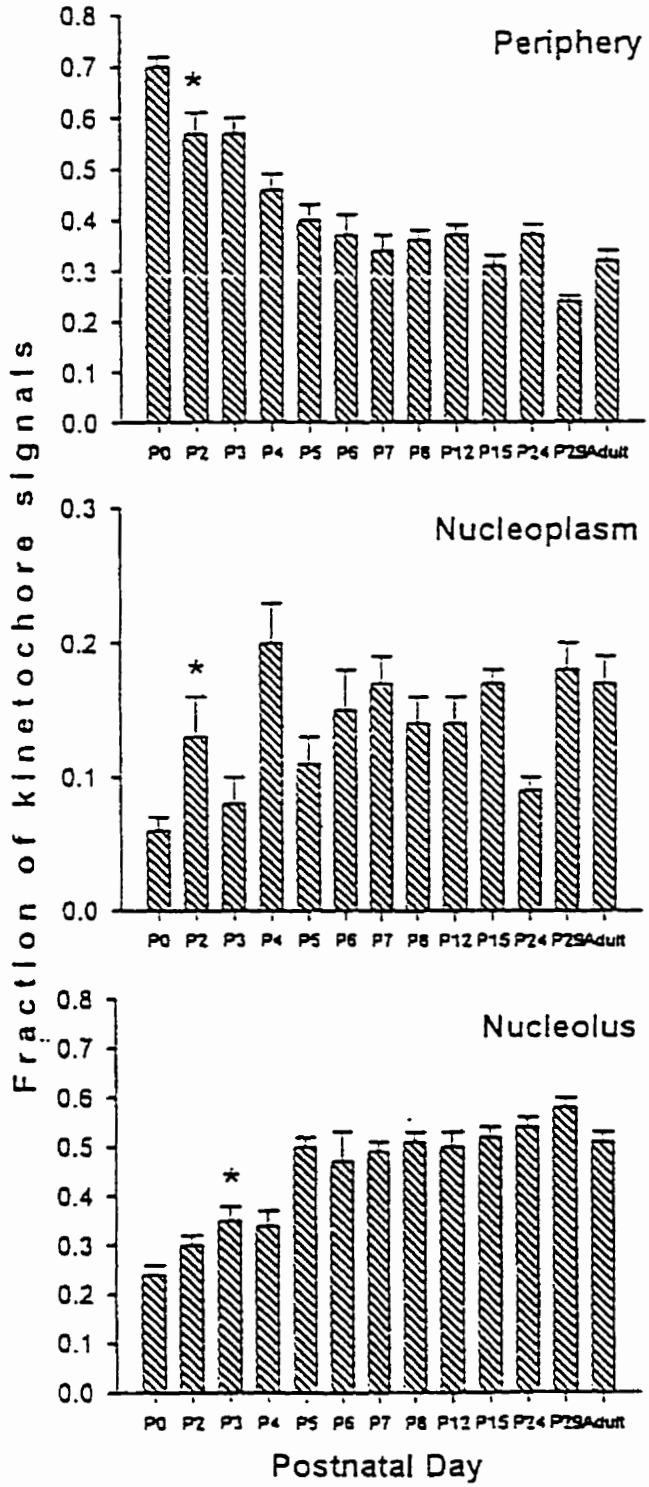
Periphery
Nucleoplasm
Nucleolus
Fraction of kinetochore signals
Postnatal Day
P0 P2 P3 P4 P5 P6 P7 P8 P12 P15 P24 P2SAdult
0.0 0.1 0.2 0.3 0.4 0.5 0.6 0.7 0.8
*

Figure 17: (next page). Changes of the fraction of the chromosome complement with postnatal development. The decrease in the fraction of chromosomes at the periphery by P4 is accompanied by a transient increase in the intermediate compartment and an increase in the nucleolar compartment. The latter change is followed by a further increase in the fraction of chromosomes at the nucleolus at P5. Changes in the fraction of the chromosome complement were assessed only for those postnatal ages at which the fraction of kinetochore signals changed (Fig. 16). Note different scale of y-axis for the nucleoplasmic compartment. Asterisks indicate those postnatal days showing the first significant difference (Tukey test, $p \leq 0.001$). Error bars represent SEM

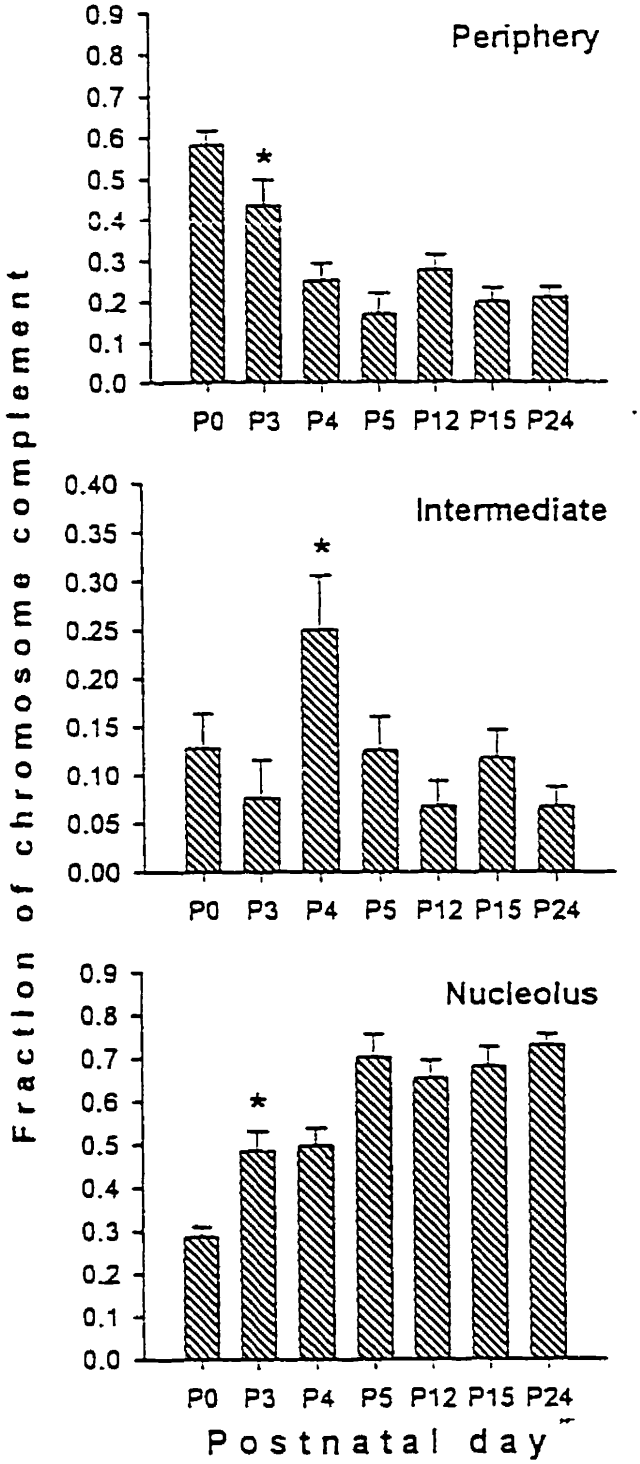
Periphery
Intermediate
Nucleolus
Fraction of chromosome complement
Postnatal day
P0 P3 P4 P5 P12 P15 P24
0.0 0.1 0.2 0.3 0.4 0.5 0.6 0.7 0.8 0.9
0.00 0.05 0.10 0.15 0.20 0.25 0.30 0.35 0.40
*

PART II: Purkinje-neuron specific sequences

Determination of number of sequence signals in Purkinje neurons

Both RORα and PLCβ3 are single copy genes, thus, two copies of each sequence should be detected in a murine cell of the standard diploid range. In agreement with this, the average number of signals per cell, representing these copies, was found to be 1.99 ± 0.0096 and 1.96 ± 0.013 for RORα and PLCβ3, respectively (Tables 2 and 3).

Table 2: Number of RORα signals in Purkinje cells

Postnatal day	n (number of cells)	Total number of signals	Signals per cell (mean ± SEM)
P3	29	58	2 ± 0.00
P5	35	70	2 ± 0.00
P8	15	29	1.93 ± 0.067
P12	26	51	1.96 ± 0.038
Adult	41	82	2 ± 0.00
Total	146	290	1.99 ± 0.0096

Table 3: Number of PLCβ3 signals per cell

Postnatal day	n (number of cells)	Total number of signals	Signals per nucleus (mean ± SEM)
P2	10	20	2 ± 0.00
P3	38	76	2 ± 0.00
P5	37	72	1.94 ± 0.038
P8	40	77	1.92 ± 0.042
P12	26	51	1.96 ± 0.038
Adult	58	114	1.96 ± 0.024
Total	209	410	1.96 ± 0.013

Changes in the spatial distribution of sequence signals as a function of development

i. RORα

The spatial, intranuclear distribution of the RORα signals did not change as a function of postnatal development (Figs. 18,19,20). At all postnatal days, P3, P5, P8, P12, and adult, the majority of the cells exhibited their signals associated with the nuclear periphery. As shown in Fig. 18, an average of 70% (± 3.36) of the RORα signals is associated with the nuclear periphery across development, whereas only 20% (± 3.59) and 10% (± 2.1) are associated with the intermediate and nucleolar compartments, respectively. This distribution pattern does not change as a function of development (Fig. 18), indicating that the association with the periphery is maintained.

Analysis of the radial distance of the RORα signals at different postnatal days also shows that the mean and distribution pattern of these signals are overall maintained across postnatal development (Fig. 19). The mean radial distance at P3 was found to be 60.5 ● 2.8 and, upon statistical comparison of the mean radial distances at different postnatal days, no significant difference could be shown (Tukey test, $p \leq 0.001$). The maintainance of the association of RORα signals with the nuclear periphery is also evident from the confocal micrographs of Purkinje neuron nuclei shown for different postnatal days (Fig. 20, A-E).

Figure 18: (next page). Changes in the spatial, intranuclear distribution of RORα (open squares) and PLCβ3 signals (solid circles) as a function of post-natal development. The majority of RORα signals (open squares) is associated with the periphery throughout development. In contrast, while the majority of PLCβ3 signals (solid circles) is associated with the periphery at early post-natal days (P2/P3), the fraction of these peripheral signals decreases at P5, concomitantly with an increase in the fraction associated with the nucleolus. This indicates a relocation of PLCβ3 signals to the nucleolus.
Note different y-scale for the intermediate compartment.

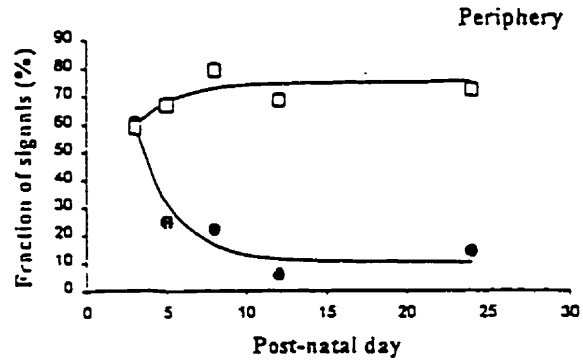
Periphery
Fraction of signals (%)
0
10
20
30
40
50
60
70
80
90
0
5
10
15
20
25
30
Post-natal day

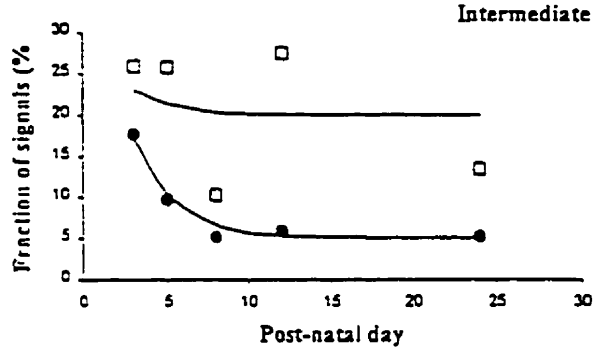
Intermediate
Fraction of signals (%
0
5
10
15
20
25
30
0
5
10
15
20
25
30
Post-natal day

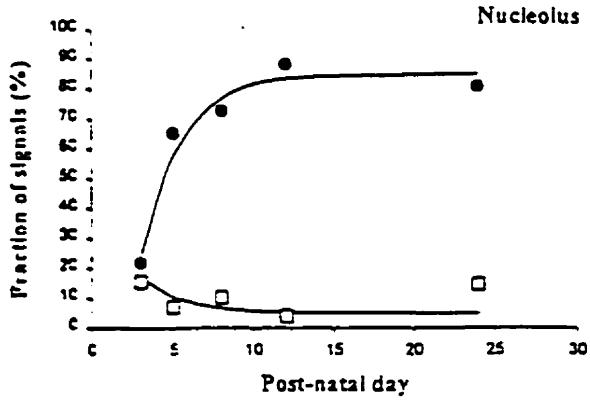
Nucleolus
Fraction of signals (%)
0
5
10
15
20
25
30
Post-natal day

PLCβ3

In contrast to RORα, the spatial, intranuclear distribution of PLCβ3 did change as a function of postnatal development (Figs. 18,19,20). The majority of young (P2-P3) Purkinje cells exhibited their PLCβ3 signals associated with the periphery. At this early stage, 60% of the signals are associated with the nuclear periphery, whereas only 20% are associated with each of the intermediate and nucleolar compartments, respectively (Fig. 18). As development progresses, this distribution is reversed. Specifically, at P5, the majority of signals (65%) is found associated with the nuclear periphery, 10% with the intermediate compartment and 25% with the nucleolus (Fig. 18). Therefore, there exists a relocation of PLCβ3 signals from the nuclear periphery towards the centrally located nucleolus, also evident in the confocal micrographs (Fig.20, A'-E'). The distribution pattern observed at P5 remained unchanged and persisted into the adult stage (Figs. 18 and 19).

Furthermore, this relocation is indicated by the significant difference in the mean radial distance of the PLCβ3 signals between P3 (58.7 ±3.2) and P5 (32.1 ± 2.4). From P5 onwards no significant difference in the mean and distribution pattern of radial distances could be shown to exist (Tukey test, $p \leq 0.001$)

It is of interest to note that the timeframe of the relocation of the PLCβ3 signals, between P3 and P5 (Fig. 18), coincides temporally with the shift of chromosomes as determined from changes in the spatial distribution of the chromosome complement across development (Fig. 17).

Figure 19: (next page). Polar plots of the radial distances for RORα (upper) and PLCβ3 (lower) as a function of postnatal development. For both plots, each quadrant represents a different postnatal day (counterclockwise; P3, P5, P8/P12 and Adult). The concentric circles represent fractions of the radial vector connecting the centroid of the nucleus to the signal, extended to the nuclear envelope. Overall, there is no change in the mean and distribution pattern of radial distances of RORα signals (upper plot) across development, besides a relatively small increase in the mean radial distance at P8/P12. The latter is most likely due to naturally occuring variability among Purkinje cells. In contrast, the mean radial distance of PLCβ3 signals (lower plot) decreased significantly between P3 and P5. No change in the mean and distribution pattern of the PLCβ3 signals exists from P5 onwards. Asterisks indicate significant difference (Tukey test, $p \leq 0.001$).

RORα

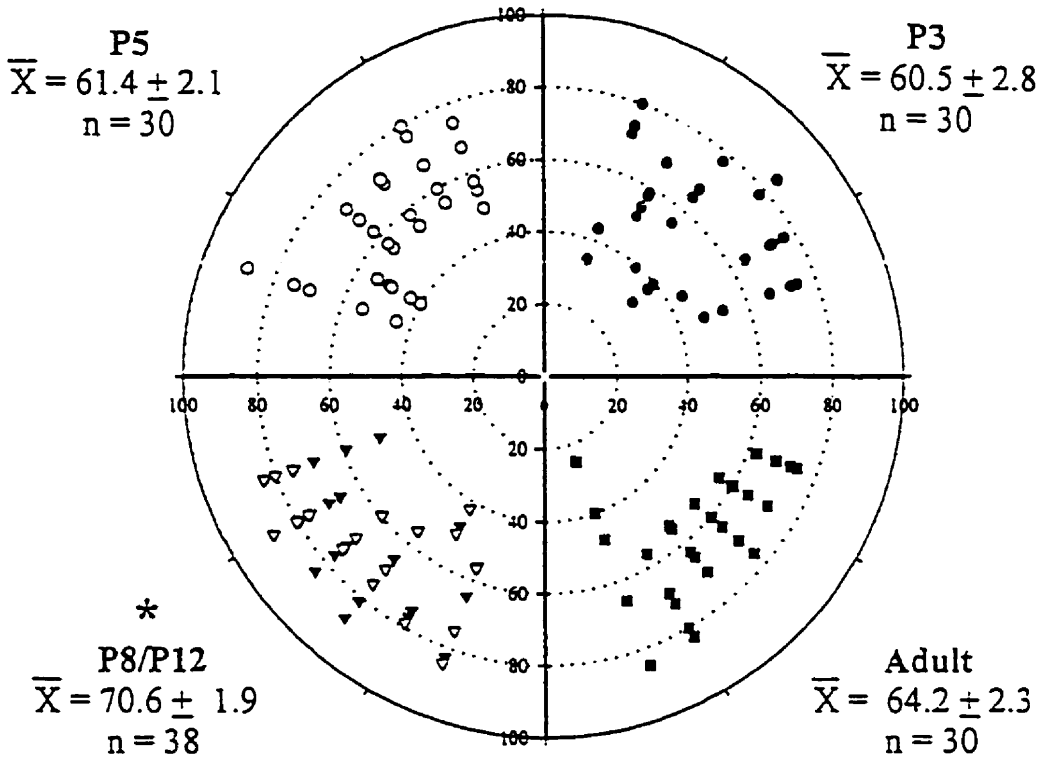
P5
$\overline{X}$ = 61.4 ± 2.1
n = 30
P3
$\overline{X}$ = 60.5 ± 2.8
n = 30
*
P8/P12
$\overline{X}$ = 70.6 ± 1.9
n = 38
Adult
$\overline{X}$ = 64.2 ± 2.3
n = 30

PLCβ3

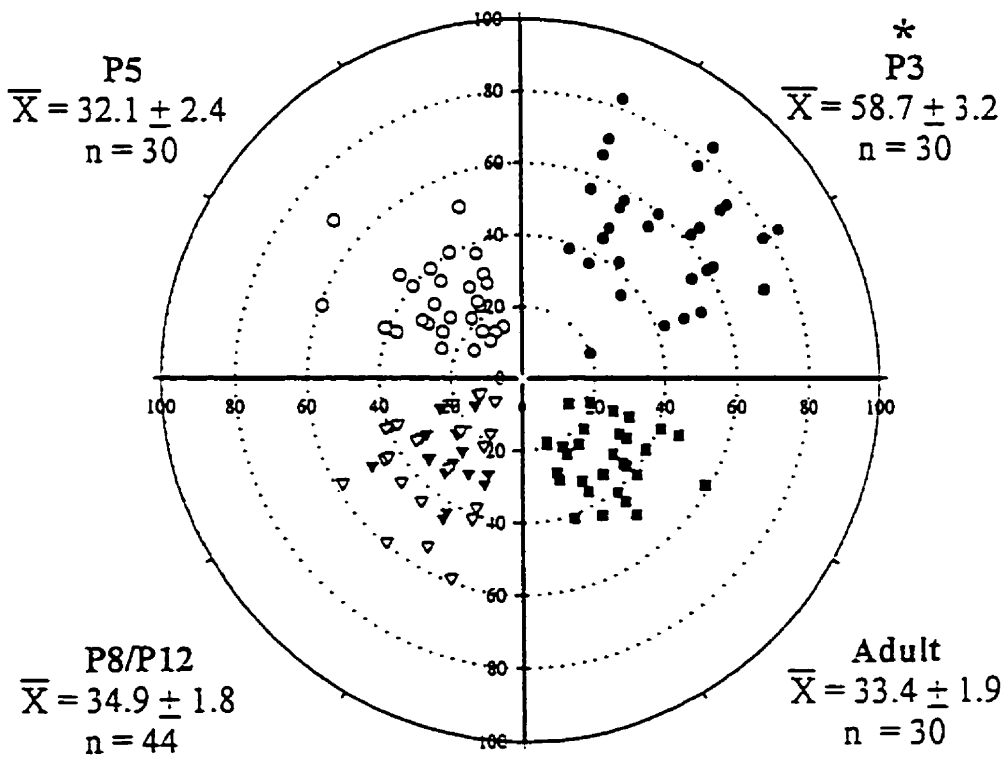
P5
$\overline{X}$ = 32.1 ± 2.4
n = 30
*
P3
$\overline{X}$ = 58.7 ± 3.2
n = 30
P8/P12
$\overline{X}$ = 34.9 ± 1.8
n = 44
Adult
$\overline{X}$ = 33.4 ± 1.9
n = 30

Figure 20: (next page). Confocal micrographs of Purkinje neuron nuclei at different postnatal days (A,A': P3; B,B' :P5; C,C', P8; D,D', P12; E,E', Adult), labelled for RORα (A to E) and PLCβ3 (A' to E'). Note the maintained association of the RORα signals (left panel) with the nuclear periphery during development. In contrast, PLCβ3 signals (right panel) relocate from the nuclear periphery at P3 (A') to the nucleolus at P5 (B'), where they remain.
Bar = 5μm.

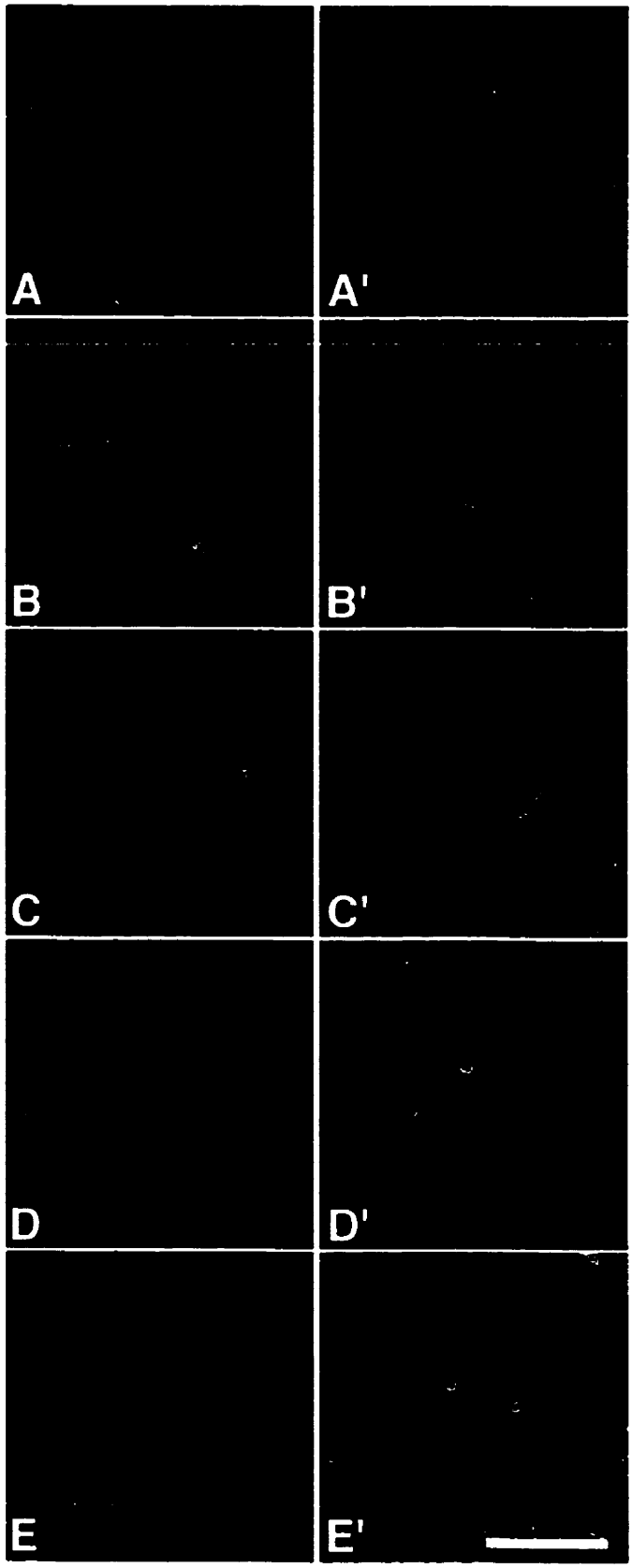
A
A'
B
B'
C
C'
D
D'
E
E'

DISCUSSION

The present study supports and extends previous findings which show that interphase nuclei exhibit a distinct, cell type-specific spatial topology of chromatin domains and in particular, centromeric domains (Manuelidis, 1984a; Billia and De Boni, 1991; Haaf and Schmid, 1991). Furthermore, the findings of this study support the existence of a temporal and potentially functional association between the topological organization of the nucleus and the functional commitment of the cell (Manuelidis, 1984a; 1985a; 1985b; Park and De Boni, 1992).

PART I: Centromeric domains

Results from this part of the study are in support of a dynamically organized nuclear topology and confirm part one of our hypothesis, according to which there is a particular developmental stage before or during which the adult topology is established.

Specifically, these results constitute evidence for major rearrangements of centromeric domains taking place during the postnatal development of PCs. Notably, there is a temporal association between the changes in both the number and the spatial, intra-nuclear position of centromeric domains and the onset of major differentiation events (Dunn *et al.*, 1998b).

The clustering events, indicated by a decrease in the total number of kinetochore signals (Fig. 13) along with the concomitant redistribution of these signals (Fig. 16) and of chromosomes (Fig. 15) from the nuclear periphery towards the centrally located nucleolus, between P3 and P5 coincide temporally with the beginning of the second developmental stage of PCs as defined by Dunn *et al.*, (1998b). Overall, this stage is characterized by a moderated progression in axonal development and an increase in the soma size while cytoplasmic

organelles and synaptic features remain poorly differentiated (Weber and Schachner, 1984: Jaeger *et al.*, 1988; Dunn *et al.*, 1998b). Notably, however, this is the stage during which significant dendritic differentiation (Dunn *et al.*, 1998b) takes place along with the parallel (Smith and Mullen, 1997; Yamada *et al.*, 1997) and climbing (Mason *et al.*, 1991) fibers contacting the PCs.

Most importantly, however, this is time of significant changes in gene expression. There is a number of Purkinje-neuron specific sequences that are either *de novo* expressed such as PLCβ3 (Watanabe *et al.*, 1998) or significantly upregulated. The latter include various subunits of the GABAA/BZ receptor (Zdilar *et al.*, 1991; 1992), the glutamate transporter EAAT4 (Yamada *et al.*, 1997), GluR 2/3 subunits of the AMPA-type glutamate receptor (GluR) (Bergmann *et al.*, 1996), δ2 subunit of the GluR (Takayama *et al.*, 1996), P400 (Maeda *et al.*, 1989), CaBPC28k (Iacopino *et al.*, 1990), calmodulin (Messer *et al.*, 1990), zebrin 1 (Sotelo and Wassef, 1991), mGluR1α (Ryo *et al.*, 1993), inositol 1,4,5- triphosphate receptor type 1 (Nakawaga *et al.*, 1996a) and L7 (Hamilton *et al.*, 1996).

Similarly, the declustering events, indicated by an increase in the total number of kinetochore signals between P12 and P15 leading to the establishment of the number of signals observed in the fully differentiated PCs (Fig. 13 and 15) is associated temporally with the onset of the third developmental stage as defined by Dunn *et al.*, (1998b). This stage is characterized by major somatic development, synaptic maturation, especially of the parallel fiber-PC synapses, and further dendritic outgrowth (Dunn *et al.*, 1998b). Sequences that undergo further upregulation during this time include the γ2 subunit of the GABAA/BZ receptor (Luntz-Leybman *et al.*, 1993), the δ2 subunit of the GluR (Takayama *et al.*, 1996) and the 2/3 subunits of the AMPA-type GluR (Bergmann *et al.*, 1996).

These temporal associations between developmental events, especially the ones related to changes in gene expression, and changes in the number and spatial distribution of kinetochore signals and of chromosomes are in support of a relationship between nuclear topology and the functional commitment of the cell. The fact that these neurons are in interphase during the course of their postnatal development allows us to exclude the possibility that the changes observed, all of them or in part, stem from variability introduced by cell cycle events.

In addition, the detection of a number of kinetochore signals, consistently less than the murine chromosome complement, along with the variability in the size of these signals (Table 1), were taken to indicate clustering of chromosomes at the kinetochore region. A representation of how such clustering is envisioned to be taking place is depicted in Fig. 21. Clustering of sDNA has been reported for a variety of cells including neurons (Manuelidis, 1984a; 1984b; Arnoldus *et al.*, 1989; Billia and De Boni, 1991), hepatocytes (Janevski *et al.*, 1995) and plant cells (Fussel, 1975; Church and Moens, 1976).

The quantification method applied in this study has been shown to be sensitive and accurate enough to provide values of fluorescence intensities that allow the determination of the number of contributing structures to each detected kinetochore signal. The finding of 40.08 signals per PC nucleus, a number equal to the murine chromosome complement, validates the changes reported here for the total number and spatial distribution of kinetochore signals. This finding also excludes the possibility that the observed changes arise from inadequate detection. Furthermore, the latter is supported by the finding of 40 individual kinetochore signals in the population of kidney fibroblasts, which served as a control and provided the unitary value corresponding to the kinetochore signal of a single chromosome.

An additional issue supported by the findings in this study regarding the number of chromosomes detected is the fact that PCs are of the standard diploid range, i.e., 40 (2n). This finding stands in contrast to the view that advocates for PC-polyploidy, an issue still surrounded by controversy. What separates our method is the detailed mathematical analysis of the calculated kinetochore signal sizes. Furthermore, in our study, the use of confocal laser microscopy corrected for any sort of contributions of out of focus fluorescence that, could, in turn, lead to deviated values of the kinetochore signal size. Our findings are in support of the results from autoradiographical (Manuelidis and Manuelidis, 1974) and certain biochemical studies (Cohen *et al.*, 1973) that also hold the view of PCs exhibiting the standard diploid murine chromosome complement. Notably, a critical review of both camps by Swartz and Bhatnagar (1981) suggested that the results from autoradiographical studies have the greatest potential for being closer to the truth and resolving the issue.

The consistent association of kinetochore signal clusters with the nucleolus is in agreement with the findings from previous studies that have shown clusters of centromeric sDNA associated with the nucleolus, via *in situ* hybridization (Haaf and Schmid, 1989; Billia and De Boni, 1991; Holowacz and De Boni, 1991). As stated previously, the chromosomes associated with the nucleolus are those which bear NORs. Furthermore, it is suggested that association of the NOR-bearing chromosomes with the nuclear matrix provides a focal point for the formation of the fibrillar centers (Hilliker and Appels, 1989). The finding in our study that the nucleolus is associated with up to 70% of the chromosome complement, i.e., 28 chromosomes, (Fig. 17) along with the fact that in murine cells NORs are associated with only three chromosomes (12, 15 and 19) (Oud and Reutlinger, 1981) indicates that centromeric regions of additional chromosomes are associated with the nucleolus in PCs.

Changes in the spatial topology of the interphase nucleus, such as those associated with activation of lymphocytes (Wachtler *et al.*, 1986; 1990) or differentiation of neurons *in vitro (De* Boni and Mintz, 1986; Fung and De Boni, 1988; Park and De Boni, 1992) and *in vivo* (Manuelidis, 1985a), involve extensive re-modeling of the relationships between various nuclear components (Park and De Boni, 1999). In fact, as shown here, kinetochores, i.e. centromeric chromosome domains, may traverse linear distances, from the nuclear periphery to the centrally located nucleolus. This distance exceeds the mean diameter of interphase chromosome territories (Park and De Boni, 1998). Thus, it may be postulated that such re-modeling involves the placement of entire chromosome territories (Cremer *et al.*, 1996) into alternate nuclear sites

Furthermore, along with data which shows an association of specific, active sequences with nuclear compartments that are considered transcriptionally competent (Park and De Boni, 1998; Vershure *et al.*, (1999), the changes in topology reported in part one support the hypothesis that the relocation of chromosomes from the periphery to the nucleolus serves the process of differentiation by placing specific sequences into transcriptionally competent nuclear sites.

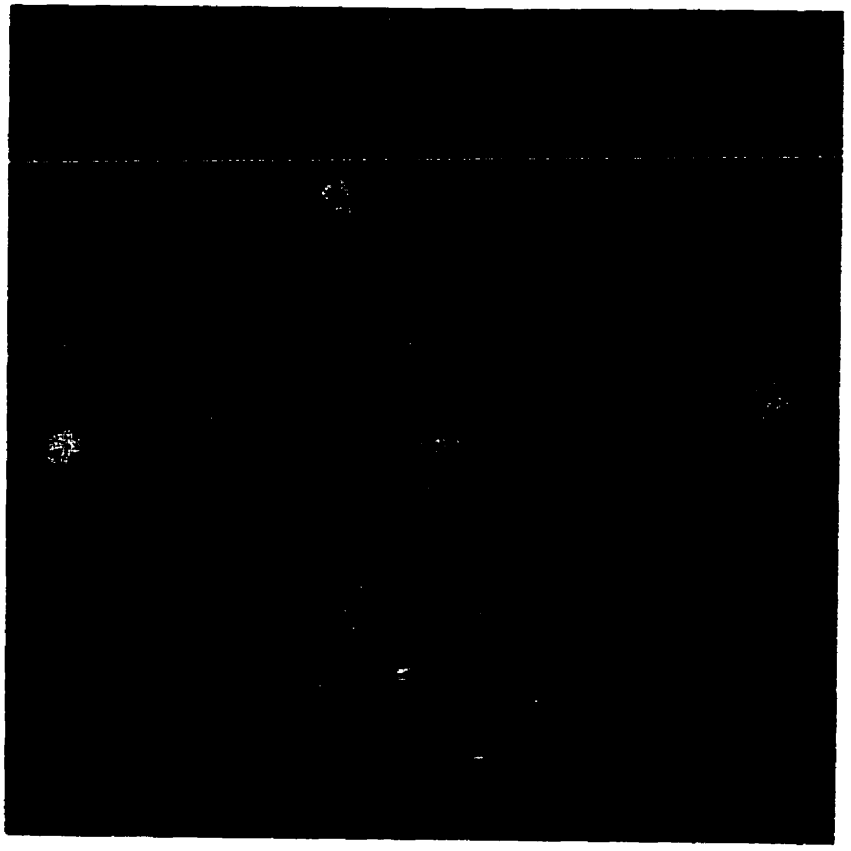

Figure 21: Nucleus of a Purkinje neuron shown as a projection of serial confocal sections. The central kinetochore signal was assumed, in this case, to arise from the clustering of three individual chromosome territories at their centromeric region. Adobe Photoshop, 4.1, was applied to depict the three participating territories, designated by different colors.

PART II: Purkinje-specific sequences

The PC-specific sequence RORα is first expressed embryonically (E15) and its levels of expression do not change throughout development. Thus, it served as the control in this study. Because this sequence is first expressed well before the timeframe of the observed chromosome shift between P3 and P5 (Fig. 17), our hypothesis predicts that the spatial position of this sequence will not change during development. The finding that the majority of the PCs exhibit reproducibly both RORα signals associated with the nuclear periphery throughout development (Figs. 18, 19) is in agreement with our hypothesis. Furthermore, according to our hypothesis, it is predicted that this sequence has already been transposed to a transcriptionally competent site. The maintained association of RORα with the nuclear periphery during the course of postnatal development (Fig. 20) indicates that the nuclear periphery is the transcriptionally competent site for this sequence.

The nuclear periphery has been proposed to be involved in gene expression by facilitating the nucleocytoplasmic transport of nascent mRNA that is, in turn, produced in this compartment (Blobel, 1985; de Graaf *et al.*, 1990; Sahlas *et al.*, 1993; Park and De Boni, 98). Such an involvement is supported by findings that show an association of DNase sensitive domains with the periphery, at least in certain cell types (Hutchinson and Weintraub, 1985; de Graaf *et al.*, 1991; Haug, *et al.*, 1994; Park and De Boni, 1996; 1998). However, there is controversy surrounding the issue of the association of the DNase sensitive domains with the nuclear periphery and the potential role of the periphery in gene expression. A recent study by Chan *et al.*, (2000), however, shows that DNase sensitive domains are indeed putatively associated with the nuclear periphery in 3T3 cells *in vitro*, in support of a functional role for the nuclear periphery.

In contrast the spatial intra-nuclear position of PLCβ3, a sequence expressed *de novo*, changes as a function of postnatal development (Figs. 18,19,20) in agreement with our hypothesis. The *de novo* expression of PLCβ3 between P2 and P7 (Watanabe *et al.*, 1998), coincides with the timeframe of the observed chromosome shift (P3-P5, Fig. 17). The relocation of the sequence signals from the nuclear periphery at P3 towards the centrally located nucleolus at P5 (Figs. 18,19) indicates that the spatial position of PLCβ3 indeed changes, in agreement of our hypothesis that an association exists between the *de novo* expression of this gene and a change in its spatial position as a function of development. Furthermore, this relocation is in agreement with the pattern of change in the fraction of chromosome complement associated with each nuclear compartment, according to which there is a redistribution of chromosomes from the nuclear periphery towards the nucleolus (Fig. 17).

It is of interest that PLCβ3 has been shown to be located on chromosome 19 (Gobl *et al.*, 1995), one of the NOR-bearing chromosomes in this species. Results from young PCs (P3) show that PLCβ3 signals are found associated with the nuclear periphery in an indirect manner, via their association with a peripherally located nucleolus. It was important, however, that the criteria for assignment of kinetochore and sequence signals to one of three nuclear compartments were kept the same. Thus a signal associated with the nuclear periphery or with a nucleolus, that was, in turn, associated with the periphery, was assigned to the compartment termed periphery in both cases. Evidence for the existence of multiple, peripherally located, smaller size nucleoli have been reported in previous studies (Park and De Boni, 1992). In that study, during the course of *in vitro* differentiation of dorsal root ganglion neurons, a fusion of nucleoli was reported resulting in the formation of a single centrally located nucleolus (Park and De Boni, 1992). Furthermore, it is of interest that for Purkinje cells with multiple nucleoli (data not

shown) the sum of the number of chormosomes associated with the small, peripherally located nucleoli was equal to the number of chromosomes found associated with the centrally located nucleolus, in support of the nucleolar fusion argument.

Thus, the relocation of PLCβ3 signals from the periphery towards the centrally located nucleolus appears to arise from the recruitment of peripherally located nucleoli towards the nucleolus located centrally. It remains to be shown whether such a relocation is passive or serves a particular functional purpose. Notably, however, in certain higher order eukaryotes, an association was shown to exist between nucleoli and the nuclear envelope via large invaginations of the latter (Dupuy-Coin *et al.*, 1986; Fricker *et al.*, 1997), an association that was previously reported and proposed to facilitate nucleocytoplasmic transport of nucleolar products (Bourgeois *et al.*, 1979). It would be of interest to examine whether such cytoplasmic invaginations indeed exist in the nuclei of PCs. Such a study would employ immunolabeling of the nuclear envelope and confocal laser microscopy, via which optical sectioning could provide more insight regarding the presence of large enough invaginations of the nuclear envelope that could accommodate its association to the centrally located nucleolus.

Conclusion

All of the observations above challenge the traditional view according to which the interphase nucleus is a membrane-bound reaction chamber in which the mode of interactions is governed solely by the laws of mass action and diffusion (Park and De Boni, 1999). However, it remains to be shown whether the re-arrangements in the number and spatial, intranuclear distribution of kinetochore signals along with the relocation of the PLCβ3 signals, as shown

here, are functionally associated with differentiation, or are merely associative. Nevertheless, results from this work provide evidence that an intimate relationship exists between the functional commitment of a cell and the topology of its nucleus during interphase. Furthermore, this evidence provides additional possibilities for future experiments that would help to enhance the further definition of structure-function relationships in the nucleus.

PROPOSAL FOR FUTURE WORK

A number of mechanisms have been proposed to be involved in the cell-specific pattern of gene expression occurring during differentiation and ultimately leading to the orderly assembly of the nervous system. In the present study, we are proposing that the appropriate spatial positioning of specific genes to particular nuclear sites may represent one such mechanism. If this is indeed the case, the spatial, intra-nuclear position of a gene with an altered expression pattern is predicted to be different in a mutant characterized by abnormal differentiation. As long as the mechanisms via which relocation of genes is accomplished within the 3-D nuclear space are unknown, a causative link between nuclear topological organization and control of gene expression will remain elusive.

However, a study examining the difference, if any, in the spatial intra-nuclear position occupied by a gene in a developmental mutant versus the wild-type is feasible. The criterion that has to be fulfilled by this candidate gene concerns its expression pattern, namely, it must be expressed in the wild-type but not in the mutant. The demonstration of a difference in the spatial position would provide a particularly strong association between nuclear topology and control of gene expression. The cerebellum represents an excellent system in which such a study can be conducted. The identification of naturally occurring cerebellar mutants and of the genes behind their abnormal development provides a number of candidate mutants and genes.

The *staggerer*, and the two PC-specific sequences encoding for RORα and cerebellin, are proposed for such a study, which ultimately represents an extension of the work conducted for this project. The *staggerer* was chosen because the PC is the primary target of this mutation and because the particularly severe compromise PCs undergo in these mutants has been characterized

in detail, especially in terms of altered gene expression patterns. RORα is an ideal sequence because its elimination causes the *staggerer* mutation, suggesting that this gene is of key importance in the postnatal differentiation of PCs. Furthermore, results from the work carried out for the present study, have already established the spatial intra-nuclear position of this sequence as a function of postnatal development in the wildtype. The other candidate sequence is cerebellin, a PC-specific neuropeptide whose expression pattern shows that it is not expressed in the *staggerer*. If the spatial positioning of specific sequences to particular nuclear sites represents one level of control of gene expression during differentiation, our hypothesis predicts that the spatial, intra-nuclear position of both RORα and cerebellin will be different in the mutant versus the wildtype PCs.

REFERENCES

Abraham, W.C., and Otani, C. (1989). Blockade of maintenance of long-term potentiation by dentate, but not entorhinal inhibition of protein synthesis. *Soc. Neurosci.* Abstracts. **15:** 85.

Altman, J., and Bayer, S.A. (1997). Development of the cerebellar system. CRC Press, Boca Raton, FL.

Amankwah, K.S., and De Boni, U. (1994). Ultrastructural localization of filamentous actin within neuronal interphase nuclei *in situ*. *Exp. Cell Res.* **210:** 315-325.

Ankenbauer, T., Kleinschmidt, J.A., Walsh, M.J., Weiner, O.H., and Franke, W.W. (1989). Identification of a wide spread actin binding protein. *Nature*. **342:** 822-825.

Araki, K., Meguro, H., Kushiya, E., Takayama, C., Inoue, Y., Misina, M. (1993). Selective expression of the glutamate receptor channel δ2 subunit in cerebellar Purkinje cells. *Biochem. Biophys. Res. Commun.* **197:** 1267-1276.

Armengol, J.A., and Sotelo, C. (1991). Early dendritic development of Purkinje cells in the rat cerebellum. A light and electron microscopic study using axonal tracing in "in vitro" slices. *Brain Res. Dev. Brain Res.* **64:** 95-114.

Arnoldus, E.P.J., Peters, A.C.B., Bots, G.T.A.M., Raaf, A.K., and van der Ploeg, M. (1989). Somatic pairing of chromosome 1 centromeres in interphase nuclei of human cerebellum. *Hum. Genet.* **83:** 231-234.

Baader, S.L., Sanlioglu, S., Berrebi, A.S., Parker-Thornburg, J., and Oberdick, J. (1998). Ectopic overexpression of Engrailed-2 in cerbellar Purkinje cells causes restricted cell loss and retarded external germinal layer development at lobule junctions. *J. Neurosci.* **18:** 1763-1773.

Baader, S.L., Schilling, M., Rosengarten, B., Pretch, W., Teutsch, H., Oberdick, J., and Schilling, K. (1996). Purkinje cell lineage and the topographic organization of the cerebellar cortex: a view from X inactivation mosaics. *Dev. Biol.* **174:** 393-406.

Baldini, A., Miller, D.A., Miller, J., Ryder, O.A., and Mitchell, A.R. (1991). A chimpanzee-derived chromosome-specific alpha satellite DNA sequence conserved between chimpanzee and human. *Chromosoma.* **100:** 156-162.

Baptista, C.A., Hatten, M.E., Blazeski, R., Mason, C.A. (1994). Cell-cell interactions influence survival and differentiation of purified Purkinje cells in vitro. *Neuron.* **12:** 243-260.

Baserga, S.J., and Steitz, J.A. (1993). The RNA World. R.F. Gesteland and J.F Atkins eds. Cold Spring Harbor Press.

Bauren, G., Jiang, W.-Q., Bernholm, K., Gu, F., and Weislander, F. (1996). Demonstration of a dynamic, transcription-dependent organization of pre-mRNA splicing factors in polytene nuclei. *J. Cell Biol.* **133:** 929-942.

Beattie, C.E., Kolva, B., and Siegel, R.E. (1995). $GABA_A$ receptor mRNA expression in the weaver cerebellum: modulation by cell-cell interactions. *Develop. Brain Res.* **88:** 171-177.

Becker, W.M., and Deamer, D.W. (1991). The world of the cell. The Benjamin/Cummings Publishing Company, Inc. Redwood City, California.

Bekers, A.G.M., Pieck, A.C.M., Rijken, A.A.M., and Wanka, R. (1981). Ultrastructure of the nuclear matrix from *Physarum polycephalum* during the mitotic cycle. *J. Ultrastruct. Res.* **75:** 352-362.

Bekers, A.G.M., Pieck, A.C.M., Rijken, A.A.M., and Wanka, R. (1986). Evidence for the persistance of a decondensed chromosome scaffold in the interphase nucleus. *J. Cell Sci.* **86:** 155-171.

Berezney, R. (1984). Chromosomal Nonhistone Proteins, Structural Association. (Hnilica, L.S. ed) CRC Press, Florida.

Berezney, R., and Coffey, D.S. (1974). Identification of a nuclear protein matrix. *Biochem. Biophys. Res. Commun.* **60:** 1410-1417.

Bergmann, M., Fox, P.A., Grabs, D., Post, A., and Schilling, K. (1996). Expression and subcellular distribution of glutamate receptor subunits 2/3 in the developing cerebellar cortex. *J. Neurosci. Res.* **43:** 78-86.

Berrebi, A.S., and Mugnaini, E. (1992). Characteristics of labeling of the cerebellar Purkinje neuron by L7 antiserum. *J. Chem. Neuroanatom.* **5:** 235-243.

Berrebi, A.S., Oberdick, J., Sangameswaran, L., Christakos, S., Morgan, J.I., and Mugnaini, E. (1991). Cerebellar Purkinje cell markers are expressed in retinal bipolar neurons. *J. Comp. Neurol.* **308:** 630-649.

Billia, F., Baskys, A., Carlen, P.L., and De Boni, U. (1992). Rearrangement of centromeric satellite DNA in hippocampal neurons exhibiting long-term potentiation. *Mol. Brain Res.* **14:** 101-108.

Billia, F. and De Boni, U. (1991). Localization of centromeric satellite and telomeric DNA sequences in dorsal root ganglion neurons, in vitro. *J.Cell. Sci.* **100:** 219-226.

Blobel, G. (1985). Gene gating: A hypothesis. *Proc. Natl. Acad. Sci. USA* **82:** 8527-8529.

Bloom, K. (1993). The centromere frontier: kinetochore components, microtubule-based motility, and the CEN-Value paradox. *Cell.* **73:** 621-624.

Bond, H.E., Flamm, W.G., Burr, H.E., and Bond, S.B. (1967). Mouse Satellite DNA. Further studies on its biological and physical characteristics and its intracellular localization. *J. Mol. Biol.* **27:** 289-302.

Borden, J. and Manuelidis, L. (1988). Movement of the X chromosome in epilepsy. *Science.* **242:** 1687-1691.

Boulikas, T. (1995). Chromatin domains and prediction of MAR sequences. *Int. Rev. Cytol.* **162A:** 279-388.

Bourgeois, C.A., Hemon, D., and Bouteille, M. (1979). Structural relationship between the nucleolus and the nuclear envelope. *J. Ultrastruct. Res.* **68:** 328-340.

Bremer, J.W., Busch, H., and Yeoman, L.C. (1981). Evidence for a species of nuclear actin distinct from cytoplasmic and muscle actin. *Biochem.* **20:** 2013-2017.

Brenner, S., Pepper, D., Berns, M.W., Tan, E., and Brinkley, B.R. (1981). Kinetochore structure, duplication and distribution in mammalian cells: Analysis by human autoantibodies from scleroderma patiants. *J. Cell Biol.* **91:** 95-102.

Brinkley, B.R., Ouspenski, I., and Zinkowski, R.P. (1992). Structural and molecular organization of the centromere-kinetochore complex. *Trends Cell Biol.* **2:** 15-21.

Burch, J.B.E., and Weintraub, H. (1983). Temporal order of chromatin structural changes associated with activation of the major chicken vitellogenin gene. *Cell.* **33:** 65-76.

Caceres, A., Potrebic, S., Kosik, K. (1991). The effect of tau antisense oligonucleotides on neurite formation of cultured cerebellar macroneurons. *J. Neurosci.* **11:** 1515-1523.

Carlson, B.M. (1997). Patten's foundations of embryology, 6th ed. McGraw-Hill, Inc.

Carmo-Fonseca, M., Cunha, C., Custodio, N., Carvalho, C., Jordan, P., Ferreira, J., and Parreira, L. (1996). The topography of chromosomes and genes in the nucleus. *Exp. Cell Res.* **229:** 247-252.

Carmo-Fonseca, M., Peppercock, R., Carvallo, M.T., and Lamond, A.I. (1992). Transcription dependent co-localization of the U1, U2, U4/U6 and U5 snRNPs in coiled bodies. *J. Cell Biol.* **117:** 1-14.

Carter, K.C., Bowman, D., Carrington, W., Fogarty, K., McNeil, J.A., Fay, F.S., and Lawrence, J.B. (1993). A three-dimension view of precursor messenger RNA metabolism within the mammalian nucleus. *Science.* **259:** 1330-1335.

Carter, K.C., Taenja, K.L., and Lawrence, J.B. (1991). Discrete nuclear domains of poly(A)RNA and their relationship to the functional organization of the nucleus. *J. Cell Biol.* **115:** 1191-1202.

Chaly, N., and Brown, D.L. (1988). The prometaphase configuration and chromosome order in early mitosis. *J. Cell Sci.* **91:** 325-335.

Chan, J.K.L., Park, P.C., and De Boni, U. (2000). Association of DNAse sensitive domains with the nuclear periphery in 3T3 cells in vitro. *Biochem. Cell Biol.* **78:** 67-78.

Chen, L., Bao, S., Qiao, X., and Thompson, R.F. (1996). Impaired cerebellar synapse maturation in waggler, a mutant mouse with a disrupted neuronal calcium channel g subunit. *Proc Nat Acad Sci.* **96:** 12132-12137.

Choh, V., and De Boni, U. (1996). Spatial repositioning of centromeric domains during regrowth of axons in nuclei of murine dorsal root ganglion neurons *in vitro*. *J. Neurobiol.* **31:** 325-331.

Christakos, S., Gabrielides, C., and Rhoten, W.B. (1989). Vitamin-D dependent calcium binding proteins: chemistry, distribution, functional considerations, and molecular biology. *Endocr. Rev.* **10:** 3-26.

Church, K., and Moens, P.B. (1976). Centromere behavior during interphase and meiotic prophase in Allium fistulum from 3-D E.M. reconstruction. *Chromosoma.* **56:** 249-262.

Clark, D.J., and Kimura, T. (1990). Electrostatic mechanism of chromatin folding. *J. Mol. Bio.* **211:** 883-896.

Clark, T.G., and Rosenbaum, R.W. (1979a). Diffusible and bound actin in nuclei of *Xenopous laevis* oocytes. *Cell* **12:** 883-891.

Clark, T.G., and Rosenbaum, R.W. (1979b). An actin filament matrix in hand-isolated nuclei of *X. laevis* oocytes. *Cell.* **18:** 1101-1108.

Clemson, C.M., and Lawrence, J.B. (1996). Multifunctional compartments in the nucleus: insights from DNA and RNA localization. *J. Cell. Biochem.* **62:** 181-190.

Cockell, M. and Gasser, S.M. (1999). Nuclear compartments and gene regulation. *Cur. Opinion Genet. & Develop.* **9:** 199-205.

Cockerill, P.N., and Garrard, W.T.(1986). Chromosomal loop anchorage sites appear to be evolutionary conserved. *FEBS Lett.* **204:** 5-7.

Cohen, J., Mares, V., Lodin, Z. (1973). DNA content of purified preparations of mouse Purkinje neurons isolated by a velocity sedimentation technique. *J. Neurochem.* **20:** 651-657.

Cole, A.J., Saffen, D.W., Baraban, J.W., and Worley, P.F. (1989). Rapid increase of an immediate early gene messenger RNA in hippocampal neurons by synaptic NMDA receptor activation. *Nature.* **340:** 474-476.

Comingns, D.E. (1968). The rationale for an ordered arrangement of chromatin in the interphase nucleus. *Am. J. Hum. Genet.* **20:** 440-460.

Cooper, G.M. (1997). The Cell. A molecular approach. ASM Press, Washington, D.C. Sinauer Associates, Inc. Sunderlang, MA.

Cox, J.V., Schenk, E.A., and Olmsted, J.B. (1983). Human anticentromere antibodies: distribution, characterization of antigens and effect on microtubule organization. *Cell.* **33:** 331.

Cremer, T., Cremer, C., Baumann, H., Luedtke, E.K., Sperling, K., Teuber, V., and Zorn, C. (1982). Rabl's model of the interphase chromosome arrangement tested in chinese hamster cells by premature chromosome condensation and laser UV-microbeam experiments. *Hum Genet.* **60:** 46-56.

Cremer, T., Cremer, C., Schneider, T., Baumann, H., Hens, L., and Kirsch-Volder, M. (1982). Analysis of chromosome positions in the interphase nucleus of Chinese hamster cells by laser-UV-microirradiation experiments. *Hum. Genet.* **62:** 201-209.

Cremer, T., Kurz, A., Zirberl, R., Dietzel, S., Rinke, B., Schrock, E., Speicher, M.R., Mathieu, U., Jauch, A., Emmerich, P., Scherthan, H., Ried, T., Cremer, C., and Lichter, P. (1993). Role of chromosome territories in the functional compartmentalization of the cell nucleus. *Cold Spring Harbor Symp. Quant. Biol.* **LVIII:** 777-792.

Cremer, T., Lichter, P., Borden, J., Ward, D.C., and Manuelidis, L. (1988). Detection of chromosome abberations in metaphase and interphase tumour cells by in situ hybridization using specific library probes. *Hum. Genet.* **80:** 235-243.

Cremer, C., Munkel, Ch., Granzow, M., Jauch, A., Dietzer, S., Eils, R., Guan, X.Y., Meltzer, P.S., Trent, J.M., Langowski, J., and Cremer, T. (1996). Nuclear architecture and the induction of chromosomal aberrations. *Mutation Res.* **366:** 97-116.

Crepel, F.N., Delhaye-Bouchard, N., Guastivino, J.M., and Sampaio, I. (1980). Multiple innervation of cerebellar Purkinje cells by climbing fibers in *staggerer* mutant mouce. *Nature.* **283:** 483-484.

Crossin, K.L., Prieto, A.L., Hoffman, S., Jones, F.S., Friedlander, D.R. (1990). Expression of adhesion molecules and the establishment of boundaries during embryonic and neural development. *Exp. Neurol.* **109:** 6-18.

Crossley, P.H., and Martin, G.R. (1995). The mouse Fgf8 gene encodes a family of polypeptides and is expressed in regions that direct outgrowth and patterning in the developing embryo. *Development.* **121:** 439-451.

Daniel, H., Levenes, C., and Crepel, F. (1998). Cellular mechanisms of cerebellar LTD. *Trends Neurosci.* **21:** 401-407.

De Boni, U. (1994). The interphase nucleus as a dynamic structure. *Intl. Rev. Cytol.* **150:** 149-171.

De Boni, U. (1988). Chromatin and nuclear envelope of freeze-fractured, neuronal interphase nuclei, resolved by scanning electron microscopy. *Biol. Cell.* **63:** 1-8.

De Boni, U., and Mintz, A.H. (1986). Curvilinear, three-dimensional motion of chromatin domains and nucleoli in neuronal interphase nuclei. *Science* (Washington D.C). **234:** 863-866.

de Graaf, A., Van Hemert, F., Linnemans, W.A.M., Brakenhoff, J., DeJong, L, Van Renswoude, J., and Van Drie, R. (1990). Three-dimensional distribution of Dnase I-sensitive regions in interphase nuclei of embryonal carcinoma cells. *Eur. J. Cell Biol.* **52:** 135-141.

De Jager, P.L., Zuo, J., and Heintz, N. (197). An ~ 1.2Mb BAC contig refines the genetic and physical maps of the Lurcher locus on mouse chromosome 6. *Genome Res.* **7:** 736-746.

de Jong, L., Grande, M.A., Mattern, K.A., Schul, W., and van Driel, R. (1996). Nuclear domains involved in RNA synthesis, RNA processing, and replication. *Crit. Rev. Eukaryotic Gene Expression.* **6:** 215-246.

Dent., A.L., Yewdell, J., Puvion-Dutilleul, F., Koken, M.H., de The, H., Staudt, L.M. (1996). LYSP100-associated nuclear domains (LANDs): description of a new class of subnuclear structures and their relationship to PML nuclear bodies. *Blood.* **88:** 1423-1426.

Dong, F., and Jiang, J. (1998). Non-Rabl patterns of centromere and telomere distribution in the interphase nuclei of plant cells. *Chromosome Res.* **6:** 551-558.

Du, L., and Warren, S.L. (1997). A functional interaction between the Carboxy-terminal domain of RNA polymerase II and pre-mRNA splicing. *J. Cell Biol.* **136:** 5-18.

Dumesnil-Bousez, N., and Sotelo, C. (1992). Early development of the Lurcher cerebellum: Purkinje cell alterations and impairment of synaptogenesis. *J. Neurocytol.* **21:** 506-529.

Dundr, M., and Raska, I. (1993). Nonisotopic ultrastructural mapping of transcription sites within the nucleolus. *Exp. Cell Res.* **208:** 275-281.

Dunn, M.E., and Mugnaini, E. (1993). Influence of granule cells on the survival and differentiation of Purkinje cells in dissociated cerebellar cultures. *Soc. Neurosci. Abstr.* **19:** 1723.
Dunn, M.E., Schilling, K., and Mugnaimi, E. (1998a). Development and fine structure of murine Purkinje cells in dissociated cerebellar cultures: neuronal polarity. *Anat. Embryol.* **197:** 9-29.

Dunn, M.E., Schilling, K., and Mugnaimi, E. (1998b). Development and fine structure of murine Purkinje cells in dissociated cerebellar cultures: dendritic differentiation, synaptic maturation, and formation of cell-class specific features. *Anat. Embryol.* **197:** 31-50.

Dupuy-Coin, A.M., Moens, P., and Bouteille, M. (1986). Three-dimensional analysis of given cell structures: nucleolus, nucleoskeleton and nuclear inclusions. *Methods. Achiev. Exp. Pathol.* **12:** 1-25.

Earnshaw, W.C. (1991). When is a centromere not a kinetochore? *J. Cell Sci.* **99:** 1-4.

Earnshaw, W.C., Halligan, N., Cooke, C.A., and Rothfield, N. (1984). The kinetochore is part of the metaphase chromosome scaffold. *J. Cell Biol.* **98:** 352-357.

Earnshaw, W.C., and Migeon, B.R. (1985). Three related centromere proteins are absent from the inactive centromere of a stable isodicentric chromosome. *Chromosoma.* **92:** 290.

Earnshaw, W.C., and Rattner, J.B. (1989). A map of the centromere (primary constriction) in vertebrate chromosomes at metaphase. *Prog. Clin. Biol. Res.* **318:** 33-42.

Eanrshaw, W.C., and Rothfield, N. (1985). Identification of a family of human centromere proteins using auto-immune sera from patients with scleroderma. *Chromosoma.* **91:** 313-321.

Earnshaw, W.C., Sullivan, K.F., Machlin, P.S., Cooke, C.A., Kaiser, D.A., Pollard, T.D., Rothfield, N., and Cleveland, D.W. (1987). Molecular cloning of cDNA for CENP-B, the major human centromere autoantigen. *J. Cell Biol.* **104:** 817-829.

Eils, R., Dietzel, S., Bertin, E., Schrock, E., Seicher, M.R., Reid, T., Robert-Nicoud, M., Cremer, C., and Cremer, T. (1996). Three-dimensional reconstruction of painted human interphase chromosomes: active and inactive X chromosome territories have similar volumes but differ in shape and surface structure. *J. Cell. Biol.* **135:** 1427-1440.

Evans, R.M. (1988). The steroid and thyroid hormone receptor superfamily. *Science.* **240:** 889-895.

Exton, J.H. (1996). Regulation of phosphoinositide phospholipases by hormones, neurotransmitters, and other agonists linked to G proteins. *Ann. Rev. Pharmacol. Toxicol.* **36:** 481-509.

Ferreira, J., Carmo-Fonseca, M., and Lamond, A.I. (1994). Differential interaction of splicing snRNPs with coiled bodies and interchromatin granules during mitosis and assembly of daughter cell nuclei. *J. Cell Biol.* **126:** 11-23.

Ferreira, J., Paolella, G., Ramos, C., and Lamond, A.I. (1997). Spatial organization of large-scale chromatin domains in the nucleus: a magnified view of single chromosome territories. *The J. Cell Biology.* **139:** 1597-1610.

Frey, M.R., and Matera, A.G.(1995). Coiled bodies contain U7 small nuclear RNA and associate with specific DNA sequences in interphase human cell. *Proc. Natl. Acad. Sci. USA.* **92:** 5915-5919.

Fricker, M., Hollished, M., White, N., and Vaux, D. (1997). Interphase nuclei of many cell types contain deep, dynamic, tubular, membrane-bound invaginations of the nuclear envelope. *J. Cell Biol.* **136:** 531-544.

Fung, L.C. and De Boni, U. (1988). Modulation of nuclear rotation in neuronal interphase nuclei by nerve growth factor, by gamma-aminobutyric acid, and by changes in intracellular calcium. *Cell Motil. Cytoske.* **10:** 363-373.

Fussel, C.P. (1975). The position of interphase chromosomes and late replication DNA in centromere and telomere regions of *Allium cepa L. Chromsoma.* **50:** 201-210.

Gasser, S.M., and Laemmli, U.K., (1986). Cohabitation of scaffold binding regions with upstream/enhancer elements of three developmentally regulated genes of *D. melanogaster*. *Cell.* **46:** 521-530

Gerace, L., and Burke, B. (1988). Functional organization of the nuclear envelope. *Annu. Rev. Cell Biol.* **4:** 335-374.

Gilbert, S.F. (1997). Developmental biology. 5th edit. Sinauer Associates, Inc. Sutherland, MA.

Gobl, A.E., Chowdhary, B.P., Shu, W., Eriksson, L., Larsson, C., Weber, G., Oberg, K., and Skogseid, B. (1995). Assignment of the mouse homologue of a human MEN1 candidate gene, phospholipase C-beta 3 to chromosome region 19B by FISH. *Cytogenet. Cell Genet.* **71:** 257-259.

Goelet, P., Castelluci, V.F., Schacher, S., and Kandel, E.R. (1986). The long and short of long-term memory - a molecular framework. *Nature.* **322:** 419-422.

Goessens, G. (1984). Nucleolar structure. *Int. Rev. Cytol.* **87:** 107-158.

Goffinet, A.M., So, K.F., Yamamoto, M., Edwards, M., Caviness, V.S, Jr. (1984). Architectonic and hodological organization of the cerebellum in *reeler* mutant mice. *Brain Res.* **318:** 263-276.

Goldwitz, D., Cushing, R.C., Laywell, E., D'Arcangelo, G., Sheldon, M., Sweet, H.O., Davisson, M., Steindler, D., and Curran, T. (1997). Cerebellar disorganization characteristic of *reeler* in *scrambler* mutant mice despite presence of reelin. *J. Neurosci.* **17:** 8767-8777.

Goldowitz, D., and Hamre, K. (1998). The cells and molecules that make a cerebellum. *Trends Neurosci.* **21:** 375-382.

Gross, D.S., and Garrard, W.T. (1988). Nuclease hypersensitive sites in chromatin. *Ann. Rev. Biochem.* **57:** 159-197.

Guldner, H.H., Lakonsek, H.J., and Bautz, F.A. (1984). Human anticentromeric sera recognize a 19.5 kd non-histone chromosomal protein from HeLa cells. *Clin. Exp. Immunol.* **58:** 13.

Haaf, T., and Schmid, M. (1989). Centromeric association and non-random distribution of centromeres in human tumor cells. *Hum. Genet.* **81:** 137-143.

Haaf, T., and Schmid, M. (1991). Chromosome Topology in mammalian interphase nuclei. *Exp. Cell Res.* **192:** 325-332.

Hamilton, B.A., Frankel, W.N., Kerrebrock, A.W., Hawkins, T.L., FitzHugh, W., Kusumi, K., Russel, L.B., Mueller, K.L., Van Berkel, V., Birren, B.W., Kruglyak, L., and Lander, E.S. (1996). Disruption of the nuclear hormone receptor RORα in *staggerer* mice. *Nature.* **379:** 736-739.

Harpold, J.H., Wilson, M.C., and Darnell, J.E. Jr. (1981). Chinese hamster polyadenylated messenger ribonucleic acid: Relationship to non-polyadenylated sequences and relative conservation during messenger ribonucleic acid processing. *Mol. Cell Biol.* **1:** 188-198.

Hawkes, R., Faulkner-Jones, B., Tam, P., Tan, S.S. (1998). Pattern formation in the cerebellum of murine embryonic stem cell chimeras. *Eur. J. Neurosci.* **10:** 790-793.

Hawkes, R., Colonnier, M., and Leclerc, N.(1985). Monoclonal antibodies reveal sagittal banding in the rodent cerebellar cortex. *Brain Res.* **333:** 359-365.

Heintz, N., and De Jager, PL. (1999). GluR delta 2 and the development and death of cerebellar Purkinje neurons in lurcher mice. *Ann. N Y Acad. Sci.* **868:** 502-514.

Henderson, S.C., and Locke, M. (1992). A shell of F-actin surrounds the branched nuclei of silk gland cells. *Cell Mot. Cytoskel.* **23:** 169-187.

Henderson, A.S., Warburton, D., and Atwood, K.C. (1972). Location of ribosomal DNA in human chromosome complement. *Proc. Natl. Acad. Sci. USA.* **69:** 3394-3398.

Herrup, K. (1983). Role of *staggerer* gene in determining cell number in cerebellar cortex. I. Granule cell death is an indirect consequence of *staggerer* gene action. *Dev. Brain Res.* **11:** 267-274.

Herrup, K., and Basser, J.C. (1995). The induction of multiple cell cycle events precedes target-related neuronal death. *Development.* **121:** 2385-2395.

Herrup, K., Diglio, T.J., and Letsou, A. (1984). Cell lineage relationships in the development of the mammalian CNS. I.The facial nerve nucleus. *Dev. Biol.* **103:** 329-336.

Herrup, K., and Mullen, R.J.(1979a). Regional variation and absence of large neurons in the cerebellum of the *staggerer* mouse. *Brain Res.* **172:** 1-12.

Herrup, K., and Mullen, R.J. (1979b). *Staggerer* chimeras: Intrinsic nature of Purkinje cell defects and implications for normal cerebellar development. *Brain Res.* **178:** 443-457.

Herrup, K., and Mullen, R.J. (1981). Role of the *staggerer* gene in determining Purkinje cell number in the cerebellar cortex of mouse chimeras. *Dev. Brain Res.* **1:** 475-485.

Herrup, K., and Sunter, K. (1987). Numerical matching during cerebellar development: Quantitative analysis of granule cell death in *staggerer* mouse chimeras. *J. Neurosci.* **7:** 829-836.

Hilliker, A.J., and Appels, R. (1989). The arrangement of interphase chromosomes: Structural and functional aspects. *Exp. Cell Res.* **185:** 297-318.

Hiraoka, Y., Dernburg, A.F., Parmelee, S.J., Rykowski, M.C., Agard, D.A., and Sedat, J.W. (1993). The onset of homologous chromosome pairing during *Drosophila melanogaster* embryogenesis. *J. Cell Biol.* **120:** 591-600.

Hochstrasser, M., Mathog, D., Gruenbaum, Y., Saumweber, H., and Sedat, J. (1986). Spatial organization of chromosomes in the salivary gland nuclei of *Drosophila melanogaster. J. Cell Biol.* **102:** 112-113.

Hochstrasser, M., and Sedat, J.W. (1987a). Three-dimensional organization of *Drosophila melanogaster* interphase nuclei. I. Tissue-specific aspects of polytene nuclear architecture. *J. Cell Biol.* **104:** 1455-1470.

Hochstrasser, M., and Sedat, J.W. (1987b). Three-dimensional organization of *Drosophila melanogaster* interphase nuclei. II. Chromosome spatial organization and gene regulation. *J. Cell Biol.* **102:** 112-113.

Holowacz, T. and De Boni, U. (1991). Arrangement of kinetochore proteins and satellite DNA in neuronal interphase nuclei: Changes induced by gamma-aminobutyric acid (GABA). *Exp. Cell Res.* **197:** 36-42.

Houk, JC., Buckingham, J.T., and Barto, A.G.1999. Models of the cerebellum and motor learning. http://dept-www.physio.nwu.edu./Physiology/houk/bbs.html. December, 5, 1999.

Howell, W.M. (1982). Selective staining of nucleolar organizer regions (NORs). The Cell Nucleus, vol. 11. H.Busch and L. Rothblum eds. Academic Press, New York.

Hozak, P. (1996). The nucleoskeleton and attached activities. *Exp. Cell Res.* **229:** 267-271.

Huang, S., and Spector, D.L. (1992). U1 and U2 small nuclear RNAs are present in nuclear speckles. *Proc. Natl. Acad. Sci. USA.* **89:** 305-308.

Huang, S., and Spector, D.L. (1996). Intron-dependent recruitment of pre-mRNA splicing factors to sites of transcription. *J. Cell Biol.* **133:** 719-732.

Hutchinson, N., and Weintraub, H. (1985). Localization of DNAse I-sensitive sequences to specific regions of interphase nuclei. *Cell.* **43:** 471-482.

Iacopino, A.M., Rhoten W.B., and Christakos, S. (1990). Calcium binding protein (calbindin-D28k) gene expression in the developing and aging mouse cerebellum. *Brain Res. Mol. Brain Res.* **8:** 283-290.

Inoue, Y., Maeda, N., Kokubun, T., Takayama, C., Inoue, K., Terashima, T., and Mikoshiba, K. (1990). Architecture of Purkinje cells of the reeler mutant mouse observed by immunohistochemistry for the inositol 1,4,5-triphosphate receptor protein P400. *Neurosci, Res (N Y).* **8:** 189-201.

Inouye, M., and Murakami, U. (1980). Temporal and spatial patterns of Purkinje cell formation in the mouse cerebellum. *J. Comp. Neurol.* **194:** 499-503.

Ito, M. (1984). The cerebellum and motor control. Raven Press.

Ito, M. (1989). Long-term depression. *Annu. Rev. Neurosci.* **12:** 85-102.

Jackson, D.A.(1991). Structure-function relationships in eukaryotic nuclei. *Bioessays.* **13:** 1-10.

Jackson, D.A., and Cook, P.R. (1986). Replication occurs at nucleoskeleton. *EMBO (Eur. Mol. Biol. Organ.) J.* **5:** 1403-1410.

Jackson, D.A., Hassan, A.B., Errington, R.J., and Cook, P.R. (1993). Visualization of focal sites of transcription within human nuclei. *EMBO J.* **12:** 1059-1065.

Jackson, D.A., McCready, S.J., Cook, P.R. (1981). RNA is synthesized at the nuclear cage. *Nature.* **292:** 552-555.

Jackson, D.A., Iborra, F.J., Manders, E.M.M., and Cook, P.R. (1998). Numbers and organization of RNA polymerases, nascent transcripts, and transcription units in HeLa nuclei. *Mol. Biol. Cell.* **9:** 1523-1536.

Jaeger, C.B., Kapoor, R., and Llinas, R. (1988). Cytology and organization of rat cerebellar organ cultures. *Neuroscience.* **26:** 509-538.

Janevski, J., Park, P.C. and De Boni, U. (1995). Organization of centromeric domains in hepatocyte nuclei: rearrangement associated with *de novo* activation of the vitellogenin gene family in Xenopus *laevis*. *Exp. Cell Res.* **217:** 227-239.

Janevski, J., Park, P.C. and De Boni, U. (1997). Changes in morphology and spatial position of coiled bodies during NGF-induced neuronal differentiation of PC12 cells. *J. Histochem. Cytochem.* **45:** 1523-1531.

Jarman, A.P., and Higgs, D.R. (1988). Nuclear scaffold attachment sites in the human globin gene complexes. *EMBO J.* **7:** 3337-3344.

Jimenez-Garcia, L.F., and Spector, D.L.(1993). *In vivo* evidence that transcription and splicing are coordinated by a recruiting mechanism. *Cell.* **73:** 47-57.

Jones, K. (1970). Chromosomal and nuclear location of mouse satellite DNA in individual cells. *Nature.* **225:** 912-915.

Joseph, A., Mitchell, A.R., and Miller, O.J. (1989). The organization of the mouse satellite DNA at centromeres. *Exp. Cell Res.* **183:** 494-500.

Kano, M., Hashimoto, K., Watanabe, M., Kurihara, H., Offermann, S., Jiang, H., Wu, Y., Jiang, H., Wu, J., Jun, K., Shin, H.S., Inoue, Y., Simon, M.I., and Wu, D. (1998). Phospholipase cbeta4 is specifically involved in climbing fiber synapse elimination in the developing cerebellum. *Proc. Natl. Acad. Sci. USA.* **95:** 15724-15729.

Kashiwabuchi, N., Ikeda, K., Araki, K., Hirano, T., Shibuki, K., Takayama, C., Inoue, Y., Kutsuwada,T., Yagi, T., Kang, Y., Aizawa, S., Mishina, M. (1995). Impairment of motor coordination, Purkinje cell synapse formation, and cerebellar long-term depression in GluRδ2 mutant mice. *Cell.* **81:** 245-252.

Katsumata, M., and Lo, C.W. (1988). Organization of chromosomes in the mouse nucleus: analysis by *in situ* hybridization. *J. Cell Sci.* **90:** 193-199.

Kitagawa, K., Masumoto, H., Ikeda, M., and Okazaki, T. (1995). Analysis of protein-DNA and protein-protein interactions of centromere protein B (CENP-B) and properties of the DNA-CENP-B complex in the cell cycle. *Mol. Cell Biol.* **15:** 1602-1612.

Klockgether, T., and Evert, B. (1998). Genes involved in hereditary ataxias. *Trends Neurosci.* **21:** 413-418.

Kohtz, J.D., Jamieson, S.F., Will, C.L., Zuo, P., Luhrmann, R., Garcia-Blanco, M.A., and Manley, J.L. (1994). Protein-protein interaction and 5'-splice site recognition in mammalian mRNA precursor. *Nature.* **368:** 119-124.

Krainer, A.R., Conway, G.C., and Kozak, D. (1990a). Purification and characterization of pre-mRNA splicing factor SF2 from HeLa cells. *Genes Dev.* **4:** 1158-1171.

Krainer, A.R., Conway, G.C., and Kozak, D. (1990b). The essential pre-mRNA splicing factor SF2 influences 5'splice site selection by activating proximal sites. *Cell.* **62:** 35-42.

Krystosek, A., and Puck, T.T. (1990). The spatial distribution of exposed nuclear DNA in normal, cancer and reverse-transformed cells. *Proc. Natl. Acad. Sci.* **87:** 6560-6564.

Kuemerle, B., Zanjani, H., Joyner, A., and Herrup, K. (1997). Pattern deformities and cell loss in *Engrailed-2* mutant mice suggest two separate patterning events during cerebellar development. *J. Neurosci.* **17:** 7881-7889.

Kumar, A., Finlay, T.H., Thomas, J.O., and Szer, W. (1984). Isolation of minor species of actin from nuclei of *Acanthamoeba castellani. Biochem.* **23:** 6753-6757.

Kurihara, H., Hashimoto, K., Kano, M., Takayama, C., Sakimura, K., Mishina, M., Inoue, Y., and Watanabe, M. (1997). Impaired parallel fiber-Purkinje cell synapse stabilization during cerebellar development of mutant mice lacking the glutamate receptor δ2 subunit. *J. Neurosci.* **17:** 9613-9623.

Kurtz, A., Lampel, S., Nickolenko, J.E., Bradl, J., Benner, A., Zirbel, R.M., Cremer, T., and Lichter, P. (1996). Active and inactive genes localized preferentially in the periphery of chromosome territories. *J. Cell Biol.* **135:** 1195-1205.

Lamond, A.L., and Carmo-Fonseca, M. (1993). Localization of splicing snRNPs in mammalian cells. *Mol. Biol. Rep.* **18:** 127-133.

Lamond, A.I., and Earnshow, W.C. (1998). Structure and Function in the Nucleus. *Science.* **280:**547-543.

Landis, D.M.D., and Sidman, R.L. (1978). Electron microscopic analysis of postnatal histogenesis in the cerebellar cortex of *staggerer* mutant mice. *J. Comp. Neurol.* **179:** 831-863.

Lannoo, M.J., Brochu, G., Maler, L., Hawkes, R. (1991). Zebrin II immunoreactivity in the rat and in the weakly electric teleost *Eigenmannia* reveals three modes of Purkinje cell development. *J. Comp. Neurol.* **310:** 215-233.

Lawrence, J.B., Singer, R.H., and Marselle, L.M. (1989). Highly localized tracks of specific transcripts within interphase nuclei visualized by *in situ* hybridization. *Cell.* **57:** 493-502.

Leclerc, N., Gravel, C., Hawkes, R. (1988). Development of parasagittal zonation in the rat cerebellar cortex: mabQ113 antigenic bands are created postnatally by the suppression of antigen expression in a subset of Purkinje cells. *J. Comp. Neurol.* **273:** 399-420.

Leclerc, N., Jibard, N., Meng, X., Schweizer-Groyer, G., Fortin, D., Rajkowski, K., Kang, K., Catelli, M.G., Baulieu, E.E., and Cadepond, F. (1998). Quantification of the nucleocytoplasmic distribution of wild type and modified proteins using confocal microscopy: interaction between 90-kDa heat shock protein (Hsp90 alpha) and glucocorticosteroid receptor (GR). *Exp. Cell. Res.* **242:** 255-264.

Leclerc, N., Schwarting, G., Herrup, K., Hawkes, R., Yamamoto, M. 1992. Compartmentation in mammalian cerebellum: zebrin II and P-path antibodies define three classes of sagitally organized bands of Purkinje cells. *Proc. Natl. Acad. Sci. USA.* **89:** 5006-5010.

Leitch, A.R., Mosgoller, W., Schwarzacher, T., Bennet, M.D. and Heslop-Herrison, J.S. (1990). Genomic *in situ* hybridization to sectioned nuclei shows chromosome domains in grass hybrids. *J. Cell Sci.* **95:** 335-341.

Lentz, R.D., Lapham, L.W. (1970). Postnatal development of tetraploid DNA content in rat Purkinje cells: A quantitative cytochemical study. *J.Neuropath. Exp. Neurol.* **29:** 43-56.

Lerner, E.A., Lerner, M.R., Janeway, C.A., and Steitz, C.A. (1981). Monoclonal antibodies to nucleic acid-containing cellular constituents: probes for molecular biology and autoimmune disease. *Proc. Natl. Acad. Sci. USA.* **78:** 2737-2741.

Leser, G.P., Fakan, S., and Martin, T.E. (1989). Ultrastructural distribution of ribonucleoprotein complexes during mitosis. snRNP antigens are contained in mitotic granule clusters. *Eur. J. Cell Biol.* **50:** 376-389.

Lichter, P., Cremer, T., Borden, J., Manuelidis, L., and Ward, D.C. (1988). Deliniation of individual human chromosomes in metaphase and interphase cells by *in situ* supression hybridization using recombinant DNA libraries. *Hum. Genet.* **80:** 224-234.

Lichter, P., Cremer, T., Tang, C.C., Watkins, P.C., Manuelidis, L., and Ward, D.C. (1988). Rapid detection of human chromosome 21 aberration by *in situ* hybridization. *Proc. Natl. Acad. Sci. USA.* **85:** 9664-9668.

Luntz-Leybman, V., Frostholm, A., Fernando, L., De Blas, A., Rotter, A. (1993). GABAA/benzodiazepine receptor gamma 2 subunit gene expression in developing normal and mutant mouse cerebellum. *Brain Res. Mol. Brain Res.* **19:** 9-21.

Long, B.H., and Och, R.L. (1983). Nuclear matrix, hnRNA, and snRNA in friend erythroleukemia nuclei depleted of chromatin by low ionic strength EDTA. *Biol. Cell.* **48:** 89-98.

Mackay, A.M., Eckley, D.M., Chue, C., and Earnshaw, W.C. (1993). Molecular analysis of the INCENPs (inner centromere proteins): separate domains are required for association with microtubules during interphase and with the central spindle during anaphase. *J. Cell Biol.* **123:** 373-385.

Maeda, N., Niinobe, M., Inoue, Y., and Mikoshiba, K. (1989). Developmental expression and intracellular location of P400 protein characteristic of Purkinje cells in the mouse cerebellum. *Dev. Biol.* **133:** 67-76.

Mangelsdorf, D.J., Thummel, C., Beato, M., Herrlich, P., Schutz, G., Umesono, K., Blumberg, B., Kastner, P., Mark, M., Chambon, P., Evans, R.M. (1995). The nuclear receptor superfamily: The second decade. *Cell.* **83:** 835-839.

Mann, D.M., Yates, P.O., and Barton, C.M. (1978). The DNA content of Purkinje cells in mammals. *J. Comp. Neurol.* **180:** 345-347.

Manuelidis, L. (1982). Nucleotide sequence definition of a major human repeated DNA, the Hind III 1.9kb family. *Nucl. Acids Res.* **10:** 3211-3219.

Manuelidis, L. (1984a). Different central nervous system cell types display distinct and non-random arrangements of satellite DNA sequences. *Proc. Natl. Acad. Sci. USA*. **81:** 2123-2127.

Manuelidis, L. (1984b). Active nucleolus organizers are precisely positioned in adult central nervous system cells but not in neuroectodermal tumour cells. *J. Neuropath. Exp. Neurol.* **43:** 225-241.

Manuelidis, L. (1985a). Indications of centromere movement during interphase and differentiation. *Ann. N.Y. Acad. Sci.* **450:** 205-221.

Manuelidis, L. (1985b). Individual interphase chromosome domains revealed by *in situ* hybridization. *Hum. Genet.* **71:** 288-293.

Manuelidis, L. (1990). A view of Interphase chromosomes. *Science*. **250:** 1533-1540.

Manuelidis, L. and Borden, J. (1988). Reproducible compartmentalization of individual chromosomes revealed by *in situ* hybridization. *Chromosoma*. **96:** 397-410.

Manuelidis, L. and Chen, T.L. (1990). A unified model of eukaryotic chromosomes. *Cytometry*. **11:** 8-25.

Manuelidis, L., and Manuelidis , E.E. (1974). On the DNA content of cerebellar Purkinje cells in vivo and in vitro. *Exp. Neurol.* **43:** 192-206.

Mares, V.L., Lodin, Z., and Sacha, J.A. (1973). A cytochemical and autoradiographic study of nuclear DNA in mouse Purkinje cells. *Brain Res.* **53:** 273-289.

Marshall, W.F., and Sedat, J.W. (1999). Genomic Imprinting. In "Results and problems in cell differentiation" (R.Ohlsson, Ed.), Springer. **25:** 283-301.

Martin, L.J., Blackstone, C.D., Levey, A.I., Huganir, R.L., and Price, D.L. (1993). AMPA glutamate receptor subunits are differentially distributed in rat brain. *Neuroscience*. **53:** 327-358.

Martou,G., and De Boni, U. (2000). Nuclear topology of murine, cerebellar Purkinje neurons: Changes as a function of postnatal development. *Exp. Cell Res.* **256:** 131-139.

Mason, C.A., Christakos, S., and Catalano, S.M. (1990). Early climbing fiber interaction with Purkinje cells in the postnatal mouse cerebellum. *J. Comp. Neurol.* **297:** 77-90.

Masumoto, H., Masukata, H., Muro, Y., Nozaki, N., and Okazaki, T. (1989a). A human specific antigen (CENP-B) interacts with a short sequence in alphoid DNA, a human centromeric satellite. *J. Cell Biol.* **109:** 1963-1973.

Masumoto, H., Sugimoto, K., and Okazaki, T. (1989b). Alphoid satellite DNA is tightly associated with centromere antigens in human chromosomes throughout the cell cycle. *Exp. Cell Res.* **181:** 181-196.

Matera, A.G., and Ward, D.C. (1993). Nucleoplasmic organization of small nuclear ribonucleoproteins in cultured human cells. *J. Cell Biol.* **212:** 715-727.

Mathis, L., Bonnerot, C., Puelles, L., and Nicolas. J.F. (1997). Retrospective clonal analysis of the cerebellum using genetic laacZ/lacZ mouse mosaics. *Development.* **124:** 4089-4104.

Mathog, D., Hochstrasser, M., Gruenbaum, Y., Saumweber, H., and Sedat, J.W. (1984). Characteristic folding patterns of the polytene chromosomes in Drosophila salivary gland nuclei. *Nature.* **308:** 414-421.

Matsui, T., Sashihara, S., Oh, Y., Waxman, S.G. (1995). An orphan nuclear receptor, mRORa, and its spatial expression in adult mouse brain. *Mol. Brain Res.* **33:** 217-226.

Matysiak-Scholze, U., and Nehls, M. (1997). The structural integrity of RORα isoforms is mutated in *staggerer* mice: Cerebellar coexpression of RORα1 and RORα4. *Genomics.* **43:** 78-84.

McClintic, J.R. The Physiology of the Human body. 1985. wysiwyg://85/http://www.albany.net/~tjc/20-02.html.1999

McDonald, JW., Johnston, M.V. (1990). Physiological and pathophysiological roles of excitatory amino acids during central nervous system development. *Brain Res. Rev.* **15:** 41-70.

McNeilage, L.J., Whittingham, S., McHugh, N., and Barnett, A.J. (1986). A highly conserved 72,000 dalton centromeric antigen reactive with autoantibodies from patients with progressive systemic sclerosis. *J. Immunol.* **137:** 2541.

Messer, A. (1988). Thyroxine injections do not cause premature induction of thymidine kinase in sg/sg mice. *J. Neurochem.* **51:** 888-891.

Messer, A., Eisenberg, B., and Plummer, J. (1991). The *lurcher* cerebellar mutant phenotype is not expressed on a *staggerer* mutant background. *J. Neurosci.* **11:** 2295-2302.

Messer, A., Plummer-Siegard, J., and Eisenberg, B. (1990). Staggerer mutant mouse Purkinje cells do not contain detectable calmodulin mRNA. *J Neurochem.* **55:** 293-302.

Miale, I.L., and Sidman, R.L. (1961). An autoradiographic analysis of histogenesis in the mouse cerebellum. *Exp. Neurol.* **4:** 277-296.

Middleton, F.A., and Strick, P.L. (1998). The cerebellum: an overview. *Trends Neurosci.* **21:** 1-3.

Milankov, K., Amankwah, K.S., and De Boni, U. (1991). Cytochemical localization of actin and myosin aggregates within interphase nuclei of intact neurons. *J. Cell Biol.* **115:** 95a.

Milankov, K., and De Boni, U. (1993). Cytochemical localization of actin and Myosin aggregates in interphase nuclei in situ. *Exp. Cell Res.* **209:** 189-199.

Millen, K.J., Wurst, W., Herrup, K., Joyner, A.L. (1994). Abnormal embryonic cerebellar development and patterning of postnatal foliation in two mouse Engrailed-2 mutants. *Development.* **120:** 695-706.

Mitchell, A.R., Gosden, J.R., and Miller, D.A. (1985). A cloned sequence, p82H, of the alphoid repeated DNA family found at the centromeres of all human chromosomes. *Chromosoma.* **92:** 369-377.

Mitchell, A.R. (1996). The mammalian centromere: Its molecular architecture. *Mutation Res.* **372:** 153-162.

Mirkovitch, J., Mirault, M.E., and Laemmli, U.K. (1984). Organization of the higher-order chromatin loop: specific DNA attachment sites on nuclear scaffold. *Cell.* **39:** 223-232.

Misteli, T., Caceres, J.F., and Spector, D.L. (1997). The dynamics of a pre-mRNA splicing factor in living cells. *Nature.* **387:** 523-527.

Misteli, T., and Spector, D.L. (1997). Protein phosphorylation and the nuclear organization of pre-mRNA splicing. *Trends Cell Biol.* **7:** 135-138.

Moroi, Y., Hartman, A.L., Nakane, P.K. and Tan, E. M. (1981). Distribution of kinetochore (centromere) antigen in mammalian cell nuclei. *J. Cell Biol.* **90:** 254-259.

Mortillaro, M.J., Blencowe, J.B., Wei, X., Nakayasu, Y., Du, L., Warren, S.L., Sharp, P.A., and Berezney, R. (1996). A hyperphosphorylated form of the large subunit of RNA polymerase II is associated with splicing complexes and the nuclear matrix. *Proc. Natl. Acad. Sci. USA.* **93:** 8253-8257.

Mugnaini, E., Dahl, A.-L., and Morgan, J.I. (1988). Cerebellin is a postsynaptic neuropeptide. *Synapse.* **2:** 125-138.

Nakagawa, S., Okano, H., Furuichi, T., Aruga, J., Mikoshiba, K. 1991. The subtypes of the mouse InsP3R1 are expressed in a tissue-specific and developmentally specific manner. *Proc. Natl. Acad. Sci. USA.* **88:** 6244-6248.

Nakagawa, S., Watanabe, M., and Inoue, Y. (1996a). Altered gene expression of the N-methyl-D-aspartate receptor channel subunits in Purkinje cells of the staggerer mutant mouse. *Eur. J. Neurosci.* **8:** 2644-2651.

Nakagawa, S., Watanabe, M., and Inoue, Y. (1996b). Regional variation in expression of calbidin and inositol 1,4,5-triphosphate receptor type 1 mRNAs in the cerebellum of the staggerer mutant mouse. *Eur. J. Neurosci.* **8:** 1401-1407.

Nakagawa, S., Watanabe, M., and Inoue, Y. (1997). Prominent expression of nuclear hormone receptor RORa in Purkinje cells from early development. *Neurosci. Res.* **28:** 177-184.

Nakayasu, H., Mori, H., and Ueda, K., (1982). Association of small nuclear RNA-protein complex with the nuclear matrix from bovine lymphocytes. *Cell Struct. Funct.* **7:** 253-262. *Neurosci.* Abstracts **15:** 795.

Nickerson, J.A., Blencowe, B.J., and Penman, S. (1995). The architectural organization of nuclear metabolism. *Int. Rev. Cytol.* **162:** 67-123.

Nigg, E.A. (1989). The nuclear envelope. *Curr. Opin. Cell Biol.* **1:** 435-440.

Oberdick, J., Schilling, K., Smeyne, R.J., Corbin, J.G., Bocchiaro, C., and Morgan, J.I. Control of segment-like patterns of gene expression in the mouse cerbellum. (1993). *Neuron.* **10:** 1007-1018.

Oberdick, J., Baader, S.L., and Schilling, K. (1998). From zebra stripes to postal zones: deciphering patterns of gene expression in the cerebellum. *Trends Neurosci.* **21:** 383-390.

Olsen, R.W., and Tobin, A.J. (1990). Molecular biology of GABAA receptors. *FASEB J.* **4:** 1469-1480.

Oud, J.L., and Reutlinger, A.H.H. (1981). The behaviour of silver positive structures during meiotic prophase of male mice. *Chromosoma* **81:** 569-578.

Ozol, K., Hayden, J.M., Oberdick, J., and Hawkes, R. (1999). Transverse zones in the vermis of the mouse cerebellum. *J. Comp. Neurol.* **412:** 95-111.

Pardue, M.L., and Gall, J.G. (1970). Chromosomal localization of mouse satellite DNA. *Science.* **168:** 1356-1358.

Park, P.C. and De Boni, U. (1991). Dynamics of nucleolar fusion in neuronal interphase nuclei *in vitro*: Association with nuclear rotation. *Exp. Cell. Res.* **197:** 213-221.

Park, P.C., and De Boni, U. (1992). Spatial rearrangement and enhanced clustering of kinetochores in interphase nuclei of dorsal root ganglion neurons *in vitro*: Association with nucleolar fusion. *Exp. Cell Res.* **203:** 222-229.

Park, P.C., and De Boni, U. (1996). Transposition of DNase hypersensitive chromatin to the nuclear periphery coincides temporally with nerve growth factor-induced up-regulation of gene expression in PC12 cells. *Proc. Natl. Acad. Sci.* **93:** 11646-11651.

Park, P.C., and De Boni, U. (1998). A specific conformation of the territory of chromosome 17 locates *ERBB-2* sequences to a DNAase-hypersensitive domain at the nuclear periphery. *Chromosoma.* **107:** 87-95.

Park, P.C., and De Boni, U. (1999). Dynamics of structure-function relationships in interphase nuclei (minireview). *Life Sciences*. **64:** 1703-1718.

Pebusque, M.J., Robaglia, A., and Seite, R. (1981). Diurnal rhythm nucleolar volume in sympathetic neurons of the rat superior cervical ganglion. *Eur. J. Cell Biol.* **24:** 128-130.

Pfarr, C.M., Cove, M., Grissom, P.M., Hay, T.S., Porter, M.E., and McIntosh, R.J. (1990). Cytoplasmic dynein localizes to kinetochores during mitosis. *Nature*. **345:** 263-265.

Phi-Van, L., von Kries, J.P., Ostertag, W., and Stratling, W.H. (1990). The chicken lysozyme 5' matrix attachment region increases transcription from a heterologous promoter in heterologous cells and dampens position effects on the expression of transfected genes. *Mol. Cell Biol.* **10:** 2302-2307.

Pienta, K.J., and Coffey, D.S. (1984). A structural analysis of the role of the nuclear matrix and DNA loops in the organization of the nucleus and chromosome. *J.Cell Sci. Suppl.* **1:** 123-135.

Pienta, K.J., Getzenberg, R.H., and Coffey, D.S. (1991). Cell structure and DNA organization. *In* Critical Reviews in Eukaryotic Gene Expression. **1:** 355-385.

Pinkel, D., Gray, J.W., Trask, B., van den Engh, G., and Fuscoe, J. (1986). Cytogenetic analysis by in situ hybridization and fluorescently labelled nucleic acid probes. *Cold Spring Harbor Symp. Quant. Biol.* **51:** 151-157.

Pinkel, D., Landegent, J., Collins, C., Fuscoe, J., Segraves, R., Lucas, J., and Gray, J.W. (1988). Fluorescence *in situ* hybridization with human chromosome specific libraries: detection of trisomy 21 and translocations of chromosome 4. *Proc. Natl. Acad. Sci. USA* **85:** 9138-9142.

Pluta, A.F., Cooke, C.A., and Earnshaw, W.C. (1990). Structure of the human centromere at metaphase. *Trends in Biol. Sci.* **51:** 151-157.

Pluta, A.F., and Earnshaw, W.C. (1996). Specific interaction between human kinetochore protein CENP-C and a nucleolar transcriptional regulator. *The J. Biol. Chem.* **271:** 18767-18774.

Pluta, A.F., Saitoh, N., Goldberg, I., and Earnshaw, W.C. (1992). Identification of a subdomain of CENP-B that is necessary and sufficient for localization to the human centromere. *J. Cell Biol.* **116:** 1081-1093.

Pomerat, C.M. (1953). Rotating nuclei in tissue culture of adult human nasal mucosa. *Exp. Cell Res.* **5:** 191-196.

Query, C.C., Moore, J.M., and Sharp, P.A. (1994). Branch nucleophile selection in pre-mRNA splicing: evidence for the bulged duplex model. *Genes Dev.* **8:** 587-597.

Rabl, C. (1885). Uber Zelltheilung. *In*: Morphologisches Jahrbuch. (Gegangaur, C. ed.). **10:** 214-330

Rae, P.M.M., and Franke, W.W. (1972). The interphase distribution of satellite DNA-containing heterochromatin in mouse nuclei. *Chromosoma.* **39:** 443-456.

Rakic, P., and Sidman, R.L. (1973). *J. Comp. Neurol.* **152:** 133-161.

Rattner, J.B. (1991). The structure of the mammalian centromere. *Bioessays.* **13:** 51-56.

Rattner, J.B., Kingwell, B.G., and Fritzel, M.J. (1988). Detection of distinct structural domains within the primary constriction using antibodies. *Chromosoma.* **96:** 360-367.

Rattner, J.B., Rao, A., Fritzler, M.J., Valencia, D.W., and Yen, T.J. (1993). CENP-F is a .ca 400kDa kinetochore protein that exhibits a cell-cycle dependent localization. *Cell Mot. Cytoskel.* **26:** 214-226.

Rawlins, D.J., and Shaw, P.J. (1990a). Localization of ribosomal and telomeric DNA sequences in intact plant nuclei by *in situ* hybridization and three-dimensional reconstruction. *J. Micros.* **157:** 83-89.

Rawlins, D.J., and Shaw, P.J. (1990b). 3-D arrangement of genes in interphase by in situ hybridization and confocal microscopy. *J. Cell Biol.* **111:** 504a.

Rimm, D.L., and Pollard, T.E. (1989). Purification and characterization of an *Acanthamoeba* nuclear actin-binding protein. *J. Cell Biol.* **109:** 585-591.

Robinson, S.I., Small, D., Idzerda, R., McKnight, G.S., and Vogelstein, B. (1983). The association of transcriptionally active genes with the nuclear matrix of the chicken oviduct. *Nuc. Acids Res.* **13:** 2413-2431.

Romanova, L.Y., Deriagin, G.V., Mashkowa, T.D., Tumeneva, I.G., Mushegian, A.R., Kisselev, L.L., and Alexandrov, I.A. (1996). Evidence for selection in evolution of alpha satellite DNA: The central role of CENP-B/pJa binding region. *J. Mol. Biol.* **26:** 334-340.

Rossi, F., Jankovski, A., and Sotelo, C. (1995). Target neuron controls the integrity of afferent axon phenotype: a study on the Purkinje cell-climbing fiber system in cerebellar mutant mice. *J Neurosci.* **15:** 2040-2056.

Rougvie, A.E., and Lis, J.T. (1988). The RNA polymerase II molecule at the 5' end of the uninduced hsp70 gene of *D.melanogaster* is transcriptionally engaged. *Cell.* **54:** 795-804.

Rowland, R.E., and Nickless, E.M. (1999). Confocal microscopy elucidates chromosome behaviour and gene activity. *The Americas Microscopy and Analysis.* 15-17.

Rosenbluth, J. (1962). Subsurface cisterns and their relationship to the neuronal plasma membrane. *J. Cell Biol.* **13:** 405-421.

Ross, M.E.(1990). *Proc. Natl. Acad. Sci. USA.* **87:** 4189-4192.

Ruskin, B., and Green, M.R. (1985). An RNA processing activity that debranches RNA lariats. *Science.* **229:** 135-140.

Rymond, B.C., and Rosbach, M. (192). Molecular and Cellular Biology of the Yeast *Saccharomyces*. E.W Jones., J.R. Pringle and J.R. Broach eds. Cold Spring Harbor Laboratory Press.

Ryo, Y., Miyawaki, A., Furuichi, T., Mikoshiba, K. (1993). Expression of the mGluR1α and the ionotropic glutamate receptor GluR1 in the brain during postnatal development of normal mouse and in the cerebellum from mutant mice. *J. Neurosci. Res.* **36:** 19-32.

Sahlas, D.J., Milankov, K., Park, P.C., and De Boni, U. (1993). Distribution of snRNPs, splicing factor SC-35 and actin in interphase nuclei; immunocytochemical evidence for differential distribution during changes in functional states. *J. Cell Sci.* **105:** 347-357.

Saitoh, H., Tomkiel, J., Cooke, C.A., Ratrie, H., Maurer, M., Rothfield, N.F., and Earnshaw, W.C. (1992). CENP-C, an autoantigen in scleroderma, is a component of the human inner kinetochore plate. *Cell.* **70:** 115-125.

Schardin, M., Cremer, T., Hager, H.D., and Lang, M. (1985). Specific staining of human chromosomes in Chinese hamster x man hybrid cell lines demonstrates interphase chromosome territories. *Hum. Genet.* **71:** 281-287.

Scheer, U., Hensson, H., Franke, W.W. and Jockusch, B.M.(1984). Microinjection of actin-binding proteins and actin antibodies demonstrates involvement of nuclear actin in transcription of lampbrush chromosomes. *Cell.* **39:** 111-112.

Scheer, U., and Rose, K.M. (1984). Localization of RNA polymerase I in interphase cells and mitotic chromosomes by light and electron microscopic immunocytochemistry. *Proc. Natl. Acad. Sci. USA.* **81:** 1431-1435.

Scheer, U., and Weisenberger, D. (1994). The nucleolus. *Curr. Opin. Cell Biol.* **6:** 354-359.

Scherini, E. (1982). "Hyperdiploidy" in the Purkinej neuron population: chromatin status or extra-DNA? The influence of fixatives on Feulgen-DNA. *Basic Appl. Histochem.* **26:**173-183.

Schiffmann, S.N., Bernier, B., and Goffinet, A.M. (1997). Reelin mRNA expression during mouse brain development. *Eur, J. Neurosci.* **9:** 1055-1071.

Schilling, K., Dickenson, M.H, Connor, J.A., Morgan, J.I. (1991). Electrical activity in cerebellar cultures determines Purkinje cell dendritic growth patterns. *Neuron.* **7:** 891-902.

Schmid, W., and Steinlein, C. (1991). Chromsome banding in amphibia; XVI. High-resolution replication banding patterns in Xenopus laevis. *Chromosoma.* **101:** 123-132.

Sidman, R.L., Lane, P.W., and Dickie, M.M. (1962). Staggerer: A new mutation in the mouse affecting the cerebellum. *Science*. **137:** 610-612.

Sidman, R.L., and Rakic, P. (1973). Neuronal migration, with special reference to developing human brain: a review. *Brain Res*. **62:** 1-35.

Slemmon, J.R., Blacher, R., Danho, W., Hempstead, J.L., and Morgan, J.I. (1984). Isolation and sequencing of two novel cerebellum-specific peptides. *Proc. Natl. Acad. Sci. USA*. **81:** 6866-6870.

Slemmon, J.R., Danho, W., Hempstead, J.L., and Morgan, J.I. (1985). Cerebellin, a quantifiable marker for Purkinje cell maturation. *Proc. Natl. Acad. Sci. USA*. **82:** 7145-7148.

Slemmon, J.R., Goldowitz, D., Blacher, R., and Morgan, J.I. (1988). Evidence for the transneuronal regulation of cerebellin biosynthesis in developing Purkinje cells. *J Neurosci*. **8:** 4603-4611.

Smeyne, R.J., Oberdick, J., Schilling, K., Berrebi, A.S., Mugnaini, E., and Morgan, J.I. (1991). Dynamic organization of developing Purkinje cells revealed by transgene expression. *Science*. **254:** 719-721.

Smeyne, R.J., Chu, T., Lewin, A., Bian, F., Crisman, S.S., Kunsch, C., Lira, S.A., Oberdick, J. (1995). Local control of granule cell generation by cerebellar Purkinje cells. *Mol. Cell. Neurosci*. **6:** 230-251.

Smith, H.C., Harris, S.G., Zillmann, M., and Berget, S.M. (1989). Evidence that a nuclear matrix protein participates in pre-mRNA splicing. *Exp. Cell Res*. **182:** 521-533.

Smith, A.M., and Mullen, R.J. (1997). Parallin, a cerebellar granule cell protein the expression of which is developmentally regulated by Purkinje cells: evidence from mutant mice. *Develop. Brain Res*. **104:** 79-89.

Smith, H.C., and Rothblum, L.I., (1987). Ribosomal DNA sequences attached to the nuclear matrix. *Biochem. Genet*. **25:** 863-876.

Soha, J.M., and Herrup, K. (1993). Purkinje cell dendrites in staggerer - wild type chimeras lack the aberrant morphologies found in lurcher-wildtype chimeras. *J. Comp. Neurol*. **331:** 540-550.

Soha, J.M., and Herrup, K. (1995). Stunted morphologies of cerebellar Purkine cells in *lurcher* and *staggerer* mice are cell intrinsic effects of the mutant genes. *J. Comp. Neurol*. **357:** 65-75.

Soha, J.M., Kim, S., Crandall, J.E., and Vogel, M.W. (1997). Rapid growth of parallel fibers in the cerebella of normal and *staggerer* mutant mice. *J Comp Neurol*. **389:** 642-654.

Sotelo, C., and Alvarado-Mallart, R.M. (1987). Reconstruction of the defective cerebellar circuitry in adult Purkinje cell degeneration muntant mice by Purkinje cell replacement through transplantation of solid embryonic implant. *Neurosci.* **20:**1-22.

Sotelo, K. and Wassef, M. (1991a). Cerebellar development: afferent organization and Purkinje cell heterogeneity. *Philos. Trans. R. Soc. Lond. B. Biol. Sci.* **331:** 307-313.

Sotelo, K. and Wassef, M. (1991b). Purkinje cell heterogeneity in four cerebellar mutations revealed by zebrin I expression. *Soc. Neurosci. Abstr.* **17:** 918.

Spector, D.L. (1990). Higher order nuclear organization: three-dimensional distribution of small nuclear ribonucleoprotein particles. *Proc. Natl. Acad. Sci.* **87:** 147-151.

Spector, D.L. (1993). Macromolecular domains within the cell nucleus. *Annu. Rev.Cell Biol.* **9:** 265-315.

Stein, G.S., Van Wijnen, A.J., Montecino, M., Stein, J.L., and Lian, J.B. (1999). Nuclear structure/gene expression interrelationships. *J Cell. Physiol.* **181:** 240-250.

Strata, P., and Rossi, F. (1998). Plasticity of the olivocerebellar pathway. *Trends Neurosci.* **21:** 407-413.

Stuurman, N. (1991). Structure and composition of the nuclear matrix. Ph.D. thesis, University of Amsterdam.

Sutherland, M.L., Delaney, T.A., and Noebels, J.L. (1996). Glutamate Transporter mRNA expression in proliferative zones of the developing and adult murine CNS. *J. Neurosci.* **16:** 2191-2207.

Swartz, F.J., and Bhatnagar, K.P. (1981). Are CNS neurons polyploid? A critical analysis based upon cytophotometric study of the DNA content of cerebellar and olfactory bulbar neurons of the bat. *Brain Res.* **208:** 267-281.

Swisher, D.A., and Wilson, D.B. (1977). Cerebellar histogenesis in the Lurcher (*Lc*) mutant mice. *J. Comp. Neurol.* **173:** 205-218.

Tagawa, Y., Nanashima, A., Yasutake, T., Hatano, K., Nishizawa-Takano, J.E., and Ayabe, H. (1997). Differences in spatial localization and chromatin pattern during different phases of cell cycle between normal and cancer cells. *Cytometry.* **27:** 327-335.

Takayama, C., Nakagawa, S., Watanabe, M., Mishina, M., and Inoue, Y. (1996). Developmental changes in expression and distribution of the glutamate receptor 2 subunit according to the Purkinje cell maturation. *Dev. Brain Res.* **92:** 147-155.

Takei, K., Stukenbrok, H., Metcalf, A., Mignery, G., Sudhof, T., Volpe, P., De Camilli, P. (1992). Calcium stores in Purkinje neurons: endoplasmic reticulum subcompartments demonstrated by the heterogeneous distribution of the Ins-P3 receptor, calcium-ATPase and calsequestrin. *J. Neurosci.* **12:** 489-505.

Teyler, J.T. 1999. Cerebellum-Anatomy and Physiology. http://web.neoucom.edu/DEPTS/NEUR/WEB/demo/cerebellumdemo.html. December, 5,1999.

Thomas, J.O., Rees, C., and Finch, J.T. (1992). Cooperative binding of the globular domains of histones H1 and H5 to DNA. *Nucl. Acids Res.* **20:** 187-194.

Thompson, E.M., Christians, E., Stinnakre, M.G., and Renard, J.P. (1994). Scaffold attachment regions stimulate HSP70.1 expression in mouse pre-implantation embryos but not in differentiated tissues. *Mol. Cell Biol.* **14:** 4694-4703.

Thorburn, A., and Knowland, J. (1993). Attachment of the vitellogenin genes to the nucleoskeleton accompanies their activation. *Biochem. Biophys. Res. Comm.* **191:** 308-313.

Tischendorf, G., Sawitzky, D., and Werz, G. (1987). Antibodies specific for vertebrate actin, myosin, actinin or vinculin recognize epitopes in the giant nucleus of the marine green algae *Acetabularia*. *Cell Mot. Cytoskel.* **7:** 78-86.

Tomkiel, J., Cooke, C.A., Saitoh, H., Bernat, R.L., and Earnshaw, W.C. (1994). CENP-C is required for maintaining proper kinetochore size and for a timely transition to anaphase. *J. Cell Biol.* **125:** 531-545.

Trenkner, E., and Hoffman, M.K. (1986). Defective development of the thymus and immunological abnormalities in the neurological mouse mutation "staggerer". *J. Neurosci.* **6:** 1733-1737.

Tsukiyama, T., Becker, P.B., and Wu, C. (1994). ATP-dependent nucleosome disruption at a heat-shock promoter mediated by binding of GAGA transcription factor. *Nature*. **367:** 525-532.

Ueyama, H., Nakayasu, H., and Ueda, K. (1987). Nuclear actin and transport of RNA. *Cell Biol. Int. Reports*. **11:** 671-677.

Vafa, O., and Sullivan, K.F. (1997). Chromatin containing CENP-A and a-satellite DNA is a major component of the inner kinetochore plate. *Current Biol.* **7:** 897-900.

Valdivia, M.M., and Brinkley, B.R. (1985). Fractionation and initial characterization of the kinetochore from mammalian metaphase chromosomes. *J. Cell Biol.* **101:** 1124-1134.

van der Valden, H.M.W., and Wanka, F. (1987). The nuclear matrix - its roles in the spatial organization and replication of eukaryotic DNA. *Mol. Biol. Rep.* **12:** 69-77.

van Driel, R., Wansink, D.G., van Steensel, B., Grande, M.A., Schul, W., and de Jong, L. (1995). Nuclear domains and the nuclear matrix. *Int. Rev. Cytol.* **162A:** 151-189.

Van Eekelen, C.A.G., and Van Venrooij, W.J. (1981). hnRNA and its attachment to a nuclear protein matrix. *J. Cell Biol.* **88:** 554-563.

Verheijen, R., van Venrooij, W., and Ramaekers, F., (1988). The nuclear matrix structure and composition. *J. Cell Sci.* **90:** 11-36.

Vershure, P.J., van Der Kraan, I., Manders, E.M., and van Driel, R. (1999). Spatial relationship between transcription sites and chromosome territories. *J. Cell Biol.* **147:** 13-24.

Vig, B.K., and Rattner, J.B. (1989). Centromere, kinetochore, and cancer. *Oncogenesis.* **1:** 343-370.

Visa, N., Puvion-Dutilleul, F., Harper, F., Bachellerie, J.P., and Puvion, E. (1993). Intranuclear distribution of poly (A)RNA determined by electron microscope *in situ* hybridization. *Exp. Cell Res.* **208:** 19-34.

Vogel, M.W., and Herrup, K. (1993). A theoritical and exprerimental examination of cell lineage relationships among cerebellar Purkinje cells in the mouse. *Dev.Biol.* **156:** 49-68.

Vogelstein, B., Pardoll, D.M., and Coffey, D.S. (1980). Supercoiled loops and eukaryotic DNA replication. *Cell.* **22:** 79-85.

Voogd, J., and Bigare, F. (1980). The Inferior Olivary Nucleus: Anatomy and Physiology. Raven Press.

Voogd, J., and Glickstein, M. (1998). The anatomy of the cerebellum. *Trends Neurosci.* **21:** 370-375.

Wachtler, F., Hartung, M., Devictor, M., Wiegant, J., Stahl, A., and Schwarzacher, H.G. (1989). Ribosomal DNA is located and transcribed in dense fibrillar component of human sertoli cell nucleoli. *Exp. Cell Res.* **184:** 61-71.

Wachtler, F., Hopman, A.H.N., Wiegant, J., and Schwarzacher, H.G. (1986). On the position of nucleolus organizer regions (NORs) in interphase nuclei. *Exp. Cell Res.* **167:** 227-240.

Wachtler, F., Mosgoller, W. and Schwarzacher, H.G. (1990). Electron microscopic *in situ* hybridization and autoradiography: localization and transcription of rDNA in lymphocyte nucleoli. *Exp. Cell Res.* **187:** 346-348.

Wallace, V.A. (1999). Purkinje-cell derived Sonic hedgehog regulates granule neuron precursor cell proliferation in the developing mouse cerebellum. *Curr. Biol.* **22:** 445-448.

Wang, J., Cao, L.G., Wang, Y.L., and Pederson, T. (1991). Localization of pre-mRNA at discrete nuclear sites. *Proc. Natl. Acad. Sci. USA.* **88:** 7391-7395.

Wanner, I., Baader, S.L., Brich, M., Oberdick, J., Schilling, K. (1997). Subcellular localization of specific mRNAs and their protein products in Purkinje cells by combined fluorescence in situ hybridization and immunocytochemistry. *Histochem. Cell Biol.* **108:** 345-357.

Wansink, D.G., Nelissen, R.L.H., and de Jong, L. (1994). *In vitro* splicing of pre-mRNA containing bromo-uridine. *Mol. Biol. Rep.* **19:** 109-113.

Wassef, M., Angaut, P., Arsenio-Nunes, M.L., Bourrat, F., and Sotelo, C. (1990). Purkinje cell heterogeneity: its role in organizing the topography of the cerebellar cortex connections. The cerebellum revisited (ed. R. Llinas and C. Sotelo). Berlin: Springer-Verlag.

Watanabe, M., Nakamura, M., Sato, K., Kano, M., Simon, M.I., and Inoue, Y. (1998). Patterns of expression for the mRNA corresponding to the four isoforms of Phospholipase Cβ in mouse brain. *European J. Neuroscience.* **10:** 2016-2025.

Weber, A., and Schachner, M. (1984). Maintenance of immunocytologically identified Purkinje cells from mouse cerebellum in monolayer culture. *Brain Res.* **311:** 119-130.

Weintraub, H.. (1984). Histone-H1-dependent chromatin superstructures and the suppression of gene activity. *Cell.* **38:** 17-27.

Wetts, R., and Herrup, K. (1982). Cerebellar Purkinje cells are descended from a small number of progenitors committed during early development: quantitative analysis of lurcher chimeric mice. *J. Neurosci.* **2:** 1494-1498.

Wilkie, T.m., Scherle, P.A., Strathmann, M.P., Slepak, V.Z., and Simon, M.I. (1991). Characterization of G-protein α subunits in the Gq class: Expression in murine tissue and in stromal and hematopoietic cell lines. *Proc. Natl. Acad. Sci. USA.* **88:** 10049-10053.

Wong, A.K.C., and Rattner, J.B. (1988). Sequence organization and cytological localization of the minor satellite of mouse. *Nuc. Acids Res.* **16:** 11645-11661.

Wood, W.I., and Felsenfeld, G. (1982). Chromatin structure of the chicken beta-globin gene region. Sensitivity to DNase I, micrococcal nuclease, and DNase II. *J. Biol. Chem.* **257:** 7730-7736.

Wu, Z., and Maniatis, T. (1993). Specific interactions between proteins implicated in splice site selection and regulated alternative splicing. *Cell.* **75:** 1061-1070.

Wurst, W., Auerbach, A.B., Joyner, A.L (1994). Multiple developmental defects in Engrailed-1 mutant mice: an early min-hindbrain deletion and patterning defects in forelimbs and sternum. *Development.* **120:** 2065-2075.

Xing, Y., Johnson, C.V., Dobner, P., and Lawrence, J.B. (1993). Higher level organization of individual gene transcription and RNA splicing: integration of nuclear structure and function. *Science*. **259:** 1326-1330.

Xing, Y., Johnson, C.V., Moen, Jr.P.T., McNeil, J.A., and Lawrence, J.B. (1995). Non-random gene organization: structural arrangements of specific pre-mRNA transcription and splicing with SC-35 domains. *J. Cell Biol.* **131:** 1635-1647.

Yamada, K., Wada, S., Watanabe, M., Tanaka, K., Wada, K., and Inoue, Y. (1997). Changes in expression and distribution of the glutamate transporter EAAT4 in developing mouse Purkinje cells. *Neurosci. Res.* **27:** 191-198.

Yen, T.J., Compton, D.A., Wise, D., Zinkowski, R.P., Brinkley, B.R., Earnshaw, W.C., and Cleveland, D.W. (1991). CENP-E, a novel human centromere-associated protein required for progression from metaphase to anaphase. *Embo. J.* **10:** 1245-1254.

Yuasa, S., Kawamura, K., Ono, K., Yamakuni, T., and Takahashi, Y. (1991). Development and migration of Purkinje cells in the mouse cerebellar primordium. *Anat. Embryol.* **184:** 195-212.

Yuryev, A., Patturajan, Y., Litingtun, Y., Joshi, R.V., Gentile, C., Gebara, M., and Corden, J.L. (1996). The C-terminal domain of the largest subunit of RNA polymerase II interacts with a novel set of Serine/Arginine-rich proteins. *Proc. Natl. Acad. USA*. **93:** 6975-6980.

Zamore, P.D., and Greem M.R.(1991). Biochemical characterization of U2 snRNP auxiliary factor: an essential pre-mRNA splicing factor with a novel intranuclear distribution. *EMBO J.* **10:** 207-214.

Zanjani, H.S., Herrup, K., and Guastavino, J.M., Delhaye-Bouchard, N., and Mariani, J. (1994). Developmental studies of the inferior olivary nucleus in *staggerer* mutant mice. *Brain Res. Dev. Brain Res.* **82:** 18-28.

Zanjani, H.S., Vogel, M.W,m Delhaye-Bouchaud, N., Martinou, JC., and Mariani, J. (1996). Increased cerebellar Purkinje cell numbers in mice overexpressing a human bcl-2 gene. *J. Comp. Neurol.* **374:** 332-341.

Zdillar, D., Luntz-Leybman, V., Frostholm, A., and Rotter, A. (1992). Differential expression of GABAA/Benzodiazepine receptor β1, β2, and β3 subunit mRNAs in the developing mouse cerebellum. *J. Comp. Neurol.* **326:** 580-594.

Zdillar, D., Rotter, A., and Frostholm, A. (1991). Expression of GABAA/benzodiazepine receptor alpha 1-subunit mRNA and [3H]flunitrazepam binding sites during postnatal development of the mouse cerebellum. *Brain Res. Dev. Brain. Res.* **61:** 63-71.

Zhang, W., Ghetti, B., and Lee, W.H. (1997). Decreased IGF-I gene expression during the apoptosis of Purkinje cells in pcd mice. *Brain Res. Dev. Brain Res.* **98:** 164-176.

Zhang, G., Taneja, K.L., Singer, R.H., and Green, M.R. (1994). Localization of pre-mRNA splicing in mammalian nuclei. *Nature.* **372:** 809-812.

Zhang, L., and Goldman, J.E. (1996a). *Neuron.* **16:** 47-54.

Zhang, L., and Goldman, J.E. (1996b). Developmental fates and migratory pathways of dividing progenitors in the postnatal rat cerebellum *J. Comp. Neurol.* **370:** 536-550.

Zhao, K., Kas, E., Gonzalez, E., and Laemmli, U.K. (1993). SAR-dependent mobilization of histone H1 by HMG I/Y *in vitro*: HMG I/y is enriched in H1 depleted chromatin. *EMBO J.* **12:** 3237-3247.

Zirbel, R.M., Mathieu, U.R., Kurtz, A., Cremer, T., and Lichter, P. (1993). Evidence for a nuclear compartment of transcription and splicing located at chromosome domain boundaries. *Chromosome Res.* **1:** 92-106.

Zou, L., Hagen, S.G., Strait, K.A., and Oppenheimer, J.H. (1994). Identification of thyroid hormone response element in rodent Pcp-2, a developmentally regulated gene of cerebellar Purkinje cells. *J. Biol. Chem.* **269:** 13346-13352.

Zuo, J., De Jager, P.L., Takahashi, K.A., Jiang, W., Linden, D.J., and Heintz, N. (1997). Neurodegeneration in Lurcher mice caused by mutation in δ2 glutamate receptor gene. *Nature.* **388:** 769-773.